学位授与年月 平成 26 年 3 月
関西大学審査学位論文

New application to public health and environmental analysis using photoionization and high-resolution mass spectrometry

理工学研究科総合理工学専攻
無機・物理化学研究領域
12D6011 山本敦史

博士論文要旨

理工学研究科総合理工学専攻
無機・物理化学研究領域
126011
山本　敦史

《論題》

New application to public health and environmental analysis using photoionization and high-resolution mass spectrometry

《概要》

保健衛生・環境分野において迅速・簡便な分析手法は不可欠なものとなっている。近年は特に、禁止薬物による事件・事故、残留農薬における大規模食中毒、不法投棄による環境汚染等の様々な社会問題の増加に伴う分析対象とする物質の急増という課題を抱えている。光イオン化は、Robb らにより質量分析における大気圧イオン化法として、液体クロマトグラフ質量分析計（LC/MS）に導入された。LC/MS における大気圧光イオン化（APPI）は比較的新しい手法の一つであり、これまでその適用範囲は低極性化合物に対して有利であるとされてきた。保健衛生・環境分野における分析対象物質の物性は極めて多様であり、多くの分析対象に用いることができる分析方法の確立は急務である。また、これらの事件・事故においては原因物質が不明であることも多く、物質同定を行う必要があることが多い。未知物質の同定において、高分解能質量分析装置は極めて有用であり、生じるイオンを精密質量により解析することで分子の構造を決定する手法の確立は大いに期待されている。

近年の環境問題は、市民生活に身近な医薬品や化粧品および機能性の高い新規の化学物質、規制にともなう代替物質による汚染が注目されている。また、有害化学物質に限らず、保健衛生・環境分野においては感染症対策も大きな課題の一つである。本論文は、保健衛生・環境分野における諸課題に関して APPI イオン化法や高分解能質量分析を適用し、新規分析手法の確立と物質同定やイオン化、フラグメンテーション機構について新たに得られた知見をまとめたものである。また、開発した手法を用いた大阪地域における実態調査についての内容が含まれる。

《各章の要旨》

第 1 章は、人畜由来の性ホルモン物質の分析について、APPI 法を用いた分析法の確立、都市河川中における実態調査の結果を示した。遊離体の性ホルモンは低極性物質であり、APPI はこれまで主に用いられてきたエレクトロスプレーイオン化よりもより高感度であ

り、より詳細な性ホルモンの環境中での挙動を明らかにすることができた。大半の分析対象は下水処理場放流水由来の物質に特徴的な挙動と示していた。

第 2 章は、低極性物質である塩素系農薬クロロタロニルとその分解物に関する APPI を用いた同時分析法の開発について示した。分解物は前駆物質と物性が大きく異なることが多いが、APPI を用いることで同時に迅速な分析が可能となった。ウリ科の野菜等に多く用いられるが、環境試料に限らず食品に対しても適用可能な手法を開発できた。

第 3 章は、2000 年以降使用されるようになったネオニコチノイド農薬について APPI を用いた分析法開発と環境調査について示した。高質量分解能の質量分析計を用い、ネオニコチノイド農薬の APPI のメカニズムを明らかにした。大阪地域は耕作が盛んな地域からは離れているが、一部のネオニコチノイド農薬は使用時期に矛盾しない濃度の推移を示していた。

第 4 章では、フルオロキノロン系の抗菌剤について、その分析法開発、フルオロキノロン耐性菌の関連を踏まえた実態調査について示した。APPI による、対象としたフルオロキノロン系抗菌剤の一斉分析が可能であり、その挙動は 1 章で述べた性ホルモン等の下水処理場由来の物質のものに似ていた。耐性菌との関連は明確ではなく、都市河川が耐性の発現の場となっているとは言えない結果であった。

第 5 章では、感染症に関して結核菌に特有のミコール酸の APPI を用いた分析について示した。ミコール酸は炭素原子数が 80 程度の低極性脂質であるが、APPI による分析が可能であった。脂質の組成は微生物種によって大きく異なっており、菌種の同定に用いることができるだけでなく、脂質組成はその菌種の特性に大きく影響している。APPI を用いた方法はより詳細な細胞壁構造の解明に適用できると考えられた。

第 6 章では、有機フッ素化合物の質量分析を用いた構造決定について示した。市販製品中に含まれる、これまで環境汚染と考えられてこなかった分子量の大きな成分についてその構造決定および、生分解試験による分解生成物の同定に、高質量分解能質量分析を適用した。製品中には多くの高分子量の有機フッ素化合物が含まれ、ペルフルオロオクタン酸等の環境汚染物質に分解し得ることを示した。

以上

Table of Contents

General Introduction

Photoionization has been applied in analytical chemistry in the 1970s as a detection principle after chromatographic separation.[1,2] As an atmospheric pressure ionization, Robb et al introduced atmospheric pressure photoionization (APPI) to ionization technique of liquid chromatography /mass spectrometry (LC/MS) in 2000 for the first time.[3] As of now, APPI sources have become commercially available from a number of mass spectrometer manufacturers as well as electrospray (ESI) and atmospheric pressure chemical ionization (APCI) sources. APPI is one of relatively new techniques and it has been considered a major advantage that its application range includes non-polar compounds such as aromatic hydrocarbons that were not ionized by ESI and APCI.[4] In the public health and environmental research fields, the development of rapid and easy analytical methods is essential. Particularly, the fields have a problem that the number of analytes increases rapidly with increase in social problems such as crime and accidents by illicit drugs, severe food poisoning by residual pesticides, and environmental pollution by illegal dumping. Because properties of the analytes vary a great deal, it is urgent to establish robust analytical methods that can be applied to various analytes. In addition, it often happens that the identification of unknown offending substances needs to be made. The development of analytical instruments in the mass spectrometry has been significantly advancing. In 2013, a mass spectrometer with a mass resolving power of 10,000,000 is already launched on the market. In the identification of unknown offending substances, such an ultra-high resolution mass spectrometer is quite useful and is highly anticipated to be applied in the determination of whole molecular structures by interpretation of generated ion species using accurate masses.

Past environmental problems were usually caused by pollution that has an obvious source origin as in the case of heavy metal and polychlorinated biphenyl, for example. Recent environmental problems are, however, caused by more familiar substances included in medicines and cosmetics. In addition, various substituents that associate with the regulations also draw attention. Not only toxic chemical substances but also

provision for infection diseases is one of the most urgent issues in the fields of public health and environment. This thesis is a compilation of new knowledge about the development of analytical methods, procedure of structural identification, mechanisms of ionization and fragmentation, and filed surveys with the developed methods.

References

(1) Schmermund, J. T.; Locke, D. C. *Anal. Lett.* **1975,** *8* (9), 611-625.

(2) Driscoll, J. N.; Spaziani, F. F. *Res./Dev.* **1976,** *27* (5), 50-54.

(3) Robb, D. B.; Covey, T. R.; Bruins, A. P. *Anal. Chem.* **2000,** *72,* (15), 3653-3659.

(4) Raffaelli, A.; Saba, A. *Mass Spectrom. Rev.* **2003**, *22*, (5), 318-331.

CHAPTER 1

Steroid Hormone Profiles of Urban and Tidal Rivers Using Liquid Chromatography/Mass Spectrometry/Mass Spectrometry with Electrospray Ionization and Atmospheric Pressure Photoniozation Sources

1.1 Introduction

The trace-level presence of compounds with estrogenic properties in the water environment has become a worldwide concern. Researchers in environmental science are interested in the discovery of substances behaving as exogenous endocrine-disrupting chemicals and in detecting their presence.

The estrogenic compounds in wastewater treatment effluent and in sewage runoff from agriculture and stockbreeding have been identified by various techniques such as chromatography fractionation, *in vitro* bioassay, and mass spectrometry (*1-4*) and the main estrogenic components have been thought to be reproductive hormones from living creatures. It is known that the majority of estrogens is excreted in urine or feces in conjugated forms (i.e. sulfate or glucuronide) (*5*). It is therefore necessary to examine the behavior of estrogens including their conjugates in the water environment. D'Ancenzo *et al.* showed in a laboratory simulation using domestic wastewater that conjugates dissipated within a few days (*6*). However, sulfuric conjugates have been detected in environmental waters (*7*). Furthermore, although there are many studies of the fate of unconjugated estrogens in environmental water (e.g. photodecomposition, biodegradation, sorption to sediment) (*8-10*), estrogens, especially estrone, appear frequently in the water environment (*4, 10-12*).

Meanwhile, there is sparse information on the occurrence of androgen in the water environment. Paper mill effluent is suspected of involvement in the masculinization of fish, which inhabits the receiving river (*13*). Jenkins *et al.* revealed the presence of 4-androstene-3,17-dione in a river containing paper mill effluent (*14*). Reproductive androgens are associated with the same problems as estrogens.

Gas chromatography/mass spectrometry (GC/MS) and LC/MS are recognized as the most sensitive and reliable methods in environmental science. These instruments have been used in order to evaluate the presence, the behavior, and the source of reproductive hormones in the environment. In the analysis of conjugated steroids using GC/MS, complicated modification steps, such as derivatization and deconjugation, are generally

required because of the involatility and thermal instability of the conjugated steroids. ESI has frequently been adopted as an ion source in hormonal analysis using LC/MS, but unconjugated steroids are less polar compounds, which were fundamentally unsuited to ESI. In 2002, Leinonen *et al.* detected anabolic hormones using APPI-MS and compared this method with ESI and APCI (*15*). Guo *et al.* showed superior sensitivity and precision in APPI-MS compared with immunoassay for nine hormones (*16*).

In this chapter, the applicability of LC/APPI-MS/MS to the simultaneous detection of steroids in urban rivers and their estuaries was investigated. The target steroids included following 17 reproductive hormones: testosterone (T), 4-androstene-3,17-dione (AD), androsterone (A), epiandrosterone (EA), dehydroepiandrosterone (DHEA), 5*α*-dihydrotestosterone (DHT), estrone (E1), 17*β*-estradiol (E2), estriol (E3), dehydroepiandrosterone-3-sulfate (DHEA-3S), estrone 3-sulfate (E1-3S), 17*β*-estradiol 3-sulfate (E2-3S), estriol 3-sulfate (E3-3S), estrone 3-*β*-$_D$-glucuronide (E1-3G), 17*β*-estradiol 3-*β*-$_D$-glucuronide (E2-3G), estriol 3-*β*-$_D$-glucuronide (E3-3G) and synthetic estrogen ethynylestradiol (EE2). Stepwise fractionation for unconjugates and conjugates was also investigated using solid-phase extraction. The fractionation method reported here is based on the method of Gentili *et al.* (*4*). The fractions were separately determined by LC/MS/MS with ESI and APPI.

1.2 Experimental Section

1.2.1 Reagents

T, AD, EA, DHEA, DHT, E1, 17*α*-estradiol (*α*E2), E2, E3 and EE2 were purchased from Wako Pure Chemical Industries, Ltd (Osaka, Japan). Androsterone and the conjugated steroids DHEA-3S, E1-3S, E2-3S, E3-3S, E1-3G, E2-3G, and E3-3G were purchased from Sigma-Aldrich (St. Louis, MO, USA). The internal standards 17*β*-estradiol 2,4,16,16-d_4 (d_4-E2) and 17*β*-estradiol 2,4,16,16-d_4 3-sulfate (d_4-E2-3S) were purchased from Cambridge Isotope Laboratories, Inc. (Andover, MA, USA) and C/D/N Isotopes INC (Pointe-Claire, Quebec, Canada), respectively.

Tetramethylammonium chloride, ammonia, and formic acid were

purchased from Nacalai Tesque Inc. (Kyoto, Japan). Acetonitrile and methanol were HPLC grade (Wako) and used as supplied. Water purified with an ultra-pure water manufacturing device (TORAY PURE LV-10T, Tokyo, Japan) was used.

1.2.2 Sample Collection

Aqueous samples were collected in glass bottles from the rivers and estuaries of Osaka City in three rounds (Aug. 3-4, 2004, Feb. 7-8, 2005, and Aug. 2-3, 2005). The sampling locations are shown in Figure 1.1. Osaka City has a population of about 2.6 million and many streams and watercourses. Because the difference of altitude is small and tidal currents periodically press back rivers, brackish water flows upstream to around station 14. Furthermore, because rivers with quite different quantities flow into each other, some rivers flow backward for more than 20 km from the estuary. Grab samples were taken only when the flow was in the downstream direction. Almost all locations receive final treated effluent from a number of municipal wastewater treatment plants (WWTPs). All samples were extracted on the same day.

1.2.3 Extraction Procedure

The analytes were extracted from 2 L of an aqueous sample and fractionated into neutral and acidic analytes by stepwise elution based on the method of Gentili (*4*). Speclean ENVI-CARB (Supelco, Belefonte, PA, USA) was used as the solid-phase extraction (SPE) cartridge. Aqueous samples were forced through the cartridges using a Sep-Pak Concentrator (Waters, Milford, MA, USA), with the flow rate adjusted to 20 ml min^{-1}. The eluents were dichloromethane/methanol (80:20, v/v) for unconjugated steroids and 5 mM tetramethylammonium chloride in dichloromethane /methanol (80:20, v/v) for conjugated steroids. Although Gentili used acidified methanol in order to remove some compounds that interfere with analysis of E3, the purification of the Osaka river samples was insufficient for this. Further purification using a Sep-pak Florisil cartridge (Waters) was therefore carried out for the analysis of unconjugated steroids. The eluates of

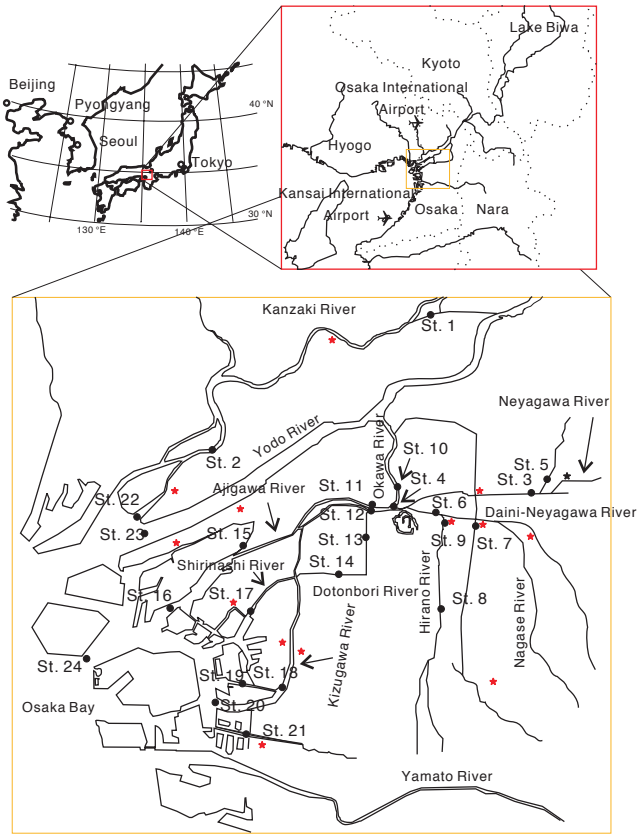

Figure 1.1 Sites of water sampling in Osaka City. The filled stars denote municipal WWTPs.

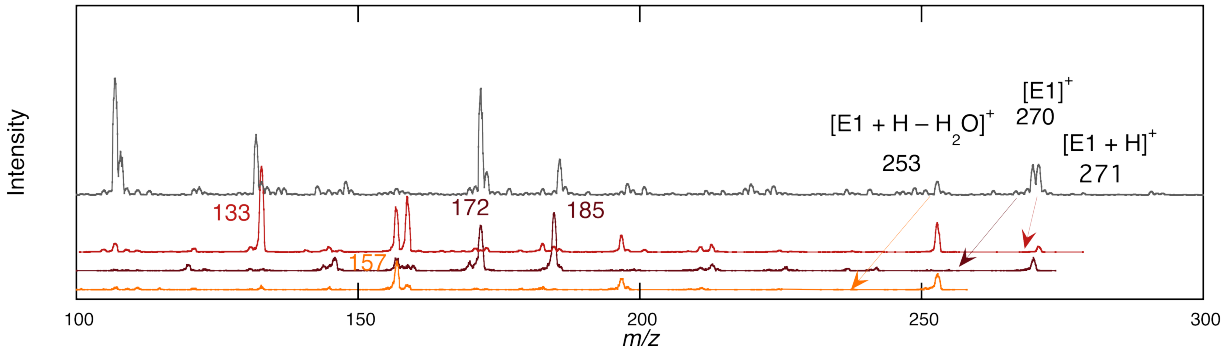

Figure 1.2 Full-scan Q1 and CID spectra for E1. Upper spectra represent full-scan mass spectrum and lower spectra CID spectrum for corresponding precursor ions.

the unconjugated steroids were reconstituted in 1 ml of dichloromethane/hexane (1:1, v/v) and the solutions loaded onto the florisil cartridges, which were conditioned with dichloromethane/methanol (80:20) and dichloromethane/hexane (1:1). The florisil cartridges were then washed with 10 ml of hexane/dichloromethane (1:1) and the unconjugated steroids re-eluted from the florisil cartridges with 6 ml of dichloromethane/methanol (80:20), following which 200 μL of methanol containing 2 ng of the internal standard was added to the eluates. The internal standard was d_4-E2 for unconjugates and d_4-E2-3S for conjugates. Each eluate was concentrated by evaporation in a water bath at 40 °C under a gentle stream of nitrogen and transferred into 200 μL of mobile phase for LC.

1.2.4 LC/MS/MS analysis

An Agilent 1100 series (Agilent Technologies, Palo Alto, CA, USA) HPLC system was used for the chromatography. The analytes were chromatographed on a 15 cm × 2 mm i.d. ODS-100S column packed with 5 μm C18 reversed-phase packing (TOSOH CORP., Tokyo, Japan). The effluent from the column was brought directly to the LC/MS interface without postcolumn split. The flow rate of the mobile phase was 200 μL min^{-1}. Injected volume was 10 μL for unconjugates and 5 μL for conjugates.

An API 2000 tandem triple quadrupole mass spectrometer (AB Sciex, Foster City, CA, USA) equipped with an electrospray source operated in the negative ion mode and a photoionization source operated in the positive ion mode was used for hormonal detection. The selected reaction monitoring (SRM) mode was used for the quantitation. The working parameters for ESI source were below. The ion spray voltage was –4500 V. The source temperature was maintained at 550 °C. The settings for both the nebulizer and heater gases were 90 psi, while the setting of gas pressure in the collision cell was 4. In the APPI experiment, the photoionization lamp was a 10 eV Cathodeon Ltd. krypton discharge lamp model PKS 100. Toluene was selected as a dopant. In APPI, dopant is used to increase the efficiency of ion formation. The optimal flow rate of toluene was 50 μL min^{-1}. The ion transfer voltage was 1550 V. The source temperature was maintained at

450 °C. The settings for the nebulizer and auxiliary gases were respectively 90 and 50 psi, while the setting of gas pressure in the collision cell was 2. For chromatography of unconjugated steroid hormones, the mobile phases were acetonitrile (A) and water (B). The concentration of formic acid was 2 mM for both mobile phases. In the mobile phase, the initial content of phase A was adjusted to 10% and maintained for 2 min. It then increased from 10% to 90% in 10 min and this composition was maintained for 5 min. For chromatography of conjugated steroid hormones, the mobile phases were the same as unconjugated steroid analysis but both mobile phases contained ammonia instead of acid. Optimized ammonia concentration was 20 mM. In the mobile phase, the content of phase A increased from 10% to 100% in 5 min and then this composition was maintained for 5 min. For each analyte, the calibration curve was obtained from the peak area ratios of the analyte to its internal standard. Six-point calibration curves were constructed using a least-square linear regression analysis within the linear range of the instrument (10-500 ng ml^{-1} for DHT, DHEA, E1-3G, and E2-3G; 50-500 ng ml^{-1} for E3-3G; 1-500 ng ml^{-1} for other steroids). Curves were linear with r^2 values higher than 0.99.

1.3 Results and Discussions

1.3.1 LC/MS/MS Optimization

Preliminary experiments were performed in order to detect the steroids using SRM mode. First, full-scan Q1 and product ion spectra of each steroid were acquired. In the analysis of unconjugated steroids using the APPI source, Q1 spectra indicated that unconjugated steroids produced three kinds of cations: radical cation $[M]^{+\cdot}$, protonated molecule $[M + H]^+$, and dehydrated fragment ion $[M + H - H_2O]^+$. For some steroids, the dehydrated fragment ion was selected as the precursor ion instead of the radical cation and protonated molecule, which had poor sensitivity. The Q1 and product ion spectra of E1 were shown in Figure 1.2. Photoionization reactions involve many steps, such as photoexcitation, photodissociation, quenching, charge transfer, and proton transfer. Analyte molecules are finally ionized through either charge transfer or proton transfer. Robb *et al.* showed that a radical

cation of an analyte could be generated in the ionization process of the APPI (*17*). The present results were consistent with them. In the present experiments, within a range of 10-50 ml min^{-1}, the flow rate of dopant increased the intensity of the analytes. The two transitions that provided the best sensitivity were selected for the combination of precursor and product ions in the SRM study. The two SRMs and mass-dependent tuning parameters are listed in Table 1.1.

In the analysis of conjugated steroids using ESI source running in negative ion mode, Q1 spectra showed that deprotonated ion $[M - H]^-$ was predominant, as reported elsewhere. These ions were selected as the precursor ions for collision induced dissociation (CID) fragmentation in ESI mass spectrometry. The two SRMs and mass-dependent parameters are listed in Table 1.1. Identification of analytes was confirmed by both the LC retention time and the abundance rate of the two SRMs.

1.3.2 Method performance

The instrumental detection limit (IDL) for each steroid, estimated from the standard deviations of seven rounds of quantitation of standard solution at the lowest concentration of calibration curves is listed also in Table 1.1. T and AD were extremely sensitive while DHEA and DHT were rather insensitive due to their fragmentation.

The analyte recoveries from environmental aqueous samples were evaluated by simultaneously analyzing spiked and not spiked river samples of same location. E1, E3-3G of 50 ng, and other steroids of 20 ng were added to 2 L river samples. Five recovery experiments were performed. The results are summarized in Table 1.1. Analyte recoveries were higher than 70% for all analytes examined. The method quantitation limit (MQL) of steroids in environmental samples was defined as 10-fold background noise intensity near the analyte. The values of MQL are also listed in Table 1.1. MQLs for E3 and DHEA-3S were relatively high for their IDL due to the high background noise of the SRM transitions.

The method developed was highly sensitive and uncomplicated and did not require the addition of any reagents such as triethylamine which are

Table 1.1 Two SRMs, mass-dependent tuning parameters, IDL, and MQL for the determination of steroidal hormones.

		SRM[a]	DP[b] / V	CE[c] / V	IDL / pg	MQL / ng L–1
APPI	E1	271/133 253/157	21 36	8 31	5.1	0.7
	E2	255/159 255/133	31	23 23	4.1	0.7
	E3	271/253 271/133	16	17 27	7.2	1.5
	EE2	279/133 279/105	21	23 49	12	0.9
	T	289/97 289/109	31	31 35	0.8	0.06
	AD	287/97 287/109	21	33 33	1.6	0.1
	DEHA	271/91 253/197	16 21	63 31	40	3.3
	DHT	291/255 273/255	21 16	21 19	62	7.0
	A	273/255 291/273	16 6	19 15	10	1.3
	EA	273/255 291/273	16 6	19 15	15	1.2
	d_4-E2	259/161 259/135	16	23 25	-	-
ESI	E1-3S	349/269 349/145	–41	-48 –70	2.4	0.4
	E2-3S	351/271 351/80	–81	–60 –60	3.5	0.5
	E3-3S	367/287 367/80	–56	–52 –62	2.3	0.6
	E1-3G	445/269 445/113	–11	–56 –34	19	0.7
	E2-3G	447/271 447/113	–36	–58 –38	18	0.9
	E3-3G	463/287 463/113	–11	–60 –38	140	12
	DEHA-3G	367/97 367/80	–76	–124 –60	2.1	2.4
	d_4-E2-3S	355/275 355/80	–81	–60 –60	-	-

[a]Selective reaction monitoring, [b]Declustering potential, [c]Collision energy.

undesirable in mass spectrometry. Specifically, the APPI source enabled simultaneous analyses of androgen and estrogen in water environment. This result shows that APPI source is superior to ESI or APCI in terms to ionize low polarity molecules and suitable for research of the environmental behavior of reproductive hormones.

1.3.3 Environmental Levels

LC/MS/MS with ESI or APPI source was applied to the analysis of the target compounds in water samples. Figure 1.3 shows typical LC/MS/MS chromatograms obtained from the water samples. Figure 1.4 summarizes the quantitative results as a box plot. For estrogens, E1, E1-3S, E1-3G, E2, and E3 were detected, while *α*E2, synthetic estrogen EE2, and conjugated estrogens other than E1-3S and E1-3G were never detected. For androgens, T and AD only were detected. E1, E1-3S, and AD were detected at almost all stations.

As to seasonal variation, steroid levels in water were greater in winter at most stations than in summer. Jürgens *et al.* showed that aerobic biodegradation of estrogens in river water predominated over other forms of degradation (e.g. photolysis) and that the half-lives owing to biodegradation were roughly halved by an increase of temperature from 10°C to 20°C (*8*). The higher winter levels detected in the present study are consistent with the results of Jürgens. T was also detected only in winter. The values measured in the river water were very high locally, and were of the same order of magnitude as for effluents from municipal WWTPs reported elsewhere (*1-4, 6, 11, 18*). The levels of steroidal hormones were especially high in the stations around the Neyagawa and Daini-Neyagawa River. The 14 stations out of 20 where the concentration of E1 exceeded 10 ng L^{-1} in the three sampling rounds were concentrated around these two rivers. The Okawa River receives from the Yodo River, which supplies drinking water to about 16 million people and has not been generally affected by effluent from WWTPs. The flow of the Okawa River is about 10 times greater than that of the Neyagawa and Daini-Neyagawa Rivers, which, like nearly all the city's rivers, are periodically pressed back by tidal currents. Station 4 is near the

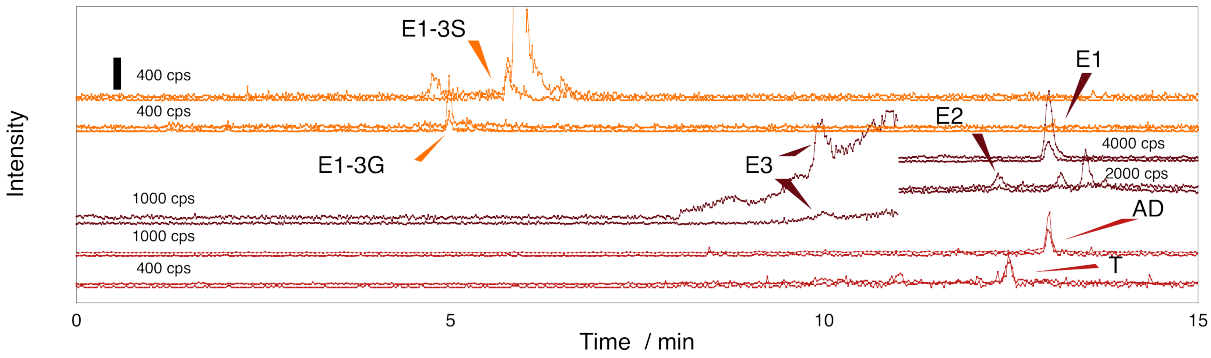

Figure 1.3 Chromatograms from MRM analysis of an aqueous sample at station 18. To identify each analyte, data from two transitions were collected.

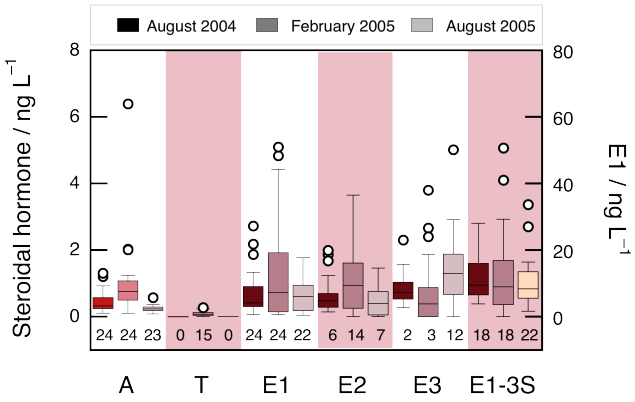

Figure 1.4 Box plot for three sample collections. The boxes are arranged from the left in order of age. The scale for E1 is 10 times larger than that for the others. The open circles represent extremes. The numbers under the boxes represent the number of detections in 24 samples.

confluences of the Okawa, Neyagawa, and Daini-Neyagawa Rivers. In the upstream region beyond station 4 of the Neyagawa and Daini-Neyagawa Rivers, there is therefore a frequent alternation between two-way flow and stagnancy.

The more a river is affected by WWTP effluent, the warmer the water temperature becomes. Water temperature therefore sometimes has good correlation with chemical oxygen demand or inorganic nitrogen levels. A similar relationship was found between E1 and water temperature (Figure 1.5). These correlations became stronger in winter. There are several WWTPs in the upstream region beyond station 4 of the Neyagawa and Daini-Neyagawa Rivers, which respectively receive effluent from WWTPs capable of treating approximately 650,000 and 770,000 tons per day. Both continuous input and irregularity of river flow seem to result in local accumulation of steroidal hormones in this region.

1.3.4 Hormonal Profile

The levels of estrogens were higher than those of androgens, and the majority of detected steroid was E1. The levels of AD were of the same order of magnitude as those of E2 and E3. Generally, contamination owing to chemical compounds is diluted in the estuarial region as the flow of the river becomes larger. Figure 1.6 shows the behavior of E1 and AD along the rivers was completely different. Steroid hormones except for AD resembled rather E1 and had positive correlation with each other (Figure 1.7). The correlation coefficients of E1 against E2 and AD were 0.80 and 0.21, respectively. Although biodegradation and sorption to sediment of steroids in rivers and soil have been reported by a number of researchers (*9, 19, 20*), critical behavior discrepancies between estrogen and androgen were not mentioned in the relevant papers. Unlike other steroid examined, levels of AD showed the same broad dispersion in bays and estuarial regions as in the upstream region (Figure 1.6). Identification of AD in paper mill effluent has been reported (*14, 21*). Although there are several paper mills in Osaka City, the present concentration of AD was considerably less than the reported value. It is thought that ubiquitous phytosterols could become the source of AD (*22*)

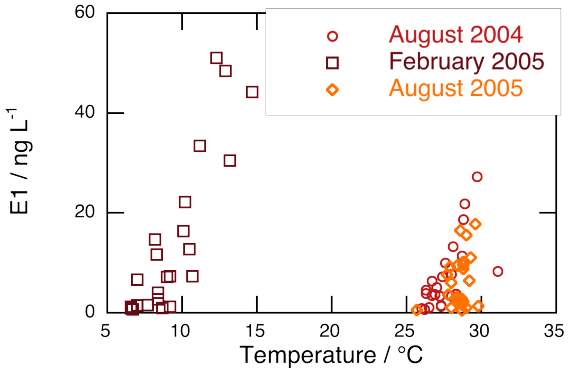

Figure 1.5 Correlation plot of water temperature against the concentration of E1.

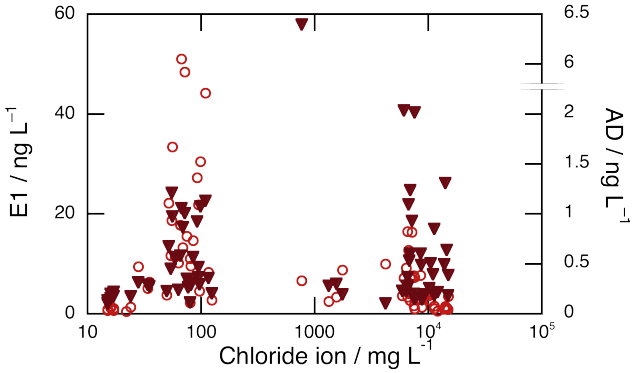

Figure 1.6 Correlation plot of steroid against chloride ion concentration. The open circles represent E1; the filled triangles represent AD.

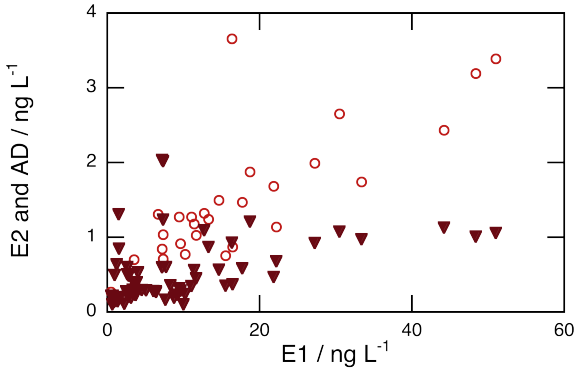

Figure 1.7 Correlation plot of E2 and AD concentration against E1 concentration. The open circles represent E2; the filled triangles represent AD.

and AD did seem to be greatly influenced by phytosterols.

Although conjugated steroids were detected, their concentrations were much lower than unconjugated steroids. E1-3G was detected only at stations 18, 19 and 20 in the first summer sampling round (Aug. 2004). The concentrations were 5.8, 4.5, and 0.7 ng L^{-1}, respectively. These stations were in the same watershed and received effluent from two WWTPs. D'Ascenzo *et al.* report that estrogen glucuronides immediately dissipate in wastewater within a day (*6*). Furthermore, there are almost no reports of the detection of estrogen glucuronides in river water or WWTP effluents.

The high correlation among steroid hormones other than AD seems to emphasize accumulative mechanism in the rivers of Osaka City. On the other hand, in national reconnaissance of U.S. streams (*12*), steroid hormones were detected in few places and no correlations were observed. In the present study, the features of urban and tidal rivers were conspicuous.

1.4 Conclusions

In this chapter, a highly sensitive and uncomplicated method of analyzing steroidal hormones in river and estuarine water samples was examined. Steroidal hormones included not only estrogen but also androgen and conjugates of these two were successfully analyzed. APPI displayed greater sensitivity than did ESI for most of the unconjugated steroids examined, with very high sensitivity for T and AD in particular. For conjugated hormones, in contrast ESI was more effective. The method developed was applied to the determination of hormones in the rivers of Osaka City and their estuaries, where the hormones detected were affected by the effluent from municipal WWTPs and hormone concentration values were comparable to those reported in previous studies of such effluent. Because of the two-way flow and stagnancy of streams and watercourses, continuous input of steroidal hormones from WWTPs seems to bring about local accumulation. Levels of androgen were one order of magnitude lower than those of estrogen. E1, E1-3S, and AD were detected in almost all water samples, with maxima of 51ng L^{-1}, 5.1ng L^{-1} and 6.4ng L^{-1}, respectively.

References

(1) Desbrow, C.; Routledge, E. J.; Brighty, G. C.; Sumpter, J. P.; Waldock, M. *Environ. Sci. Technol.* **1998,** *32,* (11), 1549-1558.

(2) Baronti, C.; Curini, R.; D'Ascenzo, G.; Gentili, A.; Samperi, R. *Environ. Sci. Technol.* **2000,** *34,* (24), 5059-5066.

(3) Thomas, K.; Hurst, M. R.; Matthiessen, P.; Waldock, M. J. *Environ. Toxicol. Chem.* **2001,** *20,* (10), 2165-2170.

(4) Gentili, A.; Perret, D.; Marchese, S.; Mastropasqua, R.; Curini, R.; Di Corcia, A. *Chromatographia* **2002,** *56,* (1-2), 25-32.

(5) Andreolini, F.; Borra, C.; Caccamo, F.; Di Corcia, A.; Samperi, R. *Anal. Chem.* **1987,** *59,* (13), 1720-1725.

(6) D'Ancenzo, G.; Di Corcia, A.; Gentili, A.; Mancini, R.; Mastropasqua, R.; Nazzari, M.; Samperi, R. *Sci. Total Environ.* **2002,** *302,* (1-3), 199-209.

(7) Isobe, T.; Shiraishi, H.; Yasuda, M.; Shinoda, A.; Suzuki, H.; Morita, M. *J. Chromatogr., A* **2003,** *984,* (2), 195-202.

(8) Jürgens, M. D.; Holthaus, K. I. E.; Johnson, A. C.; Smith, J. J. L.; Hetheridge, M.; Williams, R. J. *Environ. Toxicol. Chem.* **2002,** *21,* (3), 480-488.

(9) Lee, L. S.; Strock, T. J.; Sarmah, A. K.; Rao, P. S. C. *Environ. Sci. Technol.* **2003,** *37,* (18), 4098-4105.

(10) Labadie, P.; Budzinski, H. *Environ. Sci. Technol.* **2005,** *39,* (14), 5113-5120.

(11) Belfroid, A. C.; Van der Horst, A.; Vethaak, A. D.; Schäfer, A. J.; Rijs, G. B. J.; Wegener, J.; Cofino, W. P. *Sci. Total Environ.* **1999,** *225,* (1-2), 101-108.

(12) Kolpin, D. W.; Furlong, E. T.; Meyer, M. T.; Thurman, E. M.; Zaugg, S. D.; Barber, L. B.; Buxton, H. T. *Environ. Sci. Technol.* **2002,** *36,* (6), 1202-1211.

(13) Drysdale, D. T.; Bortone, S. A. *Bull. Environ. Contam. Toxicol.* **1989,** *43,* (4), 611- 617.

(14) Jenkins, R. L.; Angus, R. A.; McNatt, H.; Howell, W. M.; Kemppainen, J. A.; Kirk, M.; Wilson, E. M. *Environ. Toxicol. Chem.* **2001,** *20,* (6), 1325-1331.

(15) Leinonen, A.; Kuuranne, T.; Kostiainen, R. *J. Mass Spectrom.* **2002,**

556 *37,* (7), 693-698.
(16) Guo, T.; Chan, M.; Soldin, S. J. *Arch. Pathol. Lab. Med.* **2004,** 560 *128,* (4), 469-475.
(17) Robb, D. B.; Covey, T. R.; Bruins, A. P. *Anal. Chem.* **2000,** *72,* (15), 3653-3659.
(18) Ingrand, V.; Herry, G.; Beausse, J.; de Roubin, M. R. *J. Chromatogr. A* **2003**, *1020*, (1), 99-104.
(19) Das, B. S.; Lee, L. S.; Rao, P. S. C.; Hultgren R. P. *Environ. Sci. Technol.* **2004**, *38*, (5), 1460-1470.
(20) Jacobsen, A. M.; Lorenzen, A.; Chapman, R.; Topp, E. *J. Environ. Qual.* **2005**, *34*, (3), 861-871.
(21) Thomas, K. V.; Hurst, M. R.; Matthiessen, P.; McHugh, M.; Smith, A.; Waldock, M. J. *Environ. Toxicol. Chem.* **2002**, *21*, (7), 1456-1461.
(22) Nagasawa, M.; Bae, M.; Tamura, G.; Arima, K. *Agric. Biol. Chem.* **1969**, *33*, (11), 1644-1650.

CHAPTER 2

Simultaneous Analysis of Organochlorine Pesticide Precursor and Its Metabolite by Liquid Chromatography/Mass Spectrometry with Dopant-assisted Photoionization

2.1 Introduction

Residual pesticides are one of the major concerns for public health. In Japan, a positive list system for residual pesticides in food is adopted and includes more than 800 pesticides. In addition, another regulation for drinking water determines target values for more than 100 pesticides. There has been an increase in the number of regulated pesticides. Some pesticides undergo a chemical change in the environment after their application. This involves more potent derivatives than precursor pesticides.

Chlorothalonil, 2,5,6-trichloroisonapththonitrile (TPN), is a foliar fungicide commonly used on turf grass, fruits, and vegetables. Because of its high consumption, chlorothalonil has been frequently detected in food (*1,2*) and the environment (*3*). The primary degradation product of chlorothalonil, 4-hydroxy-chlorothalonil (4OH-TPN), has been reported to have greater stability and persistency than does that of the precursor compound (*4*). TPN has been analyzed by a gas chromatograph/electron capture detector or GC/MS (*5*). Trace analysis of TPN and its metabolites using gas chromatography requires complex analytical methods that include not only separate extractions under acidic and basic conditions but derivatization of polar metabolites. Therefore, novel analytical methods for TPN to complement methods based on GC are anticipated. Recently, LC/MS has been applied to the trace analysis of polar compounds. Although there are some studies of TPN using LC/MS equipped with an APCI source (*4,6-8*), the sensitivity of APCI was, for the most part, insufficient for detection in an aqueous environment. Furthermore, the analyses of TPN and its degradation products required two separate runs on LC/MS (*8*).

APPI technique has the potential to complement the deficit. So far, the technique enables LC/MS to quantify apolar compounds (*9*), as well as polar ones (*10*). In addition, negative-ion APPI was also examined in detail (*11,12*), so that its application range of APPI has been extended. Indirect ionization considered as photo-induced chemical ionization seems to be an important pathway in APPI. Consequently, the LC/APPI-MS technique ought to have a potential to improve the detection limit of TPN and to simplify the analytical pretreatment. In this chapter, an analytical method for food and aqueous

samples of TPN and 4OH-TPN by LC/MS using dopant-assisted APPI was examined.

2.2 Experimental Section

2.2.1 Reagents

TPN was purchased from Wako Pure Chemical Industries, Ltd. (Osaka, Japan). Its degradation product, 4OH-TPN, was purchased from Dr. Ehrenstorfer GmbH (Augsburg, Germany). Dacthal-d_6 (Dimethyl-d_6-tetrachloroterephthalate) was used as an internal standard, and purchased from C/D/N Isotopes Inc. (Pointe-Claire, Quebec, Canada). All other chemicals were of residue analysis grade. A stock solution with a concentration of 1 mg mL^{-1} was prepared by dissolution of the analyte in acetone. The solution was stored at –18 °C in the dark. Working standards were prepared by serial dilution of the stock solution with methanol for the acquisition of mass spectra and with methanol/water (20:80, v/v) for the LC/MS quantitation. Working standards for the quantification were prepared so that they would also contain 1 μg mL^{-1} of the internal standard.

2.2.2 LC/MS and LC/MS/MS analysis

The APPI-MS observation was performed using an API 2000 triple-quadrupole system. APPI source for the API 2000 was used as an ionization module. The photoionization lamp was a 10 eV model PKS 100 krypton discharge lamp. A micro-syringe pump (Harvard Apparatus, Holliston, MA, USA) or an Agilent 1200 isocratic pump (Agilent Technologies, Palo Alto, CA, USA) was used for dopant delivery. Toluene was used as the dopant in the APPI experiments. The full-scan mass spectrum was obtained in the range of *m/z* 100-500 at a scan rate of 1 scan s^{-1}. Selective ion monitoring (SIM) and SRM modes were examined. Two each of the SIMs and SRMs that provided the best sensitivity were selected and applied to identification and quantitation. The APPI conditions were as follows: nitrogen curtain gas, 20 psi; ion transfer voltage, –1200 V; heater temperature, 450 °C; lamp gas flow, 1.5 L min^{-1}; and declustering voltage, –41 V. The flow rates of the LC solvent and dopant were optimized by flow

injection analysis (FIA) in which water/methanol (1:1) was used as the solvent. An Agilent 1100 series HPLC system was applied to the FIA and chromatography. The analytes were chromatographed on a 15cm × 2mm i.d. ODS-100S column packed with 5 μm C18 reversed-phase packing (Tosoh Corp.). The effluent from the column was brought directly to the LC/MS interface without any post-column split. For fractionation, a gradient that was composed of mobile phase A (water) and mobile phase B (methanol) was applied. Both mobile phase A and B contained 2 mM ammonium bicarbonate for chromatographic retention. The gradient, expressed as changes in mobile phase B, was as follows: 0–5 min, a linear increase from 20% to 100% B; 5–10 min, hold at 100% B; 10–15 min, equilibration at 20% B. The flow rate of the mobile phase was optimized, and then determined to be 200 μL min^{-1}. The injected volume was 5 μL.

2.2.3 Aqueous Sample Preparation

Aqueous samples were collected from rivers of Osaka City and their estuaries for the examination of a recovery study and the environmental occurrence of TPN. Twenty-seven samples were collected on 6–7 February 2008. The analytes were extracted from 0.5 L of an aqueous sample by SPE. A Presep-C Agri cartridge (Wako Pure Chemical Industries, Ltd., Osaka, Japan) was sequentially conditioned by acetonitrile and water. Aqueous samples were forced through the cartridges using a Sep-Pak Concentrator (Waters) with the flow rate adjusted to 20 mL min^{-1}. The analytes were eluted from the cartridges with 5 mL of acetonitrile. The eluates were spiked with 1 μg dacthal-d_6 and concentrated in 1 mL by evaporation in a water bath at 40 °C under a gentle stream of nitrogen.

2.2.4 Food Sample Preparation

Because cucumber is one of the vegetables in which TPN has frequently been detected (*2*), we examined food sample preparation with cucumber. The extraction procedure from food samples was based on the method described by Hernández *et al.* (*13*) with some modification. A 20 g portion of chopped cucumber was weighed and homogenized with 60 mL of water/methanol

(20:80) containing 0.1% formic acid for 2 min. After filtration of the homogenate through a glass fiber filter (GA-100, Advantec, Tokyo, Japan) on a Buchner funnel under vacuum, the residue was washed. The filtrate was mixed with washing solvent and diluted to 100 mL. A mixed solution of water/methanol (20:80) containing 0.1% formic acid was used for washing and dilution. Subsequently, an aliquot of 2.5 mL was taken from the extract and diluted eightfold with 0.1% formic acid solution. As with the environmental samples, Presep-C Agri was used as an SPE cartridge. Following loading the sample, a wash step was examined in order to elute any interference without premature elution of the analytes. Appropriate washing solvents were examined with various organic solvent contents. After washing the cartridges, the cartridges were dried by passing air for 5 min. The analytes were eluted with 5 mL of acetonitrile. The eluates were spiked with 1 μg of dacthal-d_6 and concentrated in 1 mL by evaporation in a water bath at 40 °C under a gentle stream of nitrogen.

2.3 Results and Discussions

2.3.1 Ionization of TPN and 4OH-TPN

The mass spectrum of TPN is shown in Figure 2.1. Since the intensity ratio of the emphatic ions corresponded to that of the ions that had three chlorine atoms, it was considered that TPN generated $[M - Cl + O]^-$ during negative-ion APPI. In the absence of a dopant, the intensity of the peaks assigned to $[M - Cl + O]^-$ decreased thoroughly. Although $O_2^{-\cdot}$ was not directly observed in the present experiment, the existence of $O_2^{-\cdot}$ has been revealed during negative-ion APPI (*12*). As does the rearrangement of polychlorinated aromatic hydrocarbons with O_2 generate characteristic phenoxides in a process of negative chemical ionization (*14,15*), it is inferred that TPN was also transformed to $[M - Cl + O]^-$ by negative-ion APPI. A similar phenoxide was generated for dacthal-d_6. On the other hand, 4OH-TPN generated deprotonated molecules as a base peak.

The effects of LC solvent and dopant flow rates on the ionization efficiency in APPI were examined by FIA. The LC flow rate and the dopant flow rate were adjusted to 50–1000 and 50–500 μL min^{-1}, respectively. The

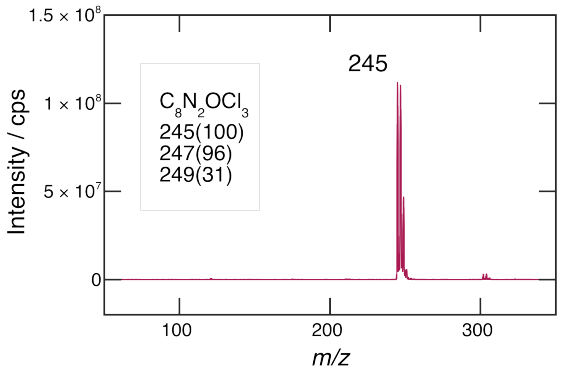

Figure 2.1 Mass spectrum of chlorothalonil by negative APPI. Predicted formula and its mass are also shown.

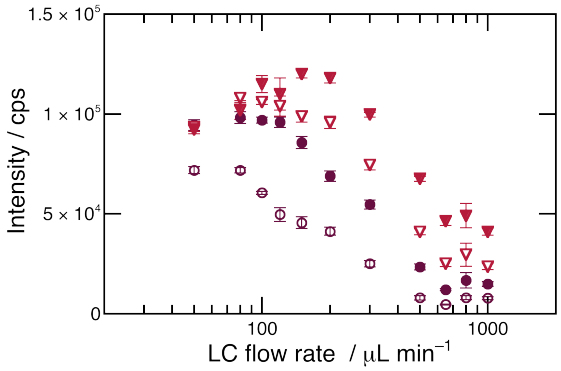

Figure 2.2 Plots of $[M–Cl+O]^-$ signal intensity versus LC flow rate, where the symbols denote dopant flow rate as follows: open circle, 50 μL min^{-1}; solid circle, 100 μL min^{-1}; open triangle, 200 μL min^{-1}; filled triangle, 500 μL min^{-1}. The standard deviation from five replicates is drawn as error bar.

results from the FIA with various flow rates are presented in Figure 2.2. The intensity decreased as the LC flow rate increased in all dopant flow rates. Ionization efficiency in positive-ion APPI has been described in detail (*16-18*). Although the effects of the solvent and dopant flow rates on the formation of $[M - Cl + O]^-$ resemble the proton transfer that occurs in positive APPI, the optimum proportion of dopant flow rate to solvent flow rate was greater than was that in positive APPI. It is inferred that the optimum proportion markedly depends on a reaction pathway. In order to maintain favorable chromatographic retention, the LC flow rate and dopant flow rate were set at 200 and 100 μmL min^{-1}, respectively.

LC/MS acquisition was performed in SIM mode with *m/z* 245 and 247. A typical chromatogram running in SIM mode for a TPN standard solution of 1 ng mL^{-1} is shown in Figure 2.3. The peak of TPN was sufficiently separated from that of 4OH-TPN, quantified by the same *m/z* value. Although use of acids was examined, acids seriously depleted the ionization efficiency. An excess use of base also showed an adverse effect. A calibration curve obtained for TPN using a series of working standard solutions over a concentration range from 0.3 to 300 ng mL^{-1} showed excellent linearity (r^2 > 0.99). Although moderate hydrolysis of TPN under a basic condition was previously reported (*19*), obvious degradation was not observed during the LC/MS measurement. The IDL was determined by multiplying the standard deviation of the quantified values of standard solutions for seven replicate measurements. The IDLs of TPN and 4OH-TPN were 0.15 ng mL^{-1} and 0.16 ng mL^{-1}, respectively. The value was lower than that of TPN by GC/MS (100 ng/mL) (*5*).

2.3.2 LC/MS/MS analysis

The product-ion mass spectrum of the generated ion (*m/z* 245) for TPN was acquired in the range *m/z* 20-300 at a scan rate of 1 scan s^{-1}. The major product ion was *m/z* 35. The optimum collision energy was –48 V. A series of Cl eliminated ions $[M - Cl_n + O]^-$ was also observed with subtle intensity. LC/MS/MS acquisition was performed in SRM mode with the following SRM transitions: *m/z* 245 → 35 and 247 → 35. A calibration curve ranging from 1

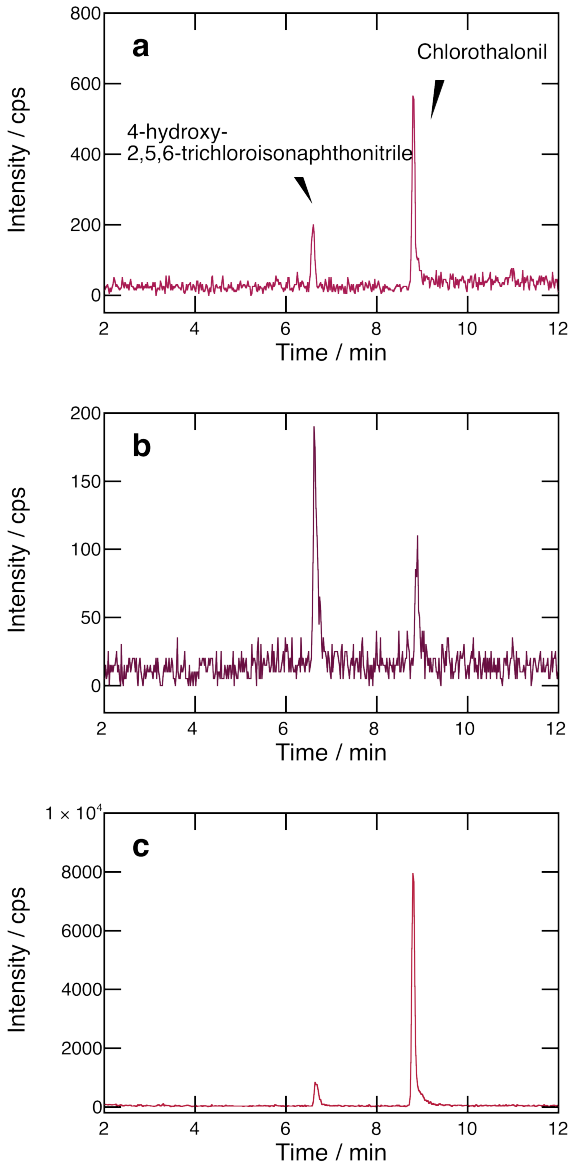

Figure 2.3 SIM chromatograms at *m/z* 245 of a) a standard solution containing both chlorothalonil and 4-hydroxy-2,5,6-trichloroisonaphthonitrile (4OH-TPN) of 1 ng mL^{-1}, b) an extract from river water collected from Osaka City, and c) an extract from cucumber containing chlorothalonil as a pesticide residue of 17 ng g^{-1}.

to 1000 ng mL^{-1} was constructed and showed good linearity ($r^2 > 0.99$). The IDL of TPN by SRM estimated in the same manner as SIM was 1.8 ng mL^{-1}. The IDL by SRM was not better than that by SIM. It appeared that the absence of a dominant product ion with a large *m/z* value caused this result. For 4OH-TPN, the product-ion mass spectrum of the deprotonated molecule (*m/z* 245) was substantially the same as that of the ion (*m/z* 245) generated from TPN. The IDL of 4OH-TPN by MRM was determined to be 2.2 ng mL^{-1}. Consequently, SIM mode was used to determine TPN and 4OH-TPN.

2.3.3 APCI vs APPI

The generation of $[M - Cl + O]^-$ from TPN by LC/APCI-MS has also been reported (*6,7*). Martínez *et al.* quantified TPN by a calibration curve whose minimum concentration was 25 ng mL^{-1} (*6*). As the IDL of TPN by the APPI method was 0.15 ng mL^{-1}, it can be said that APPI is outstanding with respect to instrumental sensitivity. As to the generated ions other than $[M - Cl + O]^-$, it was reported that APCI generated solvent adducts and a fragment ion corresponding to the loss of Cl (*7*), whereas APPI generated some solvent adducts and $[M - Cl + O_2]^-$ with a relative abundance of 5% or less.

Although the analysis of 4OH-TPN by APCI was also examined (*7,8*), Scribner *et al.* used only ESI for the determination of 4OH-TPN because of the sensitivity (*8*). The APPI method could provide simultaneous determination of TPN and its polar degradation product with sub-ppb level sensitivity differing from other ionization methods.

2.3.4 Elution from SPE cartridge

The sorbent of Presep-C Agri is a copolymer composed of styrene, divinylbenzene, and methacrylate. Presep-C Agri has a capability to adsorb both polar and nonpolar compounds, as well as Oasis HLB (styrene, divinylbenzene, and N-vinyl-pyrrolidone; Waters), which was used in other studies (*6-8,13*). The elution profiles from Presep-C Agri cartridges with 5 mL of various solvents are shown in Figure 2.4. Acetonitrile was stronger than methanol in the elution of TPN and 4OH-TPN. Since the use of

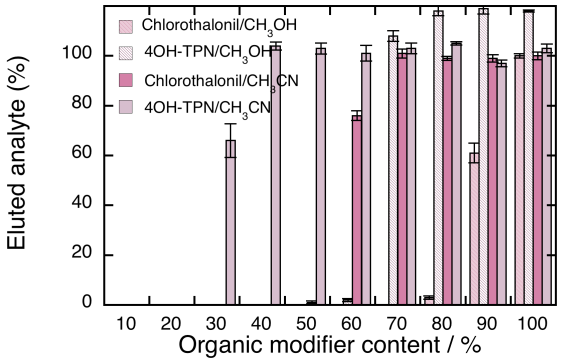

Figure 2.4 Elution profiles of chlorothalonil and 4OH-TPN from SPE cartridges using eluents with different organic solvent contents.

methanol brought excess recovery of 4OH-TPN, 15% acetonitrile solution was selected as a washing solvent.

Oasis HLB was also examined. Since it strongly adsorbed 4OH-TPN, the eluent required additives such as ammonia to elute 4OH-TPN from Oasis HLB. Presep-C Agri was selected to avoid degradation of TPN under a basic condition.

2.3.5 Method Validation

For the recovery study, 0.5 L of river water and 20 g of cucumber samples were spiked with 5 ng and 0.2 μg of both TPN and 4OH-TPN, respectively. The recovery was satisfactory for extracting TPN from both the river water and cucumber samples, as listed in Table 2.1. Presep-C could be used for the extraction of 4OH-TPN as well as TPN. LC/APPI-MS chromatograms for the extracts from actual river water and cucumber are also shown in Figure 2.3. The cucumber contained TPN as a pesticide residue at 17 ng g^{-1}. The MQL calculated from seven replicate extractions is also listed in Table 2.1. The MQL for the aqueous sample enabled to quantify the concentration, which was potent for aquatic organisms (*20*). Inter-day variation was evaluated by analyses of spiked water and cucumber samples over a period of three days. The reproducibility of the method was expressed in terms of relative standard deviation ranged from 3.8 to 7.5%.

2.3.6 Environmental Level

At several estuarial locations, TPN was detected with a maximum of 1.1 ng L^{-1}. Although some pesticides are currently also used as antifouling agents in boat paint, the concentration was still lower than that of other pesticides (*6*). As for 4OH-TPN, it was principally detected not from estuaries but from river water with a maximum of 14 ng L^{-1}. The difference of biota between rivers and estuaries might be one of the factors. The locations where 4OH-TPN was detected have received much effluent from sewage treatment plants and some agricultural water. In order to elucidate environmental occurrence of TPN, further investigation will be required especially in the peak season when TPN is frequently used.

Table 2.1 Recoveries from 0.5 L of river water and 20 g of cucumber spiked with TPN and 4OH-TPN so as to respectively adjust the concentration to 1 ng L^{-1} and 10 ng g^{-1}.

		Mean recovery ± SD[a] (%, *n* = 7)	MDL[b]
River water	TPN	89 ± 3	0.18 ng L^{-1}
	4OH-TPN	93 ± 8	0.71 ng L^{-1}
Cucumber	TPN	93 ± 8	3.2 ng g^{-1}
	4OH-TPN	105 ± 7	2.4 ng g^{-1}

[a]Standard deviation, [b]Method detection limit (MDL) calculated from the standard deviation of seven replicated analyses.

2.4 Conclusions

This investigation demonstrated the applicability of LC/MS using an APPI source to the determination of TPN and its polar degraded product, 4OH-TPN, in environmental and food samples. Dopant-assisted negative-ion APPI brought a rearrangement reaction of TPN with O_2 and generated $[M - Cl + O]^-$ with great sensitivity. The flow rates of dopant and solvent were definitive for high sensitivity. Extraction and purification methods using solid phase cartridges were applied to actual samples. TPN was detected in the estuarial location with a maximum of 1.1 ng L^{-1}. The location where 4OH-TPN was detected did not coincide with that of TPN. This is the first example of detecting TPN by LC/APPI-MS. This method provided superb sensitivity compared with other techniques (*4,5,7,8*) and simultaneous quantification with 4OH-TPN.

References

(1) Newsome, W. H.; Doucet, J; Davies, D; Sun, W. F. *Food Addit. Contam.* **2000**, *17*, 847-854.

(2) Pharmaceutical and Food Safety Bureau, Ministry of Health, Labour and Welfare of Japan. Test Results of Agricultural Chemical Residues on Farm Products in 2004.

(3) Sakai, M. *J. Environ. Sci. Health B*, **2002**, *37*, (3), 247-254.

(4) Potter, T. L.; Wauchope, R. D.; Culbreath, A.K. *Environ. Sci. Technol.*, **2001**, *35*, (13), 2634-2639.

(5) Alder, L.; Greulich, K.; Kempe, G.; Vieth, B. *Mass Spectrom. Rev.*, **2006**, *25*, (6), 838-865.

(6) Martínez, K.; Ferrer, I.; Barceló, D. *J. Chromatogr. A*, **2000**, *879*, (1), 27-37.

(7) Chaves, A.; Shea, D.; Danehower, D. *Chemosphere*, **2008**, *71*, (4), 629-638.

(8) Scribner, E. A.; Orlando, J. L.; Battaglin, W. A.; Sandstrom, M. W.; Kuivila, K. M.; Meyer, M. T. *"Results of analyses of the fungicide chlorothalonil, its degradation products, and other selected pesticides at 22 surface-water,"* **2006**, U.S. Geological Survey Open-File Report 2006-1207.

(9) Moriwaki, H.; Ishitake, M.; Yoshikawa, S.; Miyakoda, H.; Alary, J. F. *Anal. Sci.*, **2004**, *20*, (2), 375-377.
(10) Moriwaki, H.; Harino, H.; Yoshikura, T.; Ohe, T.; Nukaya, H.; Terao, Y.; Sawanishi, H.; Wakabayashi, K.; Miyakoda, H.; Alary, J. F. *J. Environ. Monit.*, **2004**, *6*, (11), 897-902.
(11) Kauppila, T. J.; Kotiaho, T.; Kostiainen, R.; Bruins, A. P. *J. Am. Soc. Mass Spectrom.*, **2004**, *15*, (2), 203-211.
(12) Song, L.; Wellman, A. D.; Yao, H.; Bartmess, J. E. *J. Am. Soc. Mass Spectrom.*, **2007**, *18*, (10), 1789-1798.
(13) Hernández F.; Pozo, O. J. ; Sancho, J. V. ; Bijlsma, L.; Barreda, M.; Pitarch, E. *J. Chromatogr. A*, **2006**, *1109*, (2), 242-252.
(14) Dougherty, R. C. *Anal. Chem.*, **1981**, *53*, (4), 625A-636A.
(15) Luosujärvi, L.; Karikko, M. M.; Haapala, M.; Saarela, V.; Huhtala, S.; Franssila, S.; Kostiainen, R.; Kotiaho, T.; Kauppila, T. J. *Rapid Commun. Mass Spectrom.*, **2008**, *22*, (4), 425-431.
(16) Kauppila, K. J.; Bruins, A. P.; Kostiainen, R. *J. Am. Soc. Mass Spectrom.*, **2005**, *16*, (8), 1399-1407.
(17) Robb, D. B.; Blades, M. W. *J. Am. Soc. Mass Spectrom.*, **2005**, *16*, (8), 1275-1290.
(18) Cai, S. S.; Syage, J. A. *J. Chromatogr. A*, **2006**, *1110*, (1-2), 15-26.
(19) Szalkowski, M. B.; Stallard, D. E. *J. Agric. Food Chem.*, **1977**, *25*, (1), 208-210.
(20) USEPA Reregistration Eligibility Decision (RED): Chlorothalonil, **1999**.

CHAPTER 3

Analysis of Newly-introduced Neonicotinoids by Liquid Chromatography/Mass Spectrometry with Dopant-assisted Photoionization

3.1 Introduction

Neonicotinoids are new-generation pesticides that began to be used around the year 2000. In 1978, Soloway *et al.* reported the insecticidal activity of 2-nitromethylene-1,3-thiazinane, nithiazine (*1*). Since then, a diverse array of chemicals were screened for practical application and several chemicals were determined to be neonicotinoids based on their structural similarity to nicotine and their common mode of action. Because neonicotinoids specifically inhibit nerve transmission in insects and have high affinity for nicotinic acetylcholine receptors in insects, they are considered to be safe to creatures other than insects. Hence, the use of neonicotinoid pesticides has markedly increased in Japan and other regions worldwide. In Japan, more than 18,000 metric tons of neonicotinoid formulations were shipped in 2009 (*2*). Changes in the shipment quantities from 1990 to 2009 in Japan are shown in Figure 3.1. Of course, neonicotinoids do not only affect harmful insects. Given the importance of beneficial insects such as pollinators in agriculture, the environmental impact of neonicotinoids has aroused considerable concern. Despite the heavy consumption, the environmental presence of neonicotinoids remains unclear. Attractive techniques such as carbon nanotubes as a sorbent of solid phase extraction and thermal lens spectroscopy have been applied to the analysis of neonicotinoids (*3,4*). Few techniques, however, are applicable to environmental analysis due to poor specificity and sensitivity. LC/MS is regarded as an optimal instrument for detecting polar analytes, and has been applied to the analysis of neonicotinoids using APCI (*5,6*) and ESI (*7-11*). Different monitoring ions in APCI of imidacloprid were reported separately, making it difficult to understand the ionization of neonicotinoids. In this chapter, a detailed examination of the atmospheric pressure ionization of neonicotinoids was conducted. In addition, the presence of neonicotinoids in the aquatic environment using the developed method was investigated.

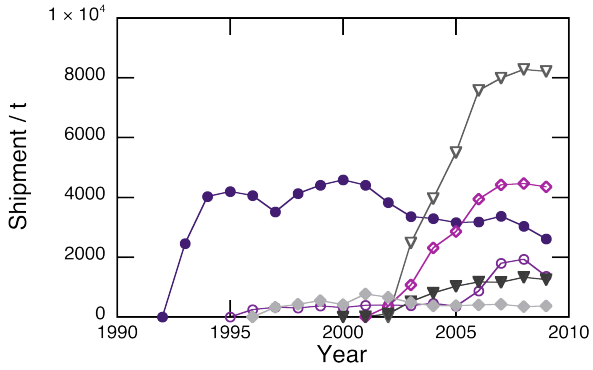

Figure 3.1 Changes in shipment quantity of neonicotinoid formulations from 1990 to 2009 in Japan. The symbols denote compounds as follows: open circles, acetamiprid; open squares, clothianidin; open triangles, dinotefuran; filled circles, imidacloprid; filled squares, nitenpyram; and filled triangles, thiamethoxam.

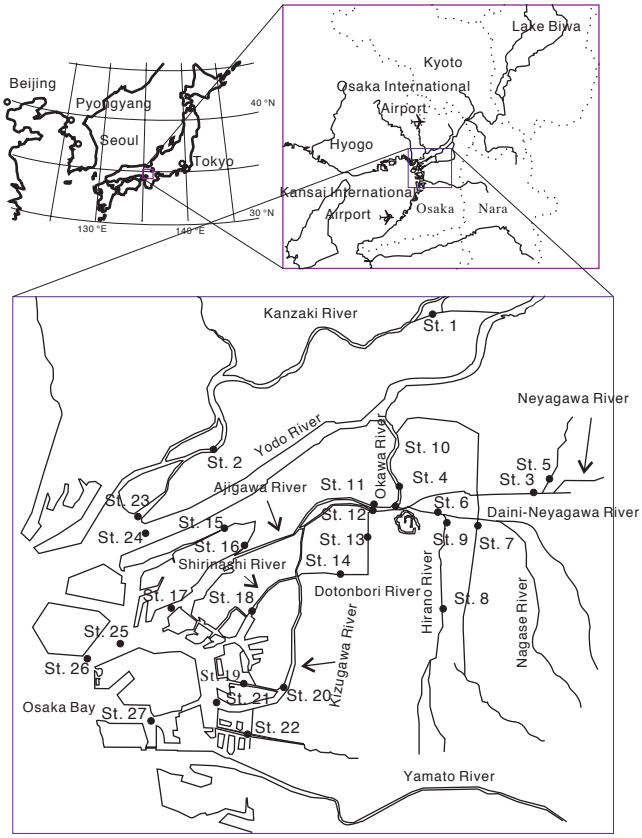

Figure 3.2 Sites of water sampling in Osaka City.

3.2 Experimental Section

3.2.1 Reagents

Acetamiprid, imidacloprid, dinotefuran, and nitenpyram were purchased from Wako Pure Chemicals Industries, Ltd. Thiamethoxam was purchased from Hayashi Pure Chemical Ind. Ltd. (Osaka, Japan). Clothianidin was purchased from Dr. Ehrenstofer GmbH. Imidacloprid-d_4 was used as internal standards and purchased from Fluka (Steinheim, Switzerland).

3.2.2 Sample Collection

Aquatic samples were collected in glass bottles from the rivers and estuaries of Osaka City on 18 and 24, August, 2009; and 26 and 28, May, 2010. The sampling locations are shown in Figure 3.2. To understand the changes in the neonicotinoids in the environment over time, river water was successively collected at St. 2 from 18 May to 5 September, 2010. Osaka City has a population of about 2.6 million and the drinking water source is the Yodo River (St. 2). Rice-producing areas are located upstream of the Yodo River. Grab samples were obtained only when the flow was in the downstream direction. All samples were extracted on the same day.

3.2.3 Sample Extraction

The analytes were extracted from 0.5 L of river water. Oasis HLB plus extraction cartridges (Waters) were used for solid phase extraction. One hundred microliters of methanol containing 0.1 μg of imidacloprid-d_4 were spiked as surrogates before the extraction. Aquatic samples were forced through the cartridges using a Sep-Pak Concentrator (Waters), with the flow rate was adjusted to 20 mL min^{-1}. The analytes were eluted with 5 mL of methanol solution. The composition of the eluent was optimized for the elution of each neonicotinoid and determined to be 80:20 methanol/water. Each eluate was concentrated to 1 mL by evaporation in a water bath at 40 °C under a gentle stream of nitrogen.

3.2.4 LC/MS/MS analysis

An Exactive mass spectrometer (ThermoFisher Scientific Inc., Waltham, MA, USA), with a resolving power of 100,000 was used for detailed study of the ionization of neonicotinoids for ESI, APCI, and APPI. An Agilent 1100 series (Agilent Technologies) HPLC system was used for the chromatography. A wide variety of HPLC columns were investigated during method development. The best retention and resolution were achieved by a TSK-GEL ODS-100V column (15 cm × 2 mm i.d. 3 μm; Tosoh Corp.). The effluent from the column was directly introduced to the LC/MS interface without a postcolumn split. For the chromatography, a gradient of mobile phase A (water) and mobile phase B (methanol) was applied. Both mobile phases contained 2 mM formic acid. The gradient, expressed as change in mobile phase B, was as follows: 0–5 min, a linear increase from 10% to 100% B; 5–10 min, hold at 100% B; 15–20 min, equilibration at 10% B. The flow rate of the mobile phase was 200 μL min^{-1}. The injected volume was 5 μL. An AB Sciex API 2000 tandem triple quadrupole mass spectrometer (AB Sciex) equipped with a photoionization source operated in positive ion mode was used. SRM mode was selected for the quantitation. The working parameters for the APPI source were as follows. The ion transfer voltage was 1200 V. The source temperature was maintained at 400 °C. The gas pressure of the nebulizer and auxiliary gases was adjusted to 40 psi and 80 psi, respectively. The setting of gas in the collision cell was 2. The photoionization lamp was a 10 eV krypton discharge lamp, model PKS 100 (Cathodeon Ltd.). Toluene was selected as a dopant and introduced into the APPI source separately from the LC eluate. The optimal flow rate of toluene was 50 μL min^{-1}.

3.3 Results and Discussions

3.3.1 Ionization of Neonicotinoids

Although protonated molecules were generated in positive-ion ESI as reported in the literature, the protonated molecules generally showed subtle intensity. Other adduct ions such as sodiated molecules were predominant and the intensity ratios of adduct ion/protonated molecule were usually over 10. On the other hand, adduct ions were rarely observed in positive-ion APCI

and APPI. Instead, some smaller ions such as $[M - 43]^+$ were generated, as shown in Figure 3.3 for thiamethoxam. $[M - 43]^+$ was also generated for clothianidin, dinotefuran, and imidacloprid. This result was basically observed with both the Exactive and API 2000 mass spectrometers and was consistent with other observations (*5*). Accurate mass measurements revealed $[M - 43]^+$ to be $[M + H - 2N - O]^+$. Thermal decomposition of nitroguanidine yields N_2O. In addition, the prior elimination of N_2O from nitroguanidine by TG/DSC-MS-FTIR studies has been reported (*12*). Because $[M + H - 2N - O]^+$ became predominant at a higher temperature, a similar reaction of the nitroguanidine-structure would occur in positive-ion APCI and APPI. Elimination of the nitro group in APCI was reported by Bonmatin *et al.* (*6*). In the ionization of dinotefuran with APCI and APPI using the Exactive spectrometer, both $[M + H - N_2O]^+$ and $[M + H - NO_2]^+$ were observed. The relation between the appearance and factors such as temperature and solvent composition, however, is obscure. The definitive SRMs for quantitation are listed in Table 3.1. Among the three ionization techniques, APCI and APPI were superior to ESI with regard to signal intensity and APPI showed particularly low background noise level at most SRM. Signal-to-noise (S/N) values of each neonicotinoid in a standard and an extract are shown in Table 3.2. Consequently, APPI demonstrated the highest sensitivity.

3.3.2 Elution from SPE cartridge

The sorbent of the Oasis HLB is a copolymer composed of styrene, divinylbenzene, and N-vinyl-pyrrolidone. The Oasis HLB adsorbs water-soluble compounds such as neonicotinoids. The elution profile of neonicotinoids from the Oasis HLB plus cartridge was examined. Five hundred milliliters of ultrapure water fortified by 50 ng of each neonicotinoid was loaded onto cartridges, and then analytes were eluted by 5 mL of eluents with a range of water/methanol ratio. Figure 3.4 shows the elution profiles of three replicates. Dinotefuran and nitenpyram were eluted with a relatively low methanol content. These results are consistent with those reported in the literature (*8*). Because the recovery was satisfactory at 80% methanol,

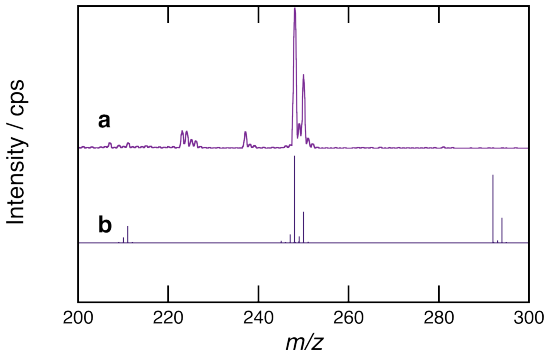

Figure 3.3 Mass spectra of thiamethoxam with (A) API2000 and (B) Exactive. Several ions were observed except $[M + H]^+$. $[M\ \ 43]^+$ was observed in both mass spectrometers. The accurate mass was determined to be 248.0246. The exact mass of $[M + H – 2N – O]^+$ is 248.0255.

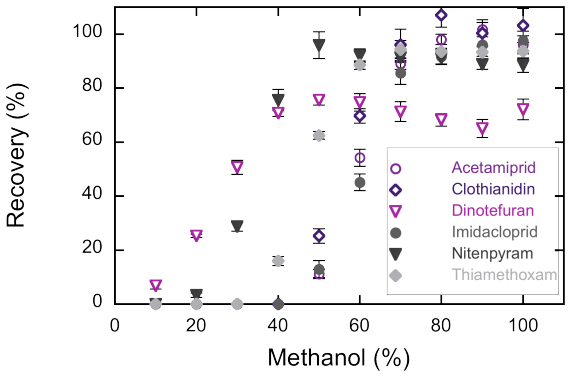

Figure 3.4 Elution profile of neonicotinoids from solid phase extraction cartridge. The symbols are the same as those in Figure 1. Even in low methanol content, dinotefuran and nitenpyram were barely eluted from the cartridge.

Table 3.1 Optimized parameters of ionisation and fragmentation. Two transitions for each compound were acquired.

Compound	Molar mass	SRM	DP[a] / V	CE[b] / V
Acetamiprid	227.7	223.1/125.9 223.1/73.0	41 41	27 71
Clothianidin	249.7	250.0/168.9 250.0/131/9	31 31	19 23
Dinotefuran	202.2	203.1/129.0 203.1/113.0	6 6	19 19
Imidacloprid	255.7	256.1/174.9 256.1/208.9	36 36	29 21
Nitenpyram	270.7	271.1/225.0 273.1/227.0	46 46	17 17
Thiamethoxam	291.7	248.0/174.9 292.0/211.0	31 21	27 21
Imidacloprid-d4	259.7	260.1/213.0 260.1/179.0	31 31	25 29

[a]Declustering potential, [b]Collision energy.

Table 3.2 Signal-to-noise (S/N) values of each neonicotinoid in a standard and an extract.

Compound	Standard solution[a]			Real sample extract[b]		
	ESI	APCI	APPI	ESI	APCI	APPI
Acetamiprid	7.4	8.4	99	3.0	11	31
Clothianidin	2.2	27	11		18	15
Dinotefuran	4.8	5.3	41	3.1	7.1	24
Imidacloprid	1.5	30	59		21	38
Nitenpyram	11	6.5	11	6.7	5.0	5.5
Thiamethoxam[c]	2.8	9.8	56		13	31

[a]The concentration was adjusted to 5 ng mL^{-1}. [b]The extract was fortified with neonicotinoids at 5 ng mL^{-1}. [c]Except for thiamethoxam, same SRMs as APPI were monitored in positive ion mode. SRM of thiamethoxam for ESI and APCI was 292.0 → 210.9.

the eluent composition was set at 80% methanol.

3.3.3 Method Validation

Analyte recoveries from river water were evaluated by simultaneously analyzing fortified and non-fortified river samples obtained at St. 2. The river water was fortified with two levels of neonicotinoids. For each quantitation, 100 ng of imidacloprid-d_4 was added in extracted samples and six-point calibration curves using analytes/imidacloprid-d_4 abundance ratio were prepared in the range from 0.01 to 3. The r^2 values for the regression line were over 0.99. Seven recovery experiments were respectively performed. The method detection limit was determined from the standard deviation of the quantified values for seven replicate measurements. Recovery was estimated from subtraction of quantitative values of unfortified river water samples from fortified ones. The results are summarized in Table 3.3. For low fortified levels, neonicotinoids, except acetamiprid and nitenpyram, were detected in unfortified river samples at nonnegligible concentrations compared with fortified levels, causing rather variable recoveries. Analyte recovery was validated also using fortified ultrapure water (n = 7). The analyte recovery from fortified ultrapure water was not variable.

For nitenpyram, using an absolute calibration method improved the recovery (100%, n = 7, relative standard deviation [RSD] 4.1%) over that using an internal standard method (147%, n = 7, RSD 5.8%). Differences in ionization efficiency, due to structural differences resulting from nitenpyram in nitromethylene neonicotinoid might decrease measurement accuracy when imidacloprid-d_4, nitroguanidine neonicotinoid, is used as the internal standard.

3.3.4 Environmental Level

An example of SRM chromatograms of neonicotinoids in the analysis of a sample collected from St. 2 is shown in Figure 3.5. Detection frequency and concentration of neonicotinoids in the rivers of Osaka City and their estuaries in two sampling rounds are listed in Table 3.4. Degradation of imidacloprid in surface water was relatively rapid (*13*). Photolysis plays an

Table 3.3 Optimized parameters of ionisation and fragmentation. Two transitions for each compound were acquired.

Compound	Fortified level / ng L^{-1}	Recovery[a] (%)	RSD[b] (%)	MDL[c] / ng L^{-1}
Acetamiprid	2	104	13	0.82
	200	99	3.8	
Clothianidin	2	113	9.8	0.62
	200	92	7.0	
Dinotefuran	2	58.9	7.5	0.47
	200	105	5.7	
Imidacloprid	2	134	14	0.88
	200	101	6.2	
Nitenpyram	2	72.4	33	2.1
	200	147	5.8	
Thiamethoxam	2	69.7	10	0.63
	200	117	5.9	

[a]Seven recovery experiments were perfomed. [b]RSD, relative standard deviation. [c]MDL, method detection limit.

Table 3.4 Detection frequency and concentration of neonicotinoids in the rivers of Osaka City and their estuaries. The results of two sampling campaigns are shown: Aug 2009 in the upper rows and May 2010 in the lower row.

Compound	Frequency	Geometric mean / ng L^{-1}	Mimimum / ng L^{-1}	Maximum / ng L^{-1}
Acetamiprid	0/24	–	—	—
	2/21	1.4	nd[a]	1.4
Clothianidin	20/24	3.5	1.0	12
	21/21	2.9	9.4	7.8
Dinotefuran	24/24	30	3.7	100
	21/21	9.9	nd	31
Imidacloprid	16/24	2.5	nd	7
	20/21	8.6	nd	25
Nitenpyram	0/24	–	—	—
	0/21	–	—	—
Thiamethoxam	18/24	1.5	nd	3.2
	21/21	3.8	1.5	11

[a]nd, Not detected.

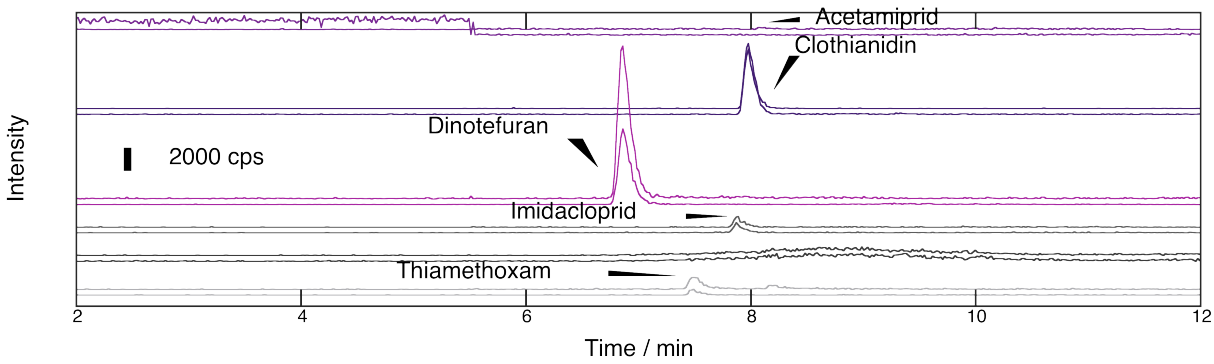

Figure 3.5 Chromatograms from SRM analysis of an aquatic sample at St. 2. To identify each analyte, data from two transitions were collected.

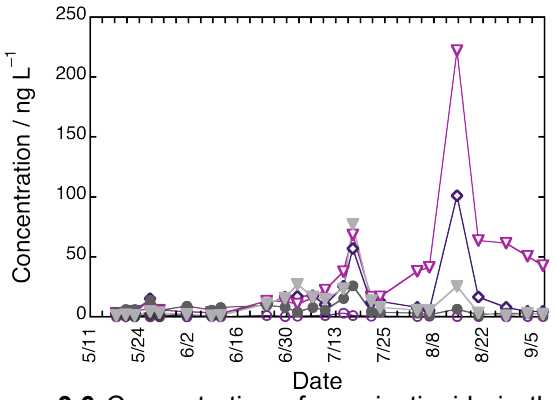

Figure 3.6 Concentration of neonicotinoids in the river water collected at St. 2 from May to September 2010. The symbols are the same as those in Figure 1. The concentration markedly increased since late July.

important role in the degradation of imidacloprid (*14,15*). Nonetheless, neonicotinoids other than nitenpyram were detected in the aquatic environment. Among neonicotinoids examined, dinotefuran was the most frequent and was present in the highest quantities, consistent with its shipment (Figure 3.1). In Japanese wet-paddy rice agriculture, the application of clothianidin, imidacloprid, and thiamethoxam to the nursery box is recommended by the agricultural society. Around Lake Biwa (Figure 3.2), rice planting begins in May. The usage pattern might be reflected in the higher concentration of imidacloprid and thiamethoxam in May. The neonicotinoid concentration profile at St. 2 collected from May to September 2010 is shown in Figure 3.6. Although variations in the concentration at the early sampling rounds were rather subtle, the concentration increased markedly in late July. In Japan, dinotefuran is applied to rice after earwig emergence and it coincides with the period of increase in the concentration of dinotefuran. Although dinotefuran reached a maximum concentration of 220 ng L^{-1}, based on the LD50 values of insects and water creatures (*16–18*), these concentrations do not seem to be an immediate problem. The shipment of dinotefuran around more active rice-producing areas in northeast Japan, however, is more than five-fold the shipment around Osaka. In addition, the concentration detected here is influenced by various factors, such as photodegradation, because the sampling stations were located at the most downstream region of the Yodo River. Investigation of the occurrence of neonicotinoids in the environment should therefore be expanded. Furthermore, metabolites of neonicotinoids have high nicotinic acetylcholine receptor affinity not only in insects but also in mammals (*19,20*). To search for degradation products of neonicotinoids, an LC/high-resolution MS analysis was conducted. Some degradation products and metabolites such as desnitro-imidacloprid and chloronicotinic acid were previously identified elsewhere (*15,21*). Although putative *m/z* values of degradation products extracted from high-resolution MS data, there were no retention peaks corresponding to highly polar degradation products. Because standard reagents of degradation products are not commercially available at this time, these experiments were performed without examination of the extraction of

degradation products from aquatic samples. Further investigations with standards including degradation products are necessary for a more complete understanding of the environmental impact of neonicotinoid pesticides.

3.4 Conclusions

A highly sensitive analytical method of neonicotinoids for aquatic samples was developed. Their ionization in atmospheric pressure ionization was also examined in detail using ultra-high resolution mass spectrometer. Dopant-assisted APPI was found to be sufficiently effective for the determination of neonicotinoid levels in the rivers of Osaka City and their estuaries. The MDLs ranged from 0.47–2.1 ng L^{-1}. The environmental occurrence of neonicotinoids closely reflected their usage trend. Although the maximum concentration reached 220 ng L^{-1}, these concentrations do not seem to be an immediate problem. The method developed in the present study can be used in further investigation at the area where neonicotinoids are abundantly applied.

References

(1) Soloway, S. B.; Henry, A. C.; Kollmeyer, W. D.; Padgett, W. M.; Powell, J. E.; Roman, S. A.; Tieman, C. H.; Corey R. A.; Horne, C. A. *Advances in Pesticide Science,* Part 2, Pergamon Press, Oxford, U.K., **1978**.

(2) Food Safety and Consumer Affairs Bureau, Ministry of Agriculture, Forest, and Fisheries of Japan, *Noyaku Yoran*, Japan Plant Protection Association, Tokyo, Japan, **2009**.

(3) Zhou, Q.; Ding, Y.; Xiao, J. *Anal. Bioanal. Chem.*, **2006**, *385*, (8), 1520-1525.

(4) Guzsvány, V.; Madžgalj, A.; Trebše, P.; Gaál F.; Franko, M. V. *Environ. Chem. Lett.*, **2007**, *5*, (4), 203-208.

(5) Obana, H.; Okihashi, M.; Akutsu, K.; Kitagawa Y.; Hori, S. *J. Agric. Food Chem.*, **2003**, *51*, (9), 2501-2505.

(6) Bonmatin, J. M.; Moineau, I.; Charvet, R.; Fleche, C.; Colin, M. E.; Bengsch, E. R. *Anal. Chem.*, **2003**, *75*, (9), 2027-2033.

(7) Seccia, S.; Fidente, P.; Barbini D. A.; Morrica, P. *Anal. Chimica Acta*,

2005, *553*, (1-2), 21-26.
(8) Rodrigues, A. M.; Ferreira, V.; Cardoso, V. V.; Ferreira E.; Benoliel, M. J. *J. Chromatogr. A*, **2007**, *1150*, (1-2), 267-278.
(9) Liu, S.; Zheng, Z.; Wei, F.; Ren, Y; Gui, W.; Wu H.; Zhu, G. *J. Agric. Food Chem.*, *2010*, *58*, (6), 3271-3278.
(10) Kamel, A. *J. Agric. Food Chem.*, **2010**, *58*, (10), 5926-5931.
(11) Xiao, Z.; Li, X.; Wang, X.; Shen J.; Ding, S. *J. Chromatogr. B*, **2011**, *879*, (1), 117-122.
(12) Li, Y.; Cheng, Y. *J. Therm. Anal. Calorim.*, **2010**, *100*, (2), 949-953.
(13) Sarkar, M. A.; Biswas, P. K.; Roy, S.; Kole, R. K.; Chowdhury, A.*Bull. Environ. Contam. Toxicol.*, **1999**, *63*, (5), 604-609.
(14) Wamhoff H.; Schneider, V. *J. Agric. Food Chem.*, **1999**, *47*, (4), 1730-1734.
(15) Lavine, B. K.; Ding, T.; Jacobs, D. *Anal. Let.*, **2010**, *43*, (10-11), 1812-1821.
(16) Suchail, S.; Guez, D.; Belzunces, L. P. *Environ. Toxicol. Chem.*, **2001**, *20*, (11), 2482-2486.
(17) Iwasa, T.; Motoyama, N.; Ambrose, J. T.; Roe, R. M. *Crop Prot.*, **2004**, *23*, (5), 371-378.
(18) Tisler, T; Jemec, A.; Mozetic, B; Trebse, P. *Chemosphere*, **2009**, *76*, (7), 907-914.
(19) Chao, S. L.; Casida, J. E. *Pestic. Biochem. Physiol.*, **1997**, *58*, (1), 77-88.
(20) Tomizawa, M.; Casida, J. E. *Br. J. Pharmacol.*, **1999**, *127*, (1), 115-122.
(21) Ford, K. A.; Casida, J. E. *Chem. Res. Toxicol.*, **2006**, *19*, (11), 1549-1556.

CHAPTER 4

Occurrence of fluoroquinolones and fluoroquinolone-resistance genes in the aquatic environment

4.1 Introduction

As well as neonicotinoids, functionally-sophisticated substances detected in the environment have gotten a lot of attention. A new category called PPCPs is recently often heard. “PPCPs” is an acronym consisting of the initial letters of pharmaceuticals and personal care products. PPCPs have been identified in the aquatic environments, such as surface water, groundwater, municipal wastewater, and even in drinking water, in several countries (*1–4*). In the European Union, more than 100 PPCPs were detected in the effluents of WWTPs (*5*). PPCPs in the aquatic environment are reported to have originated primarily from effluents of WWTPs and animal excretion (*6,7*).

PPCPs involve various functionally-sophisticated substances. Among different types of PPCPs, antimicrobial agents are mainly used to control bacterial infections in humans and animals, and to increase the growth rate of animals. Antimicrobial agents target bacterial functions or growth processes. Antimicrobial agents and antimicrobial-resistant bacteria have been identified from various environmental sources globally (*8,9*). The extensive use of antimicrobial agents might increase the prevalence of antimicrobial-resistant bacteria in environmental strains as well as in clinical strains. Furthermore, long-term exposure to subtherapeutic antimicrobial agents provides selective pressure, which might change the susceptibility of bacteria to antimicrobial agents even in the environment. Whether antimicrobial agents affect the aquatic ecosystem and microbial communities is therefore of growing concern (*3*). Although many studies have examined antimicrobial resistance in the environment, methodological inconsistency complicates the interpretation of the studies (*10*).

Quinolones comprise a family of synthetic antimicrobial agents. Numerous pathogens now exhibit resistance to quinolones. The lead compound of this group is nalidixic acid (NA), followed by fluoroquinolones (FQs). FQs are extensively used because of their broad spectrum antimicrobial activity. Consequently, FQ-resistant bacteria have increased in clinical strains over the last decade (*11,12*). FQs have two enzyme targets, DNA gyrase and topoisomerase IV. DNA gyrase, the primary target of FQs, consists of two

subunits that are encoded by *gyrA* and *gyrB*. Topoisomerase IV, the secondary target of FQs, also consists of two subunits encoded by *parC* and *parE*. FQ resistance is mostly due to mutations in the quinolone resistance-determining regions (QRDRs), especially *gyrA*. Mutations in these target genes increase the minimum inhibitory concentrations (MICs) of quinolones (*13*). Furthermore, plasmid-mediated quinolone resistance (PMQR) genes were recently identified in clinical strains worldwide (*14–16*). Because resistance genes for synthetic antimicrobial agents are frequently found in the environment, bacteria in the aquatic environment can be a potential reservoir of antimicrobial-resistance genes. In this chapter, the prevalence of FQs and FQ-resistant *Escherichia coli* (*E. coli*) in rivers is discussed. In addition, in order to elucidate the environmental impact of antimicrobial agent contamination in the aquatic environment, the strains isolated from the aquatic environment are characterized.

E. coli, the most common member of the family *Enterobacteriaceae*, is used as an indicator of fecal contamination in water samples. Methodologies for its detection are well-standardized as the genetics and biochemistry of *E. coli* have been extensively studied.

In rivers that receive effluents from WWTPs and flow unstably depending on the tides and floodgate operations, compounds relevant to WWTPs tend to accumulate (*17*). Thus, it is predicted that such rivers are more polluted by antimicrobial agents and antimicrobial resistant bacteria than other rivers.

4.2 Experimental Section

4.2.1 Reagents

Enoxacin (ENX) was purchased from ICN Biochemicals (Cleveland, OH). Ciprofloxacin (CPFX), enfloxacin (ERFX), lomefloxacin (LFLX), and ofloxacin (OFLX) were purchased from Sigma-Aldrich Inc. (St. Louis, MO). Norfloxacin (NRFX) was obtained from Kanto Chemical Co., Inc (Tokyo, Japan). CPFX-d_8 hydrochloride monohydrate and OFLX-d_3 hydrochloride were used as internal standards, and purchased from Sigma-Aldrich. All other chemicals were of residue analysis grade.

4.2.2 Sample Collection

Water samples were collected from 30 sampling sites in Osaka, Japan, in February and August 2010 (Figure 4.1). Samples were collected in 500-mL glass bottles for measurement of FQs and in 200-mL sterilized bottles for detection of bacteria, and then transported to the laboratory within a few hours after sampling. The samples were stored at 4 °C until analysis.

Because rivers sometimes flow backward from the estuary for more than 20 km, grab samples were obtained only when the flow was in the downstream direction. The Yodo River supplies drinking water to approximately 16 million people as a main water source. After confluence around stations (St.) 2 and 3, it does not receive effluents from WWTPs. Sanitation coverage in the Osaka area exceeds 99%, except in part of the southern area. In some areas around the Ishikawa River, sanitation remains inadequate. Frequent alternation between two-way flow and stagnancy occurs at the downstream river and watercourse. The downstream river and watercourse may also be reservoirs of WWTP effluent.

4.2.3 Determination of FQs

4.2.3.1 LC/MS/MS analysis

An Agilent 1100 series (Agilent Technologies) high-performance liquid chromatography system was used. All FQs were separated using an L-column2 ODS analytical column (2.1 × 150 mm, 3 μm; Chemicals Evaluation and Research Institute, Tokyo, Japan). Separation was achieved using a binary elution gradient consisting of water (A) and methanol (B). Both mobile phases A and B contained 2 mM formic acid. The gradient, expressed as changes in mobile phase B, was as follows: 0–5 min, linearly increased from 20 to 100% B; 5–10 min, held at 100% B; 10–15 min, equilibrated at 20% B. The injected volume was 5 μL.

An AB Sciex API 2000 tandem triple quadrupole mass spectrometer (AB Sciex) equipped with a photoionization source operated in the positive ion mode was used. SRM mode was used for the quantitation. In dopant-assisted atmospheric pressure photoionization, the photoionization lamp was a 10 eV Cathodeon Ltd. krypton discharge lamp model PKS 100

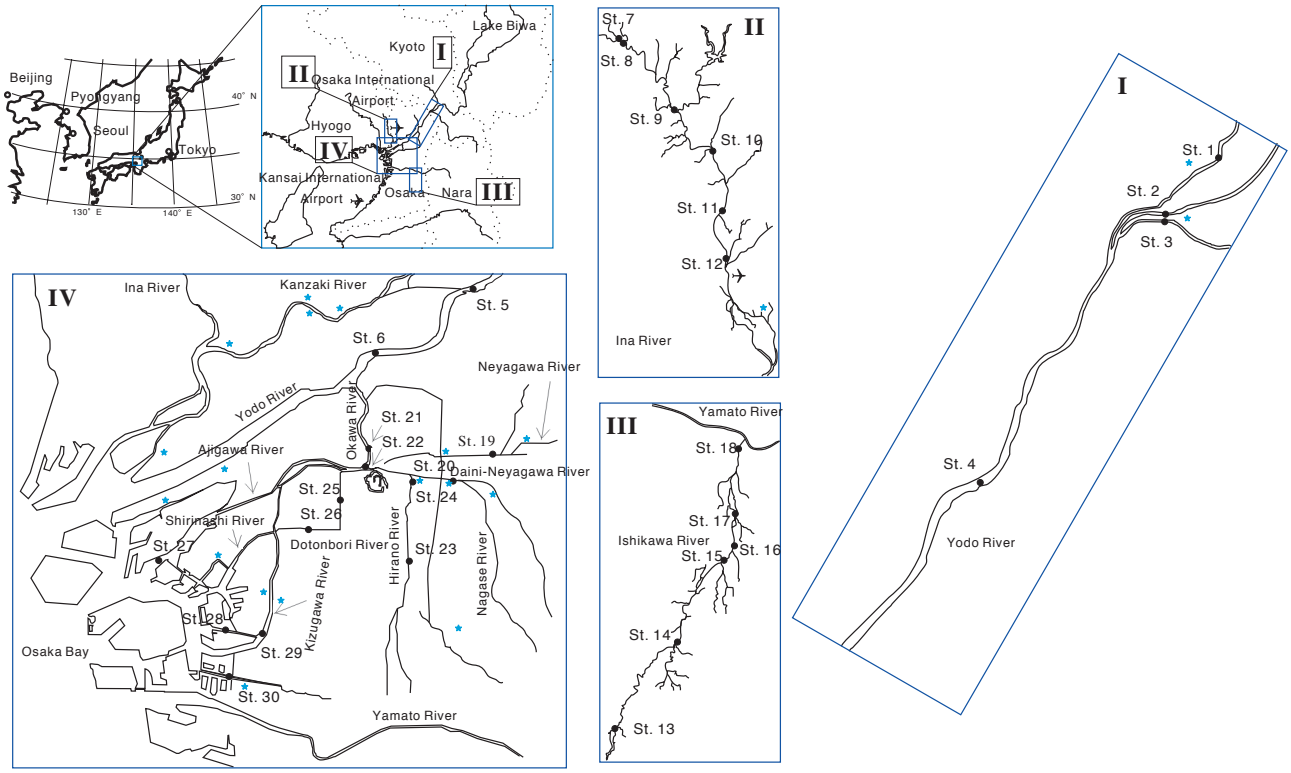

Figure 4.1 Sites of water sampling in Osaka, Japan. Filled stars denote municipal wastewater treatment plants.

and toluene was selected as the dopant. The working parameters for the APPI source were as follows: ion transfer voltage 1200 V; source temperature 350°C; nebulizer and auxiliary gas settings 30 and 80 psi, respectively; gas pressure setting in the collision cell 2; and flow rate of toluene was adjusted to 50 μL min^{-1}. The *m/z* values of SRM and SRM-dependent tuning parameters are listed in Table 4.1.

4.2.3.2 Extraction Procedure

Analytes were extracted from 0.5 L of an aqueous sample, as described by Lee et al. (*18*). Briefly, OASIS WCX plus cartridges (Waters) were preconditioned with 4 mL methanol, followed by 10 mL water adjusted to pH 3. The sample was acidified to pH 3 with 1 N hydrochloric acid solution and spiked by 50 ng of surrogates. Aqueous samples were forced through the cartridges using a Sep-Pak Concentrator (Waters), with the flow rate was adjusted to 20 mL min^{-1}. The cartridges were washed with 100 mL water at pH 3, and then washed with 5 mL methanol, and the wash eluent were discarded. The eluents were 10 mL of methanol/acetonitrile/formic acid (20:75:5, v/v). The eluates were concentrated to 0.5 mL by evaporation under a gentle stream of nitrogen.

4.2.3.3 Quantitation and Method Validation

A multipoint calibration curve for each FQ was obtained using one of two internal standards. One of two internal standards with a retention time closer to each FQ was adopted for quantitation. The effectiveness of WCX cartridges for recovering FQs from fortified river water was also examined. The river water examined was taken from St. 24. The water quality at St. 24 is greatly affected by effluent from WWTPs. The chemical oxygen demand values of this station are around 10 mg L^{-1} throughout the year. The river water was fortified with 50 ng of FQs, resulting in 100 ng L^{-1}. Following elution from the cartridges, ciprofloxacin-d_8 and ofloxacin-d_3 were added to the eluate as internal standards. Five recovery experiments were performed for both fortified and unfortified samples.

Table 4.1 Monitoring reactions and mass-dependent tuning parameters.

	SRM[a]	DP[b] / V	CE[c] / V
ENX	321/232	36	27
	332/231		47
CPFX	332/314	61	27
	332/314		51
ERFX	360/342	46	29
	360/286		47
LFLX	352/334	51	27
	352/249		53
OFLX	362/344	51	31
	362/268		47
NRFX	320/302	51	27
	320/231		53
$CPFXd_8$	340/322	61	27
	340/235		51
$OFLXd_3$	365/347	51	31
	365/271		47

[a]Selective reaction monitoring, [b]Declustering potential, [c]Collision energy.

Table 4.2 a) PCR conditions for QRDR using QIAGEN Multiplex PCR Kit. b) PCR conditions for PMQR using QIAGEN Multiplex PCR Kit. c) PCR conditions for qnrS determinants.

Reaction solution composition			Reaction condition for PCR			
	Composition	Volume / μL^{-1}		Temp. °C	Time	
a	2 × QIAGEN Multiplex Master Mix	12.5	Activation	95	15 min	
	Primers (20 μM each)	2.5	Denaturation	94	30 s	
	Template DNA	1.5	Annealing	60	90 s	30 cycles
	Q-solution	2.5	Extension	72	90 s	
	Sterilized distilled water	6.5	Extension	72	10 min	
	Total	25				
b	2 × QIAGEN Multiplex Master Mix	12.5	Activation	95	15 min	
	Primers (20 μM each)	2.5	Denaturation	94	30 s	
	Template DNA	1.5	Annealing	57	90 s	25 cycles
	Q-solution	2.5	Extension	72	60 s	
	Sterilized distilled water	6.5	Extension	72	10 min	
	Total	25				
c	*Takara Ex Taq* (5unit μL^{-1})	0.2	Activation	95	5 min	
	10 × *Ex Taq* Buffer	12.5	Denaturation	94	30 s	
	Primers (20 μM each)	1.0	Annealing	55	30 s	30 cycles
	Template DNA	1.0	Extension	72	60 s	
	dNTP Mixture (2.5 mM each)	2.0	Extension	72	7 min	
	Sterilized distilled water	8.3				
	Total	25				

4.2.4 Isolation and Identification

4.2.4.1 Isolation of FQ-resistant *E. coli*

Water samples were concentrated by centrifugation and diluted so that 10 to 50 colonies were inoculated on each plate. An aliquot of 100 or 150 μL of sediment was placed on ChromoCult Coliform agar ES (Merck, Darmstadt, Germany), which is a selective agar for *E. coli* and coliforms. In this study, CPFX was used as an indicator for examining FQ-resistance, and FQ-resistant *E. coli* was defined as *E. coli* obtained from agar plates containing CPFX. We added CPFX to agar plates at a concentration of 0.03 μg mL^{-1} to collect the strains showing low susceptibility and resistance to CPFX. The plates were incubated at 37 °C for 1 d. Colonies that were dark-blue to violet in color were selected, in accordance with manufacturer's recommendation. From each plate, one to five suspected colonies were isolated and confirmed to be *E. coli* based on biochemical tests.

4.2.4.2 Antimicrobial Susceptibility Testing

The MICs of isolates to quinolones, including CPFX and NA, were determined using a broth microdilution method with Dry Plate (Eiken Chemical Co., Ltd, Tokyo, Japan) in accordance with the Clinical and Laboratory Standards Institute guidelines (*19*).

4.2.4.3 Polymerase Chain Reaction Amplification of *gyrA*, *gyrB*, *parC,* and *parE* in the QRDR and *qnrS1* Gene

Total DNA used as a template for the polymerase chain reactions (PCR), which were performed using the following protocol. Each colony was suspended into 50 μL Tris-EDTA (TE) buffer and the cells were lysed at 95 °C for 10 min. After centrifugation, the supernatant was used as the DNA template for PCR. PCR of the *gyrA*, *gyrB*, *parC*, and *parE* genes in the QRDR was performed, containing 2×QIAGEN Multiplex PCR Master Mix (QIAGEN Inc., CA), each primer, dH2O, Q-solution, and the extracted DNA. To screen for the presence of PMQR genes, PCR was also performed by multiplex PCR. For PMQR-positive samples, another PCR was performed to determine the genotypes, containing 10× Ex *Taq* Buffer (Takara Bio Inc., Shiga, Japan),

dNTP Mix each primer, dH2O, Ex *Taq*, and the extracted DNA. The PCR protocol and primers used in this study are shown in Tables 4.2 and 4.3, respectively.

4.2.4.4 Sequencing of PCR Products

The PCR products were purified using EXO-SAP treatment (Amersham Biosciences, NJ). Cycle sequencing reactions were performed with The Big Dye Terminator v3.1 Cycle Sequencing kit (Applied Biosystems, CA). Sequencing was performed using an Applied Biosystems 3130 Genetic Analyzer. The nucleotide and derived amino acid sequences were analyzed with GENETYX Mac version 15.0.5 (Genetyx Corporation, Tokyo). DNA sequences were compared with the sequence of *E. coli K12* (GenBank accession numbers: NP_416734 for *gyrA*, YP_026241 for *gyrB*, NP_417491 for *parC,* and NP_417502 for *parE*, respectively). Sequence analysis for the amplicons of the *qnrS* fragment was performed with the BLAST programs, both the blastn and the tblastx algorithms, at the National Center for Biotechnology Information website (http://www.ncbi.nlm.nih.gov/).

4.2.5 Statistical Analysis

The factors affecting the detection probabilities of FQ-resistant *E. coli* were statistically explored using a model selection after checking the multicolinearity of each independent variable. The variance inflation factors (VIFs) were calculated and the independent variable with a larger VIF than 10.0 was removed (*20*). After that, model selection was conducted with the brute force comparison; the model with the smallest Akaike's information criteria (AIC), which is an index of the goodness of model fit (*21*), among all possible models was selected as the optimal model. The full model contained the detection of FQ-resistant *E. coli* as a binomial dependent variable (detected/not detected) and the concentration of FQs, sampling months (February/August), and regional basins as independent variables. The regional basins were categorized as the Yodo River (I in Figure 4.1), Ina River (II), Ishikawa River (III), and Osaka City River (IV). In this analysis, the effects of months and regional basins were random effects that absorbed

Table 4.3 Primers used in this study.

Gene	Primer	Sequence(5' → 3')	Reference
gyrA	gyrA forward gyrA reverse	TACACCGGTCAACATTGAGG TTAATGATTGCCGCCGTCGG	(*46*)
gyrB	gyrB forward gyrB reverse	TGAAATGACCCGCCGTAAAGG GCTGTGATAACGCAGTTTGTCCGGG	
parC	parC forward parC reverse	GTCTGAACTGGGCCTGAATGC AGCAGCTCGGAATATTTCGACAA	
parE	parE forward parE reverse	ATGCGTGCGGCTAAAAAAGTG TCGTCGCTGTCAGGATCGATAC	
qnrA	QnrAm-F QnrAm-R	AGAGGATTTCTCACGCCAGG TGCCAGGCACAGATCTTGAC	(*47*)
qnrS	QnrSm-F QnrSm-R	GCAAGTTCATTGAACAGGGT TCTAAACCGTCGAGTTCGGCG	
qnrB	QnrBm-F QnrBm-R	GGMATHGAAATTCGCCACTG TTTGCYGYYCGCCAGTCGAA	
aac(6')-Ib	aac(6')-Ib-F aac(6')-Ib-R	TTGCGATGCTCTATGAGTGGCTA CTCGAATGCCTGGCGTGTTT	(*48*)
qnrC	qnrCF qnrCR	GGGTTGTACATTTATTGAATCG CACCTACCCATTTATTTTCA	(*16*)
qnrD	qnrD_vl-142F qnrD_vl-508R	AGGAATAGCTTGGAAGGGTGTG CAGCCAAAGACCAATCAAACG	Original
qnrS1	QnrSs_forward QnrSs_reverse	AACCTACMRTCAYACATATCGRCAC TAGTCAGGAWAAACAACAATACCCARYG	This study

Table 4.4 Recovery of fluoroquinolones from water samples spiked with 50 ng of each compound (n = 5).

	Recovery (%)	Fortified sample conc. / ng L^{-1}	Unfortified sample conc. / ng L^{-1}	RSD[a] (%)	LOD[b] / ng L^{-1}
ENX	79	85	6	5.1	1.0
CPFX	67	79	12	4.5	0.6
ERFX	85	96	11	4.1	0.8
LFLX	63	67	4.3	4.7	0.5
OFLX	90	330	240	12	1.5
NRFX	90	102	12	5	1.1

[a]relative standard deviation, [b]limit of detection.

spatial-temporal variance of the response. That is, the full model was the generalized linear mixed model (*22*) because it had the binomial response and random effects. Following the model selection, the Wald test was performed with the selected model to test the significance of each factor. All statistical analyses were conducted with R 2.11.1 (*23*).

4.3 Results and Discussions

4.3.1 Method Performance

The recovery of environmental samples fortified with FQs, corresponding environmental concentrations before fortification, and MQLs are summarized in Table 4.4. MQLs were defined as the concentration with a signal-to-noise ratio (S/N) of 10. Recovery of OFLX was rather variable because the OFLX concentration of unfortified sample exceeded the fortified level. Analyte recovery was validated also using fortified ultrapure water. The analyte recovery from fortified ultrapure water was not variable.

4.3.2 Environmental Levels

Concentrations of FQs for two sampling campaigns in the aquatic environment are presented in Tables 4.5. All FQs were detected in the winter, and the concentrations ranged from 0.1 to 570 ng L^{-1}. On the other hand, only two types of FQs, CPFX and OFLX, were detected in the summer, in coucentrations ranging from 2.0 to 480 ng L^{-1}. CPFX was observed at every sampling station in the winter and at 7 of 30 stations in the summer, although the concentration was low. OFLX was observed at 24 of 30 stations in the winter and at 20 of 30 stations in the summer. To date, OFLX has been extensively studied and frequently observed in aquatic environments. In the Osaka area, however, OFLX as well as CPFX were present throughout the year.

At stations (St. 19–30) in urban rivers located in the vicinity of the WWTPs, the concentration of FQs was comparable to the level of the effluent from WWTPs in other reports (*24–28*). This predisposition was also observed for reproductive hormones (*17*). At stations (St. 13–18) in the Ishikawa River, which flows through land that includes areas with inadequate sewage

Table 4.5 Range of concentrations and mean level (expressed in brackets) detected from rivers and estuaries in Osaka area.

Analyte	Winter		Summer	
	Minimum-maximum concentration / ng L^{-1}	Frequency	Minimum-maximum concentration / ng L^{-1}	Frequency
ENX	nd-23(6.6)	22/30	nd[a]	0/30
CPFX	2.6-37(8.5)	30/30	nd-9.3(4.6)	7/30
ERFX	nd-4.4(1.9)	7/30	nd	0/30
LFLX	nd-3.1(0.5)	14/30	nd	0/30
OFLX	nd-510(70)	24/30	nd-480(76)	20/30
NRFX	nd-33(11)	25/30	nd	0/30

[a]not detected.

systems, a higher concentration of OFLX was observed between St. 13 and 14. On the other hand, at stations (St. 7–12) in the Ina River, which does not receive effluents from WWTPs, the concentrations were very low. At the stations in the Yodo River (St. 1–6), concentrations of FQs were extremely low and remained steady between stations. Because there are only a few livestock facilities in Osaka, the FQs detected in the rivers were attributed mainly to human excretion.

4.3.3 Isolation and Antimicrobial Susceptibility Analysis

A total of 57 FQ-resistant strains were isolated from 24 plates: 15 of 30 samples in the winter and 9 of 30 samples in the summer. The patterns of susceptibility to NA and CPFX for the isolates are shown in Table 4.6. Based on the MIC results, 57 isolates were divided into three groups as follows: Group 1, eight isolates (14.0%) resistant to both NA (MICs, ≥ 128 μg mL^{-1}) and CPFX (MICs, ≥ 4 μg mL^{-1}); Group 2, 43 isolates resistant to NA (MICs, ≥ 32–128 μg mL^{-1}) and low-susceptible to CPFX (MICs, 0.12–1 μg mL^{-1}); and Group 3, 6 isolates low-susceptible to both NA (MICs, 8–16 μg mL^{-1}) and CPFX (MICs, 0.12 μg mL^{-1}). These isolates were obtained mostly from samples collected from the Ishikawa and Osaka City rivers (III and IV in Figure 4.1). In particular, river waters at these stations (St. 14, 18, 22, 26, 30), in which highly resistant *E. coli* (MICs, ≥ 128 μg mL^{-1} [NA], ≥ 4 μg mL^{-1} [CPFX]) was obtained, were considerably influenced by effluents from the WWTPs, because there are many effluent outfalls from WWTPs around these watersheds. In contrast, in the Yodo and Ina rivers (I and II in Figure 4.1), only 3 and 4 isolates were detected, respectively. These data suggest that FQ-resistant *E. coli* are related to the effluent because there are few WWTPs around the Yodo and Ina rivers.

4.3.4 Statistical Analyses

The relationship between the concentration of FQs and FQ-resistant *E. coli* was examined. Because only CPFX and OFLX were detected in our summer sampling campaign, the other FQs were eliminated from the statistical analyses. The VIFs were 2.88 (CPFX concentration) at their

Table 4.6 MIC / μg mL^{-1} for CPFX and NA, and mutations detected in each gene of *E. coli* isolates.

Isolates	MIC μg mL^{-1}		Mutation[a]									
	CPFX	NA	*gyrA*		*parC*		*parE*			*qnrS*		
1002W16	>4	>128	S83L	D87N	S57T	S80I	L416F					Group 1
1008S05	>4	>128	S83L	D87N		S80I		S458A				
1002W21	>4	>128	S83L	D87N		S80I			I464F			
1002W29	>4	>128	S83L	D87N		S80I						
1008S17	>4	>128	S83L	D87N				S458A				
1008S10	>4	>128	S83L	D87N		S80R		S458T				
1002W28	4	>128	S83L	D87N		S80I						
1008S07	4	>128	S83L	D87G		S80I						
1008S22	1	>128	S83L			S80I						Group 2
1008S02	1	>128	S83L			S80R						
1008S04	1	>128	S83L									
1008S06	0.5	>128	S83L					S458A				
1002W19	0.5	>128	S83L				E84G					
1008S01	0.25	>128	S83L									
1008S03	0.25	>128	S83L									
1008S08	0.25	>128	S83L									
1008S12	0.25	>128	S83L									
1008S20	0.25	>128	S83L									
1002W01	0.25	>128	S83L									
1002W04	0.25	>128	S83L									
1002W05	0.25	>128	S83L									
1002W06	0.25	>128	S83L									
1002W12	0.25	>128	S83L									
1002W15	0.25	>128	S83L									
1002W17	0.25	>128	S83L									
1002W18	0.25	>128	S83L									
1002W20	0.25	>128	S83L									
1002W23	0.25	>128	S83L									
1002W35	0.25	>128	S83L									
1002W36	0.25	>128	S83L									
1002W34	0.25	>128	S83W									
1002W30	0.25	>128		D87N								
1002W31	0.25	>128		D87N								
1002W32	0.25	>128		D87N								
1002W33	0.25	>128		D87N								
1002W37	0.25	>128		D87N								
1002W08	0.12	>128	S83L									
1002W13	0.12	>128	S83L									
1002W22	0.12	>128	S83L									
1002W25	0.12	>128	S83L									
1002W27	0.12	>128	S83L									
1008S11	0.12	>128	S83L									
1002W02	0.12	>128		D87N								
1002W24	0.12	>128		D87Y								
1002W07	0.12	128	S83L									
1002W09	0.12	128	S83L									
1008S09	0.12	128		D87G								
1002W11	0.12	128		D87G								
1002W26	0.12	64	S83L									
1002W10	0.12	64		D87N								
1002W14	0.12	32		D87G								
1002W03	0.25	16								qnrS1		Group 3
1008S13	0.25	16								qnrS1		
1008S14	0.25	16								qnrS1		
1008S19	0.25	16								qnrS1		
1008S15	0.25	8								qnrS1		
1008S16	0.25	8								qnrS1		

[a]Substituted amino acids and position number, e.g., S83L indicates substitution of Leucine for Serine at position 83 amino acid. S:Serine, L:Leucine, W:Tryptophan, D:Aspartic acid, N:Asparagine, G:Glycine, Y:Tyrosine,T:Threonine, I:Isoleucine, R:Arfinine, A:Alanine, E:Glutamic acid, L:Leucine, F:Phenylalanine

largest and therefore no independent variable was removed from the analysis. The model selection chose the model that included continual concentrations of CPFX and OFLX as the optimal model. The AICs of full models were 76.98 with continual FQ concentrations and 80.23 with binomial detection of FQs, and that of the optimized model was 73.62. Table 4.7 shows the estimated coefficients of each factor of the selected model and their results in the Wald test. Both coefficients of the CPFX and OFLX concentrations were positive, suggesting that they increased the acquisition of FQ-resistance. The effect of the CPFX concentration, however, was marginal (Wald test, $p = 0.0494$) and that of OFLX and regional basins was not significant ($p > 0.05$). Although the possibility that resistance was acquired in the aquatic environment cannot be ruled out, the effect of the FQ concentration on the acquisition of FQ-resistance was consistently positive, but vague. These tendencies suggest that the relationship between the concentration of FQs and FQ-resistance observed in this study is indirect. That is, resistance might be previously acquired before the *E. coli* and FQs were released in the aquatic environment.

4.3.5 Genetic Analysis

The level of resistance to quinolones generally depends on the number of accumulated mutations in the QRDRs of the *gyrA*, *gyrB*, *parC*, and *parE* genes (*13*). To elucidate the correlation of the phenotype and genotype, all isolates were submitted to amplification and sequencing for QRDRs of the *gyrA*, *gyrB*, *parC*, and *parE* genes.

Among eight isolates belonging to Group 1, all isolates had two mutations in the *gyrA* gene. As for *parC*, one isolate had two mutations, six isolates had single mutations, and one isolate had no mutations. The amino acid changes in these mutations were quite similar to those in previously reported clinical strains (*29,30*). Five isolates that belong to Group 1 have a single mutation also in *parE*. There was one strain that had five mutations in the QRDRs. FQs-resistance was directly connected to these mutations.

Among 43 isolates belonging to Group 2, four isolates had double mutations in *gyrA* and either *parC* or *parE*. Three out of this four isolates

Table 4.7 Estimated coefficients in the selected model and results of the Wald test. Asterisk rep- resent the significance (Wald test, *: p < 0.05, **: p < 0.01).

Factors	Estimate ± SE	*z* value	*p* value
Conc. of CPFX	0.141± 0.072	1.965	0.0494*
Conc. of OFLX	0.008± 0.005	1.442	0.1493
Intercept	–1.369± 0.430	–3.182	0.0015**

[a]not detected.

had a mutation in *parC* and the other had a mutation in *parE*. The remaining 39 isolates had only one mutation in *gyrA*. In Group 3, all strains lacked mutations in the QRDR.

4.3.6. Screening of the prevalence of PMQR determinants

Hopkins et al. (*31*) previously reported that the presence of *qnr* gene increased the MIC of CPFX. To investigate the presence of these genes, additional PCR amplification and sequencing were performed. As a result, all strains belonging to Group 3 retained *qnrS* genes, which were identified as *qnrS1*. The phenotype of these isolates was quite unique and similar to those found in clinical isolates that have *qnrS* (*31,32*).

FQ-resistant *E. coli* was frequently obtained from river water containing FQs, suggesting that the strains isolated from environmental sources were from human waste because the application of FQs to food animals is under very strict control in Japan (*33*) and the stockbreeding activity is very low in the Osaka area compared to the Japanese average (*34*). In the present study, only six kinds of FQs and their resistance genes of *E. coli* were examined. On the other hand, previous reports demonstrated the presence of various resistance genes in bacteria, such as *E. coli*, *Enterobacter spp.*, *Salmonella spp.*, *Aeromonass spp.*, and *K. pneumoniae*, from clinical isolates and mentioned the possibility of a link between human waste and the environment. The PMQR determinants *qnrA*, *qnrB*, *qnrD*, and *qnrS* have been found worldwide (*35*). *qepA*, a PMQR determinant for a quinolone-specific efflux pump, was identified in *E. coli* (*36*) and in *Salmonella spp.* (*37*) from clinical isolates. In addition, PMQR determinants have been also isolated in the environment. *qnrS* was identified from *Aeromonass spp.* in the aquatic environment in France and Switzerland (*38,39*) and even from *E. coli* in waterbirds (*40*). Furthermore, resistance genes have been detected in both humans and the environment. *oqxA*, another PMQR related to efflux pumps, has been detected in animals, workers, and the environment in farms in China (*41*). Thus, various resistance genes have been detected worldwide in both clinical and environmental isolates. Nevertheless, little is known about the relationship

between these isolates.

qnr genes, which facilitate the selection of high-level resistance mutations, were observed in urban rivers, although the presence in clinical isolates is still uncommon in Japan. Importantly, PMQR genes are conjugatively transferable in bacteria.

Jakobsen et al. (*42*) reported the discovery of *aac(3)-II*, the resistance gene for gentamicin in *E. coli*, isolated from both patients and wastewater in Denmark. They concluded that environmental *E. coli* strains should be considered reservoirs of antimicrobial resistance. There is currently no evidence, however, that clearly links environmental strains and clinical strains. Therefore, ongoing monitoring in local areas should be conducted and the origin of antimicrobial resistant genes involved in bacteria in the environment should be traced to prevent the spread of antimicrobial resistance among bacteria.

4.4 Conclusions

The findings of the present study indicate the presence of FQs, FQ-resistant *E. coli*, and FQ-resistant genes in urban rivers. Previous studies demonstrated a high prevalence of PMQRs, mostly in Southeast Asia (*43–45*). Although Yamane et al. (*36*) tested 751 *E. coli* isolated from patients from 2002 to 2006 in Japan, no *qnr* gene was detected. Thus, the prevalence in clinical isolates appears to be low in Japan. Here, however, the *qnrS1* gene was found in six strains of 57 FQ-resistant *E. coli* isolates from water samples. This is the first report of the PMQR determinant *qnrS1* in the aquatic environment.

FQs were detected with high frequency in the samples in which FQ-resistant *E. coli* was also detected. It is highly likely that excessive use of antimicrobial agents has led to an increase in their presence in the aquatic environment and that some bacteria harboring resistance genes also occur in the environment. Furthermore the potential for conjugative transmission of PMQR genes in the environment also remains.

The finding of *qnr* determinants in the aquatic environment highlights the importance of frequent surveys of environmental strains as well as

clinical strains. Further investigation is required to evaluate the spread of resistance genes and to determine the main source of these resistance genes, the extent of the spread of antimicrobial resistance genes and bacteria in the environment.

References

(1) Vieno, N.; Tuhkanen, T; Kronberg, L. *Water Res.,* **2007**, *41*, (5),1001–1012.

(2) Fick, J.; Söderström, H; Lindberg, R. H.; Phan, C; Tysklind, M.; Larsson, D. G. J. *Environ. Toxicol. Chem.*, **2009**, *28*, (12), 2522–2527.

(3) Fernández, C.; González-Doncel, M.; Pro, J.; Carbonell, G.; Tarazona, J. V. *Sci. Total Environ.*, **2010**, *408*, (3), 543–551.

(4) Ferrer, I.; Zweigenbaum, J. A.; Thurman, E. M. *J. Chromatogr. A*, **2010**, *1217*, (36), 5674–5686.

(5) Kümmerer, K. *Pharmaceuticals in the environment: Sources, fate, effects and risks;* Springer: Berlin, Heidelberg, **2001**.

(6) Carballa, M.; Omil, F.; Lema, J. M.; Llompart, M.; García, C.; Rodriguez, I.; Gómez, M.; Ternes, T. *Water Sci. Technol.*, **2005**, *52*, (8), 29–35.

(7) Kümmerer, K. Antibiotics in the aquaticenvironment – A review – Part I. *Chemosphere,* **2009**, *75*, (4), 417–434.

(8) Martinez, J. L. *Environ. Pollut.*, **2009**, *157*, (11), 2893–2902.

(9) Zhang, X. X.; Zhang, T.; Fang, H. H. P. *Appl. Microbiol. Biotechnol.*, **2009**, *82*, (3), 397–414

(10) Allen, H. K.; Donato, J.; Wang, H. H.; Cloud-Hansen, K. A.; Davies, J.; Handelsman, J. *Nat. Rev. Microbiol.*, **2010**, *8*, (4), 251–259.

(11) Hooper, D. C. *Emerg. Infect. Dis.*, **2001**, *7*, (2), 337-341.

(12) Lautenbach, E.; Strom, B. L.; Nachamkin, I.; Bilker, W. B.; Marr, A. M.; Larosa, L. A.; Fishman, N. O. *Clin. Infect. Dis.*, **2004**, *38*, (5), 655–662.

(13) Morgan-Linnell, S. K.; Boyd, L. B.; Steffen, D.; Zechiedrich, L. *Antimicrob. Agents Chemother.*, **2009**, *53*, (1), 235–241.

(14) Wang, M.; Tran, J. H.; Jacoby, G. A.; Zhang, Y.; Wang, F.; Hooper, D. C. *Antimicrob. Agents Chemother.*, **2003**, *47*, (7), 2242–2248.

(15) Robicsek, A.; Jacoby, G. A.; Hooper, D. C. *Lancet Infect. Dis.*, **2006**, *6*,

(10), 629–640.
(16) Kim, H. B.; Park, C. H.; Kim, C. J.; Kim, E. C.; Jacoby, G. A.; Hooper, D. C. *Antimicrob. Agents Chemother.*, **2009**, *53*, (2), 639–645.
(17) Yamamoto, A.; Kakutani, N.; Yamamoto, K.; Kamiura, T.; Miyakoda, H. *Environ. Sci. Technol.*, **2006**, *40*, (13), 4132–4137.
(18) Lee, H. B.; Peart, T. E.; Svoboda, M. L. *J. Chromatogr. A*, **2007**, *1139*, (1), 45–52.
(19) Clinical and Laboratory Standard Institute (CLSI) *Performance standards for antimicrobial disk and dilution susceptibility tests for bacteria isolated from animals: Approved standard. In CLSI document M31-A3. Third edition*; CLSI: Wayne, PA, 2008.
(20) Marquardt, D. *J. Am. Stat. Assoc.*, **1980**, *75*, (368), 87–91.
(21) Akaike, H. *IEEE Trans Automat. Contr.*, **1974**, *19*, (6), 716–23.
(22) McCulloch, C. E.; Neuhaus, J. M. *Generalized linear mixed models. Encyclopedia of Biostatistics. Second edition*; John Wiley & Sons Ltd.: New York, 2005.
(23) R Development Team *A language and environment for statistical computing*; R Foundation for Statistical Computing: Vienna, Austria, 2010.
(24) Batt, A. L.; Bruce, I. B.; Aga, D. S. *Environ. Pollut.*, **2006**, *142*, (2), 295–302.
(25) Vieno, N. M.; Tuhkanen, T.; Kronberg, L. *J. Chromatogr. A*, **2006**, *1134*, (1–2), 101–111.
(26) Spongberg, A. L.; Witter, J. D. *Sci. Total Environ.*, **2008**, *397*, (1–3), 148–157.
(27) Xiao, Y.; Chang, H.; Jia, A.; Hu, J. *J. Chromatogr. A*, **2008**, *1214*, (1–2), 100–108.
(28) Gros, M.; Petrović, M.; Barceló, D. *Anal. Chem.*, **2009**, *81*, (3), 898–912.
(29) Sorlozano, A.; Gutierrez, J.; Jimenez, A.; de Dios Luna, J.; Martínez, J. L. *J. Clin. Microbiol.*, **2007**, *45*, (8), 2740–2742.
(30) Morgan-Linnell, S. K.; Zechiedrich, L. *Antimicrob. Agents Chemother.*, **2007**, *51*, (11), 4205–4208.
(31) Hopkins, K. L.; Day, M.; Threlfall, E. J. *Emerg. Infect. Dis.*, **2008**, *14*, (2), 340–342.

(32) Taguchi, M.; Kawahara, R.; Seto, K.; Inoue, K.; Hayashi, A.; Yamagata, N.; Kamakura, K.; Kashiwagi, E. *Jpn. J. Infect. Dis.*, **2009**, *62*, (4), 312–314.
(33) Ministry of Agriculture, Forestry and Fisheries, Japan. Animal Products Safety Division, Food Safety and Consumer Affair Bureau. *About risk control of fluoroquinolones that apply to cattle and swine*. Letter of Notice dated 25 June, 2012 (in Japanese).
(34) Statistics Bureau, Ministry of Internal Affairs and Communications, Japan. *Statistics of Stockbreeding and Population Survey Report*, 2012 (in Japanese).
(35) Rodríguez-Martínez, J. M.; Cano, M. E.; Velasco, C.; Martínez-Martínez, L.; Pascual, A. *J. Infect. Chemother.*, **2011**, *17*, (2), 149–182.
(36) Yamane, K.; Wachino, J.; Suzuki, S.; Arakawa, Y. *Antimicrob. Agents Chemother.*, **2008**, *52*, (4),1564–1566.
(37) Lunn, A. D.; Fàbrega, A.; Sánchez-Céspedes, J.; Vila, J. *Int. Microbiol.*, **2010**, *13*, (1), 15–20.
(38) Cattoir, V.; Poirel, L.; Aubert, C.; Soussy, C. J.; Nordmann, P. *Emerg. Infect. Dis.*, **2008**, *14*, (2), 231–237.
(39) Picão, R. C.; Poirel, L.; Demarta, A.; Silva, C. S.; Corvaglia, A. R.; Petrini, O.; Nordmann, P. *J. Antimicrob. Chemother.*, **2008**, *62*, (5), 948–950.
(40) Literak, I.; Dolejska, M.; Janoszowska, D.; Hrusakova, J.; Meissner, W.; Rzyska, H.; Bzoma, S.; Cizek, A. *Appl. Environ. Microbiol.*, **2010**, *76*, (24), 8126–8134.
(41) Zhao, J.; Chen, Z.; Chen, S.; Deng, Y.; Liu, Y.; Tian, W.;Huang, X.; Wu, C.; Sun, Y.; Zeng, Z.; Liu, J. H. *Antimicrob. Agents Chemother.*, **2010**, *54*, (10), 4219–4224.
(42) Jakobsen, L.; Sandvang, D.; Hansen, L. H.; Bagger-Skjøt, L.; Westh, H.; Jørgensen, C.; Hansen, D. S.; Pedersen, B. M.; Monnet, D. L.; Frimodt-Møller, N.; Sørensen, S. J.; Hammerum, A. M. *Environ. Int.*, **2008**, *34*, (1), 108–115.
(43) Wu, J. J.; Ko, W. C.; Tsai, S. H.; Yan, J. J. Antimicrob. Agents Chemother., **2007**, *51*, (4), 1223–1227.
(44) Vien, L. T. M.; Baker, S.; Thao, L. T. P.; Tu, L. T. P.; Thuy, C. T.; Nga, T. T. T.; Nguyen, V.M.; Campbell, J. I.; Lam, M. Y.; Nguyen, T. H.; Nguyen, V. V.; Farrar, J.; Schultsz, C. *J. Med. Microbiol.*, **2009**, *58*, (12), 1585–1592.

(45) Zhou, T. L.; Chen, X. J.; Zhou, M. M.; Zhao, Y. J.; Luo, X. H.; Bao, Q. Y. *Jpn. J. Infect. Dis.*, **2011**, *64*, (1), 55–57.
(46) Dutta, S.; Kawamura, Y.; Ezaki, T.; Nair, G. B.; Iida, K.; Yoshida, S. *Antimicrob. Agents Chemother.*, **2005**, *49*, (4), 1660–1661.
(47) Cattoir, V.; Poirel, L.; Rotimi, V.; Soussy, C. J.; Nordmann, P. *J. Antimicrob. Chemother.*, **2007**, *60*, 394–397.
(48) Park, C. H.; Robicsek, A.; Jacoby, G. A.; Sahm, D.; Hooper, D. C. *Antimicrob. Agents Chemother.*, **2005**, *50*, (11), 3953–3955.

CHAPTER 5

Molecular characterization of mycolic acid from the cell wall of *Mycobacterium bovis* BCG substrains by liquid chromatography/dopant-assisted photoionization mass spectrometry

5.1 Introduction

Mycolic acids (MAs) are one of the primary constituents in cell wall of *Mycobacterium* spp. and are high-molar-mass lipids, 2-alkyl and 3-hydroxy fatty acids that can mostly be represented by Figure 5.1. MAs present as several forms that bound to the arabinogalactan of the cell wall and some esters such as trehalose dimycolate as well as a free form. For example, the mycolates make up 34% (by weight) of the cell wall skeleton in *Mycobacterium microti* (*1*). In *M. tuberculosis*, α-, methoxy-, ketoMAs are the main subclasses. In addition, several variants with other oxygen functions (i.e. the dicarboxy-, epoxy-, and ω – 1 methoxymycolates) are included (*2*). Watanebe et al. showed the same species had similar mycolate profiles using ^{1}H-NMR, argentation chromatography, and mass spectrometry (*3,4*). Elucidation of relationship between phenotype and constituents of cell wall as well as differentiation of mycobacteria by analyses of lipids is of great concern. The constituents of the cell wall play an important role in their functions. For example, the presence of glyceropeptidolipids in the cell wall determines the survival of mycobacterium in host macrophages (*5*). To date numerous analytical platforms for MAs have been described. MAs included in Mycobacteria comprise of approximately 80 of carbon atoms and are apolar compounds (*6*). For MA analyses using mass spectrometry, mainly fast atom bombardment (*7*), matrix-assisted laser desorption ionization (*8*), and electron ionization (*9*) have been used. On the other hand, application of mass spectrometry with atmospheric pressure ionization is relatively sparse (*10,11*). APPI is favorable for ionization of compounds that are difficult to ionize with conventional ionization techniques such as ESI and APCI. As to analyses of lipids, Cai et al. evaluated the accuracy and sensitivity in three ionization techniques and demonstrated the benefit of APPI for the quantitative analysis of neutral lipids (*12*). Lipids also include a broad polarity range of compounds, such as polar phosphatidylcholines and sphingomyelins, less polar ceramids, and apolar MAs. The broad applicability of APPI has been noticed particularly in lipidmic analysis coupled with untargeted mass-detection approach (*13*). On the other hand, APPI has been mainly applied to small molecules. In analyses of

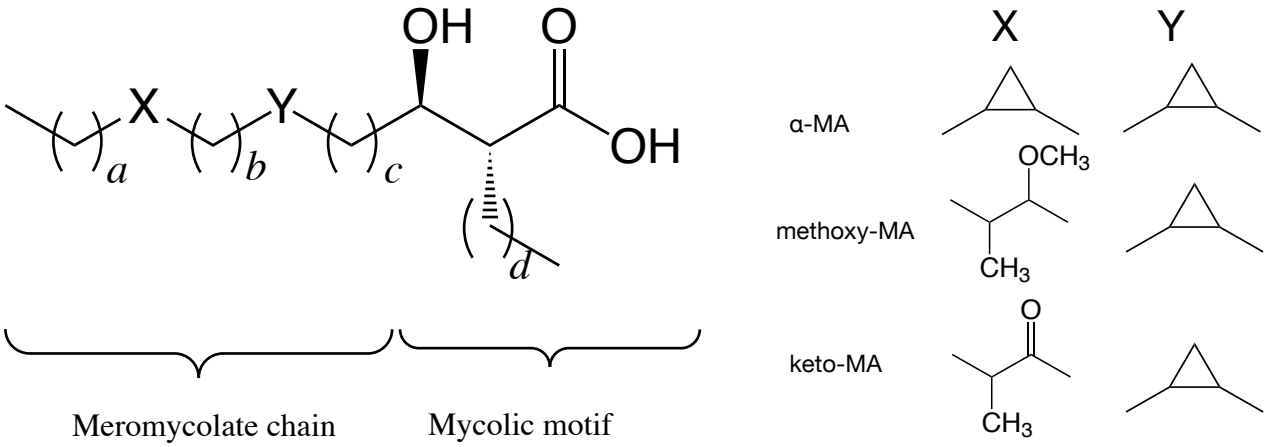

Figure 5.1 General structure of a MA. Methylene chain length varies depending on *a, b, c*, and *d*.

high-molar-mass molecules, an application to synthetic polymers was only reported (*14*). In this chapter, the applicability of APPI in the characterization of high-molar-mass MAs in mycobacteria is examined. Normal phase (NP) LC/MS was used for the chromatographic separation by MA subclasses.

5.2 Experimental Section

5.2.1 Mycolic acid preparation

MA from *M. tuberculosis* (bovine strain) was purchased from Sigma-Aldrich. The MA was used for the examination and optimization of ionization condition.

A reference strain H37Rv of *M. tuberculosis* isolated from different patients of pulmonary tuberculosis were also used in this study. BCG Tokyo 172 subpopulation types I and II were also prepared. They were cultured on Middlebrook 7H10 agar medium (Difco, Detroit, MI, USA) with 0.5% glycerol and 10% Middlebrook oleic acid-albumin-dextrose-catalase enrichment (Difco) at 37 °C for two weeks. MAs were harvested and separated as described previously (*15*). In brief, MAs of each subpopulation were liberated from the bacteria by alkaline hydrolysis using 10% potassium hydroxide in methanol at 90 °C for 2 h followed by extraction with *n*-hexane. After treatment with diazomethane, the methyl ester derivatives of total MAs were separated by thin-layer chromatography (TLC) on Silicagel G (Uniplate; 20 × 20 cm, 250 μm; Analtech, Inc., Newark, DE, USA), which was developed with *n*-hexane-diethyl ether (90:15, v/v; three runs). For each MA subclass, α-, methoxy-, and ketoMA was purified by preparative TLC until a single spot was obtained. Both TLC-separated MAs and mixtures of subclasses were forwarded to LC/MS analysis.

5.2.1 LC/MS/MS analysis

Two kinds of LC/MS were used in the present study. One of the LC/MS consisted of an Agilent 1100 series (Agilent Technologies) high-performance LC and an AB Sciex API 2000 mass spectrometer (AB Sciex). The other consisted of an UltiMate 3000 (Dionex) and an Exactive mass spectrometer

(Thermo Fisher Scientific). MAs were separated using an Inertsil NH_2 analytical column (2.1 × 150 mm, 3 μm; GL Science, Tokyo, Japan). A normal phase mobile phase of *n*-hexane and ethyl acetate (97:3, v/v) was applied to the chromatography. The flow rate was 200 μL min^{-1}. The injected volume was 10 μL. Data acquisition was conducted for 50 min. API 2000 equipped with a PhotoSpray ionization source operated in the positive ion mode was used. The Q1 scan mode at *m/z* ranging from 200 to 1500 was applied. In dopant-assisted APPI, the photoionization lamp was a Cathodeon Ltd. krypton discharge lamp model PKS 100 and toluene was selected as the dopant. The flow rate of dopant was adjusted to 50 μL min^{-1} and dopant was introduced to an exclusive port of PhotoSpray source. The working parameters for the APPI source were as follows: ion transfer voltage 1100 V; nebulizer and auxiliary gas settings 30 and 80 psi, respectively. The source temperature was examined from 250 °C to 500 °C. An Exactive equipped with a PhotoMate light source (Syagen Technology Inc., Santa Ana, CA, USA) operated in the positive ion mode was used. The *m/z* range from 200 to 3000 was acquired with a resolving power of 100 000. The working parameters for the APPI source were as follows: capillary temperature 275 °C; capillary voltage, 60 V; tube lens voltage, 115 V; sheath gas setting, 10; and axially gas setting, 10, respectively. Vaporizer temperature was changed from 200 °C to 450 °C. Dopant of 50 μL min^{-1} was introduced to the LC eluate with a tee connector. APCI sources also applied to both mass spectrometers for the comparison to APPI.

5.3 Results and Discussions

5.3.1 Ion species generated from mycolic acid methyl ester in APPI

The total ion chromatogram of an analysis of purchased MA showed successful separation of each subclass. Main peaks were α-, methoxyl-, and ketoMAs in that elution order. Before these peaks, there were some unidentified peaks with very weak retention by NP-LC. DicarboxyMA was also detected in some mycobacteria at late retention time. Although methoxy- and ketomycolates have sub-subclasses depending on the presence

of the alternative cis-cyclopropane or methyl branched trans-cyclopropane moieties, it is difficult to separate these sub-subclasses by the present NP chromatography (*3,16*). However, it is convenient to explain the APPI mass spectrum of a peak because a lipid subclass elute in the same elution window as a single peak. In the PhotoMate APPI, each peak included numerous ions and some ions had *m/z* values that did not match that of protonated molecules of MA methyl ester. The ion species generated in the PhotoMate APPI were identified by accurate mass observation as $[MeM\text{-}C\mathit{x} + H]^+$, $[MeM\text{-}C\mathit{x} + H - H_2O]^+$, $[MeM\text{-}C\mathit{x} + H - H_2O - CH_2]^+$, $[MeM\text{-}C\mathit{x} + H + 2H_2O - CH_2]^+$, $[MeM\text{-}C\mathit{x} + H + 2H_2O - 2CH_2]^+$, $[MeM\text{-}C\mathit{x} + H + 3H_2O - 2CH_2]^+$, and $[MeM\text{-}C\mathit{x} + H + 4H_2O - 2CH_2]^+$, where MeM-C*x* denotes MA methyl ester that have *x* carbon atoms in its MA moiety. All MAs had broad distribution in their alkyl chain length. In positive-ion APPI, in-source fragmentation such as a dehydration reaction of the protonated molecules is well-known. These kinds of dehydrated ions are identical to those seen in APCI. Gaudin et al. reported the generation of di-dehydrated ions for ceramides and sphingomyelins (*13*). In the present positive-ion APPI, dehydrated and methylene-eliminated ions were found by tetra-dehydrated ions, corresponding to the number of oxygen atoms in the MA molecule. Tetra-dehydrated ions, $[MeM\text{-}C\mathit{x} - 4H_2O - 2CH_2]^+$, was found only in methoxyMA methyl esters. The structure difference of MA methyl ester affected their ionization materially. The ions identified here were consistent with the results of Uenishi et al. (*11*). The intensity and profile of ions were strongly depended on the vaporizer temperature also for APCI. Concerning signal and noise ratio, APPI was superior to APCI. ESI could not ionize both MA methyl ester and underivatized MA, sufficiently. The influence of temperature on intensity and profile in APPI was weaker than that in APCI. In APPI, the dopant doubled the intensity of MA methyl esters. Given that the ionization in APPI is uniform in the homologs of each lipid subclass, the ratio of ion species with same *m/z* value, i.e. $[MeM\text{-}C\mathit{x} + H - H_2O]^+$ and $[MeM\text{-}C\mathit{x}_{+1} + H - H_2O - CH_2]^+$, can be estimated using the composition of protonated molecules. The intensity was drastically changed by source temperature and vaporizer temperature. Both the optimized temperatures

was ranging from 300–400 °C. The intensity at the optimized temperature was two orders more than that at 200 °C. Ion species generated in APPI also were influenced by temperature. At low temperature, protonated molecules were dominant ions in all lipid subclasses at 200 °C. With an increase in temperature, abundance of fragment ions preceded that of the protonated molecules. At 350 °C, where highest intensity was achieved in most observations, $[MeM\text{-}C_x + H - H_2O]^+$ was the most dominant for α-MA methyl ester and $[MeM\text{-}C_x + H - 2H_2O - CH_2]^+$ was the most dominant for methoxy- and ketoMA methyl esters. Higher temperature caused the generation of various in-source fragment ions as well as the high intensity. Consequently, signal redundancy became massive at high temperature. The presence of isotope ions, i.e. the fourth isotope ion of $[MeM\text{-}C_{x+1} + H - H_2O]^+$ that interferes with $[MeM\text{-}C_x + H]^+$ even with a high resolving power of 100 000, makes the annotation of mass spectra cumbersome, as well as the presence of ions with same m/z, $[MeM\text{-}C_{x+1} + H - H_2O - CH_2]^+$ and $[MeM\text{-}C_x + H - H_2O]^+$. In the PhotoSpray APPI, the similar in-source fragmentation to the PhotoMate was observed. The most dominant species were $[MeM\text{-}C_x + H]^+$ for α- and ketoMA methyl ester and $[MeM\text{-}C_x + H + H_2O - CH_2]^+$ for methoxy MA methyl ester. Comparing PhotoMate and PhotoSpray, the ionization of MA methyl esters was very similar to each other, although their architectures were different (*17*). By the intensity and handleability of mass spectra, subsequent examination was conducted at 350 °C.

5.3.2 Comparison between TLC purified and crude samples

The carbon number compositions of each MA methyl ester were compared between two APPI sources. There was no significant difference between two APPI sources. The composition of MAs with and without TLC purification was nearly identical in the isolates of *M. tuberculosis*. On the other hand, critical difference was found particularly in the composition of α-MAs of BCG Tokyo 172. Uenishi et al. reported that α-MAs of BCG Tokyo 172 had two sub-subclasses that consisted of α-MA with two cis-cyclopropane rings and α-MA with one cis-cyclopropane ring and cis-double bond (*18*). In the present study, the composition of one sub-subclass with one

cis-cyclopropane ring and cis-double bond was different by the presence or absence of TLC purification. In some subclasses, there were insufficient chromatographic separation for the purpose of the differentiation by the homolog composition. Further separation techniques prior to APPI such as supercritical fluid chromatography and multi-dimensional chromatography might be promising because these contaminants could interfere with the carbon number composition.

5.3.3 Mycolic acid composition of mycobacteria

The compositions of MAs were substantially different between *M. tuberculosis* and *bovis* BCG. The defect of methoxyMA in M. bovis BCG pasteur were consistent with previous studies (*3,18*). Although the number of homologs could be detected were four or five in the previous studies, NP-LC/APPI-MS could detect up to 10 homologs of each sub-subclass. This demonstrated the superiority of APPI in sensitivity to other techniques. However Naka et al. reported the identical subclass composition in *M. bovis* BCG Tokyo strains (*19*). The composition of subclasses were not completely accorded with other techniques such as densitometry. Each subclass has possibilities to have difference efficiency of ionization in APPI. The method that can normalize the difference in ionization efficiency might be needed in future studies.

References

(1) Davidson, L. A.; Draper, P.; Minnikin. D. E. *J. Gen. Microbiol.*, **1982**, *128*, (4), 823–828.

(2) Minnikin, D. E.; Minnikin, S. M.; Parlett, J. H.; Goodfellow, M.; Magnusson M. *Arch. Microbiol.*, **1984**, *139*, (2–3), 225–231.

(3) Watanabe, M.; Aoyagi, Y.; Ridell, M.; Minnikin. D. E. *Microbiol.*, **2001**, *147*, (7), 1825-1837.

(4) Watanabe, M.; Aoyagi, Y.; Mitome, H.; Fujita, T.; Naoki, H.; Ridell, M.; Minnikin, D. E. *Microbiol.*, **2002**, *148*, (6), 1881-1902.

(5) Fujiwara, N.; Naka, T.; Ogawa, M.; Yamamoto, R.; Ogura, H.; Taniguchi, H. *Tuberculosis*, **2012**, *92*, (2), 187-192.

(6) Kaneda, K.; Naito, S.; Imaizumi, S.; Yano, I.; Mizuno, S.; Tomiyasu, I.; Baba, T.; Kusunose, E.; Kusunose, M. *J. Clin. Micorobiol.*, **1986**, *24*, (6), 1060-1070.
(7) Fujiwara, N.; Jiongwei, P.; Enomoto, E.; Terao, Y.; Honda, T.; Yano I. *FEMS Immunol. Med. Microbiol.*, **1999**, *24*, (2),141-149.
(8) Laval, F.; Lanéelle, M. A.; Deon, C.; Monsarrat, B.; Daffé M. *Anal. Chem.*, **2001**, *73*, (18), 4537-4544.
(9) Batt, R. D.; Hodges, R.; Robertson, J. G. *Biochim. Biophys. Acta.*, **1971**, *239*, (3), 368-373.
(10) Song, S. H.; Park, K. U.; Lee, J. H.; Kim, E. C.; Kim Q., Song, J. *J. Microbiol. Method.*, **2009**, *77*, 165-177.
(11) Uenishi, Y.; Takii, T.; Yano, I.; Sunagawa, M. *J. Microbiol. Method.*, **2009**, *77*, (3), 320-322.
(12) Cai, S. S.; Syage, J. A. *Anal. Chem.*, 2006, 78, (4), 1191-1199.
(13) Gaudin, M.; Imbert, L.; Kibong, D.; Chaminade, P.; Brunelle, A.; Touboul, D.; Laprévote, O. *J. Am. Soc. Mass Spectrom.*, **2012**, *23*, (5), 869-879.
(14) Kéki, S.; Török, J.; Nagy, L.; Zsuga, M. *J. Am. Soc. Mass Spectrom.*, **2008**, *19*, (5), 656-665.
(15) Bhatt, A.; Fujiwara, N.; Bhatt, K.; Gurcha, S. S.; Kremer, L.; Chen, B.; Chan, J.; Porcelli, S. A.; Kobayashi, K.; Besra, G. S.; Jacobs Jr, W. R. *Proc. Natl. Acad. Sci. U.S.A.*, **2007**, *104*, (12), 5157-5162.
(16) Gernaey, A. M.; Minnikin, D. E.; Copley, M. S.; Power, J. J.; Ahmed, A. M. S.; Dixon, R. A.; Roberts, C. A.; Robertson, J. D.; Nolan, J.; Chamberlain, A. *Detecting ancient tuberculosis.* Internet Archaeol. http://intarch.ac.uk/journal/issue5/gernaey_index.html, 1998.
(17) Marchi, I.; Rudaz, S.; Veuthey, J. L. *Talanta*, **2009**, *78*, (1), 1-18.
(18) Uenishi, Y.; Fujita, Y.; Kusunose, N.; Yano, I.; Sunagawa, M. *J. Microbiol. Method.*, 2008, 72, (2), 149-156.
(19) Naka, T.; Maeda, S.; Niki, M.; Ohara, N.; Yamamoto, S.; Yano, I.; Maeyama, J.; Ogura, H.; Kobayashi, K.; Fujiwara, N. *J. Biol. Chem.*, **2011**, *286*, (51), 44153-44161.

CHAPTER 6

Structural Identification of Chemical Components and Biodegradation Products of Highly Fluorinated Products Using Two-dimensional Liquid Chromatography and High-resolution Mass Spectrometry

6.1 Introduction

At the 4th Meeting of the Conference of the Parties of the Stockholm Convention held from 4–8 May 2009, in Geneva, Switzerland, perfluorooctane sulfonic acid (PFOS), its salt, and prefluorooctane sulfonyl fluoride were listed among the Stockholm Convention Annex B substances as persistent organic pollutants (*1*). The historical intentional use of PFOS was widespread and PFOS was found in a wide range of products, such as electric and electronic parts, fire-fighting foam, photo imaging materials, hydraulic fluids, and textiles. PFOS continues to be produced in several countries (*2*). Perfluorooctanoic acid (PFOA) and its salt were also used for a variety of industrial applications and consumer products because of their versatility. Companies concluding the 2010/2015 PFOA Stewardship Program with the US Environmental Protection Agency (USEPA), however, promised to eliminate PFOA by 2015 and have begun to replace PFOA with compounds with a shorter perfluoroalkyl chain than that of PFOA. So far, the analysis of PFOS, PFOA, and their related compounds with different alkyl chain lengths or branched alkyl chains has been attempted, and valuable information regarding the worldwide distribution of these compounds has been retrieved (*3,4*). An understanding of the sources of pollution and the mechanisms of mass transfer, however, requires further investigation, in part because per(poly)fluoroalkyl substances (PFASs) that have a moiety like PFOS or PFOA are present in numerous forms (*5*). Environmental researchers have not yet elucidated the full breadth of their structures. Perfluorinated polymers are one of the most frequent forms of perfluorinated compounds. Perfluorinated polymers comprise not only high-molar-mass compounds such as poly(tetrafluoroethylene) or perfluoroalcoxyalkane, but also relatively small compounds with molar masses of ~2000. Polymerized acrylates and urethanes that have fluorinated alkyl chains at their side chains are often used in textile and leather to protect from staining and water damage (*5,6*). Because the textile industry usually comprises many small- and medium-sized enterprises, public data about the accurate application amounts are limited worldwide. In Japan, one of the few statistics available comes from a fact-finding investigation about production

and import of chemical substances by the Ministry of Economy, Trade, and Industry of Japan. According to the statistics, the domestic production volumes of fluorotelomer acrylate with 2 to 7 carbon atoms in the perfluorinated alkyl chain and fluorotelomer alcohol with 4 to 16 carbon atoms in the perfluorinated alkyl chain used as intermediates of processing of textiles and leather were several hundred tons and several dozen tons in 2007, respectively (*7*). On the other hand, the Telomer Research Program that comprises major fluorochemical manufacturers including Japanese manufacturers reported to the USEPA that the production of telomer-based compounds was over 10 000 tons in 2004 (*8*). No public statistics are available about PFOS-based chemicals in Japan. Although general polymeric acrylate and urethane are persistent, polymers with a low degree of polymerization might be biodegradable. Elucidation of the degradation pathway of these polymers and whether these polymers are broken down to PFOS and PFOA in the natural environment is a challenging task for environmental researchers (*9,10*). Due to the complexity of the polymers and experimental conditions, studies of perfluorinated polymer degradation in the environment remain scarce (*11,12*).

In the past few years, two or multidimensional liquid chromatography has become an attractive method for analyzing complex mixtures. Multidimensional chromatography coupled with MS provides comprehensive analysis and has been applied to the characterization of natural products and industrial materials such as polymers (*13,14*). Although the interpretation of the measurement data is often a laborious task, it can be simplified if the mass spectra of target materials are extracted from complex mass spectra by multidimensional chromatography. In addition, the screening and identification of emerging contaminants by accurate mass determination have attracted attention in the environmental science (*4,15,16*). For organofluorine compounds, the stability of ions and the fragmentation reaction are quite unique. For example, charge migration in the perfluoroalkyl chain should be considered during quantitative analysis using mass labeled internal standards (*17*). To identify the structure of PFASs, it is important to understand MS of organofluorine compounds (*4*).

In this chapter, applicability of a two-dimensional (2D) LC coupled with high-resolution MS (LC/HR-MS) in full-scan mode is discussed for determination of the structure of unfamiliar PFASs that have the potential to degrade into PFOS and PFOA, and elucidation of the biodegradation pathway of such PFASs. Furthermore, through annotation of fragment ions with accurate masses, an overview of the mass spectrometry of PFASs is presented.

6.2 Experimental Section

6.2.1 Materials and Reagents

The fluorinated polymeric materials examined include four fabric stain repellents. Three brands, AsahiGuard (Asahi Glass, Tokyo, Japan), ScotchGard (Sumitomo 3M, Tokyo, Japan), and Unidyne (Daikin, Osaka, Japan) were purchased in Japan. Hereafter, these brands are anonymously referred to as Brand A, B, or C. The companies that participated in the PFOA Stewardship Program with the USEPA are substituting non-bioaccumulative substances for past fluorochemical product lines. Here, Brands A, B, and C were products produced before the substitution (i.e., old products). Brand A' is a substitute from the same manufacturer as Brand A (i.e., a current product). The chemical components of products shown on the product description were as follows: Brand A and A', fluorinated urethane; Brand B, perfluoroalkylethyl acrylate copolymer; Brand C; perfluoroalkyl ethylene oxide adduct. Ammonium bicarbonate was purchased from Sigma-Aldrich (St. Louis, MO, USA). All other chemicals were of residue analysis grade. Abbreviations and suppliers of PFASs examined in this study are listed in Table 6.1.

6.2.2 LC/MS analysis

For quantitative analyses of PFASs that had been frequently analyzed, we used a tandem quadrupole mass spectrometer system, Acquity UPLC/Xevo TQ (Waters), and a headspace gas chromatograph/mass spectrometer, TurboMatrix HS-40 (Perkin Elmer, Norwalk, CT, USA)/GCMS-QP2010 (Shimadzu, Kyoto, Japan). Three analytical methods,

Table 6.1 Abbreviations and related information of PFASs examined in the present study.

Abbreviation	Formula	IUPAC name	CAS #	Supplier
n-PFBA	$C_4HF_7O_2$	2,2,3,3,4,4,4-heptafluorobutanoic acid	375-22-4	Wellington Laboratories
n-PFPeA	$C_5HF_9O_2$	2,2,3,3,4,4,5,5,5-nonafluoropentanoic acid	2706-90-3	Wellington Laboratories
n-PFHxA	$C_6HF_{11}O_2$	2,2,3,3,4,4,5,5,6,6,6-undecafluorohexanoic acid	307-24-4	Wellington Laboratories
n-PFHpA	$C_7HF_{13}O_2$	2,2,3,3,4,4,5,5,6,6,7,7,7-tridecafluoroheptanoic acid	375-85-9	Wellington Laboratories
n-PFOA	$C_8HF_{15}O_2$	2,2,3,3,4,4,5,5,6,6,7,7,8,8,8-pentadecafluorooctanoic acid	335-67-1	Wellington Laboratories
iso-PFOA	$C_8HF_{15}O_2$	2,2,3,3,4,4,5,5,6,7,7,7-dodecafluoro-6-trifluoromethylheptanoic acid	15166-06-0	Wellington Laboratories
n-PFNA	$C_9HF_{17}O_2$	2,2,3,3,4,4,5,5,6,6,7,7,8,8,9,9,9-heptadecafluorononanoic acid	375-95-1	Wellington Laboratories
iso-PFNA	$C_9HF_{17}O_2$	2,2,3,3,4,4,5,5,6,6,7,8,8,8-tetradecafluoro-7-trifluoromethyloctanoic acid	15899-31-7	Wellington Laboratories
n-PFDA	$C_{10}HF_{19}O_2$	2,2,3,3,4,4,5,5,6,6,7,7,8,8,9,9,10,10,10-nonadecafluorodecanoic acid	335-76-2	Wellington Laboratories
n-PFUdA	$C_{11}HF_{21}O_2$	2,2,3,3,4,4,5,5,6,6,7,7,8,8,9,9,10,10,10-Henicosafluoroundecanoic acid	2058-94-8	Wellington Laboratories
n-PFDoA	$C_{12}HF_{23}O_2$	2,2,3,3,4,4,5,5,6,6,7,7,8,8,9,9,10,10,11,11,11-tricosafluorododecanoic acid	307-55-1	Wellington Laboratories
n-PFTrdA	$C_{13}HF_{25}O_2$	2,2,3,3,4,4,5,5,6,6,7,7,8,8,9,9,10,10,11,11,12,12,12-pentacosafluorotridecanoic acid	72629-94-8	Wellington Laboratories
n-PFTedA	$C_{14}HF_{27}O_2$	2,2,3,3,4,4,5,5,6,6,7,7,8,8,9,9,10,10,11,11,12,12,13,13,13-heptacosafluorotetradecanoic acid	376-06-7	Wellington Laboratories
n-PFHxdA	$C_{16}HF_{31}O_2$	2,2,3,3,4,4,5,5,6,6,7,7,8,8,9,9,10,10,11,11,12,12,13,13,14,14,15,15,15-hentriacontafluorohexadecanoic acid	67905-19-5	Wellington Laboratories
n-PFBS	$C_4F_9SO_3H$	1,1,2,2,3,3,4,4,4-nonafluorobutane-1-sulfonic acid	375-73-5	Wellington Laboratories
n-PFHxS	$C_6F_{13}SO_3H$	1,1,2,2,3,3,4,4,5,5,6,6,6-tridecafluorohexane-1-sulfonic acid	355-46-4	Wellington Laboratories
n-PFHpS	$C_7F_{15}SO_3H$	1,1,2,2,3,3,4,4,5,5,6,6,7,7,7-pentadecafluoroheptane-1-sulfonic acid	375-92-8	Wellington Laboratories
n-PFOS	$C_8F_{17}SO_3H$	1,1,2,2,3,3,4,4,5,5,6,6,7,7,8,8,8-heptadecafluorooctane-1-sulfonic acid	1763-23-1	Wellington Laboratories
n-PFDS	$C_{10}F_{21}SO_3H$	1,1,2,2,3,3,4,4,5,5,6,6,7,7,8,8,9,9,10,10,10-henicosafluorodecane-1-sulfonic acid	335-77-3	Wellington Laboratories
n-4:2 FTOH	$C_6H_5F_9O$	3,3,4,4,5,5,6,6,6-nonafluorohexan-1-ol	2043-47-2	Fluorochem Ltd.
n-6:2 FTOH	$C_8H_5F_{13}O$	3,3,4,4,5,5,6,6,7,7,8,8,8-tridecafluorooctan-1-ol	647-42-7	STREM Chemical
n-8:2 FTOH	$C_{10}H_5F_{17}O$	3,3,4,4,5,5,6,6,7,7,8,8,9,9,10,10,10-heptadecafluorodecan-1-ol	648-39-7	MATRIX SCIENTIFIC
n-10:2 FTOH	$C_{12}H_5F_{21}O$	3,3,4,4,5,5,6,6,7,7,8,8,9,9,10,10,11,11,12,12,12-henicosafluorododecan-1-ol	865-86-1	Alfa Aesar
n-6:2FTAcrylate	$C_{11}H_7F_{13}O_2$	3,3,4,4,5,5,6,6,7,7,8,8,8-tridecafluorooctyl prop-2-enoate	17527-29-6	Fluorochem Ltd.
n-6:2FTMetacrylate	$C_{12}H_9F_{13}O_2$	3,3,4,4,5,5,6,6,7,7,8,8,8-tridecafluorooctyl 2-methylprop-2-enoate	2144-53-8	Fluorochem Ltd.

Table 6.1 (continued)

Abbreviation	Formula	IUPAC name	CAS #	Supplier
n-8:2FTAcrylate	$C_{13}H_7F_{17}O_2$	3,3,4,4,5,5,6,6,7,7,8,8,9,9,10,10,10-heptadecafluorodectyl prop-2-enoate	27905-45-9	MATRIX SCIENTIFIC
n-8:2FTMetacrylate	$C_{14}H_9F_{17}O_2$	3,3,4,4,5,5,6,6,7,7,8,8,9,9,10,10,10-heptadecafluorodectyl 2-methylprop-2-enoate	1996-88-9	Fluorochem Ltd.
n-4:2 FTOlefin	$C_6H_3F_9$	3,3,4,4,5,5,6,6,6-nonafluorohex-1-ene	19430-93-4	Alfa Aesar
n-6:2 FTOlefin	$C_8H_3F_{13}$	3,3,4,4,5,5,6,6,7,7,8,8,8-tridecafluorooct-1-ene	25291-17-2	Alfa Aesar
n-8:2 FTOlefin	$C_{10}H_3F_{17}$	3,3,4,4,5,5,6,6,7,7,8,8,9,9,10,10,10-heptadecafluorodec-1-ene	21652-58-4	Alfa Aesar
n-10:2 FTOlefin	$C_{12}H_3F_{21}$	3,3,4,4,5,5,6,6,7,7,8,8,9,9,10,10,11,11,12,12,12-henicosadecafluorododec-1-ene	30389-25-4	Alfa Aesar
n-4:2 FTI	$C_6H_4F_9I$	1,1,1,2,2,3,3,4,4-nonafluoro-6-iodohexane	2043-55-2	Fluorochem Ltd.
n-6:2 FTI	$C_8H_4F_{13}I$	1,1,1,2,2,3,3,4,4,5,5,6,6-tridecafluoro-8-iodooctane	2043-57-4	MATRIX SCIENTIFIC
n-8:2 FTI	$C_{10}H_4F_{17}I$	1,1,1,2,2,3,3,4,4,5,5,6,6,7,7,8,8,8-heptadecafluoro-10-iododecane	2043-53-0	Fluorochem Ltd.
n-PFOI	$C_8F_{17}I$	1,1,1,2,2,3,3,4,4,5,5,6,6,7,7,8,8-heptadecafluoro-8-iodooctane	507-63-1	MATRIX SCIENTIFIC
n-PFDI	$C_{10}F_{21}I$	1,1,1,2,2,3,3,4,4,5,5,6,6,7,7,8,8,9,9,10,10-henicosafluoro-10-iododecane	423-62-1	Fluorochem Ltd.
n-3:3FTA	$C_6H_5F_7O_2$	4,4,5,5,6,6,6-heptafluorohexanoic acid	356-02-5	Wellington Laboratories
n-5:3FTA	$C_8H_5F_{11}O_2$	4,4,5,5,6,6,7,7,8,8,8-undecafluorooctanoic acid	914637-49-3	Wellington Laboratories
n-7:3FTA	$C_{10}H_5F_{15}O_2$	4,4,5,5,6,6,7,7,8,8,9,9,10,10,10-pentadecafluorodecanoic acid	812-70-4	Wellington Laboratories
n-6:2FTA	$C_8H_3F_{13}O_2$	3,3,4,4,5,5,6,6,7,7,8,8,8-tridecafluorooctanoic acid	53826-12-3	Wellington Laboratories
n-8:2FTA	$C_{10}H_3F_{17}O_2$	3,3,4,4,5,5,6,6,7,7,8,8,9,9,10,10,10-heptadecafluorodecanoic acid	27854-31-5	Wellington Laboratories
n-10:2FTA	$C_{12}H_3F_{21}O_2$	3,3,4,4,5,5,6,6,7,7,8,8,9,9,10,10,11,11,12,12,12-henicosafluorododecanoic acid	53826-13-4	Wellington Laboratories
n-6:2FTUA	$C_8H_2F_{12}O_2$	3,4,4,5,5,6,6,7,7,8,8,8-dodecafluorooct-2-enoic acid	70887-88-6	Wellington Laboratories
n-8:2FTUA	$C_{10}H_2F_{16}O_2$	3,4,4,5,5,6,6,7,7,8,8,9,9,10,10,10- hexadecafluorodec-2-enoic acid	70887-84-2	Wellington Laboratories
n-10:2FTUA	$C_{12}H_2F_{20}O_2$	3,4,4,5,5,6,6,7,7,8,8,9,9,10,10,11,11,12,12,12-icosafluorodec-2-enoic acid	70887-94-4	Wellington Laboratories
FOSA	$C_8H_2F_{17}NO_2S$	1,1,2,2,3,3,4,4,5,5,6,6,7,7,8,8,8-heptadecafluorooctane-1-sulfonamide	754-91-6	Wellington Laboratories
N-MeFOSA	$C_9H_4F_{17}NO_2S$	N-methyl-1,1,2,2,3,3,4,4,5,5,6,6,7,7,8,8,8-heptadecafluorooctane-1-sulfonamide	31506-32-8	Wellington Laboratories
N-EtFOSA	$C_{10}H_6F_{17}NO_2S$	N-ethyl-1,1,2,2,3,3,4,4,5,5,6,6,7,7,8,8,8-heptadecafluorooctane-1-sulfonamide	4151-50-2	Wellington Laboratories

Table 6.1 (continued)

Abbreviation	Formula	IUPAC name	CAS #	Supplier
N-EtFOSE	$C_{12}H_{10}F_{17}NO_3S$	N-ethyl-1,1,2,2,3,3,4,4,5,5,6,6,7,7,8,8,8-heptadecafluoro-N-(2-hydroxyethyl)octane-1-sulfonamide	1691-99-2	Wellington Laboratories
N-MeFOSAA	$C_{11}H_6F_{17}NO_4S$	2-[(1,1,2,2,3,3,4,4,5,5,6,6,7,7,8,8,8-heptadecafluorooctylsulfonyl)(methyl)amino]acetic acid	2355-31-9	Wellington Laboratories
N-EtFOSAA	$C_{12}H_8F_{17}NO_4S$	2-[(1,1,2,2,3,3,4,4,5,5,6,6,7,7,8,8,8-heptadecafluorooctylsulfonyl)(ethyl)amino]acetic acid	2991-50-6	Wellington Laboratories
N-MeFBSAA	$C_7H_6F_9NO_4S$	2-[(1,1,2,2,3,3,4,4,4-nonafluorooctylsulfonyl)(methyl)amino]acetic acid	159381-10-9	N/A

Methods I, II, and III, were applied to different PFAS groups. To identify unknown PFASs, we used a system comprising an Ultimate 3000 (Dionex) and an Exactive Orbitrap (Thermo Fisher Scientific) (Method IV). Furthermore, an UPLC/Xevo TQ was used to acquire product ion spectra of unknown compounds that were found by scan analysis with the Exactive Orbitrap mass spectrometer. The detailed analytical conditions are described below.

Method I (PFOS congeners and PFOA congeners)

An Acquity UPLC system and a Xevo TQ mass spectrometer (Waters, Milford, MA, USA) were used for the quantitation of perfluoroalkanoic acids and perfluoroalkyl sulfonic acids. A TSK-Gel ODS-100S (15cm × 2mm i.d. 5 μm, TOSOH, Tokyo, Japan) was used for quantitative analysis. Another ODS-100S was installed before the autosampler to delay elution of the analytes from the LC pump system. The advantage of the column was reported by Flaherty et al. (*18*) The mobile phases A and B consisted of water and methanol including 2 mM ammonium bicarbonate. A gradient was applied to the quantitative analysis. The gradient, expressed as changes in mobile phase B, was as follows: 0 – 5 min, a hold at 10% B; 5 – 10 min, a linear increase from 10% to 100% B; 10 – 15 min, hold at 100% B; 23 – 28 min, equilibration at 10% B. Quantitation was performed using linear congeners of PFOA with the number of carbon atoms in perfluorinated alkyl chain ranging from 4 – 14 and 16, and linear isomeric congeners of PFOS with carbon atoms of 4, 6, 7, 8 and 10, *iso*-PFOA, and *iso*-PFNA (Wellington Laboratories,Guelph, Canada). Internal standard method was adopted in the quantitation. ^{13}C mass labeled standards (4 – 12 carbon atom congeners of *n*-PFOA, *n*-PFHxS and *n*-PFOS) were used as internal standards. Six-point calibration curve (0.15, 0.5, 1.5, 5, 15, 50 ng mL^{-1}) was prepared for each analyte. Another calibration curve for branched congeners was separately prepared because the branched standard reagent included small amount of *n*-PFOA. The SRMs used in this analysis is summarized in Table 6.2. The settings of Xevo TQ were following: ion spray voltage, 3.0 kV; desolvation gas flow, 800 L h^{-1}; desolvation temperature, 400 °C; and collision gas flow, 0.15 mL min^{-1}.

Table 6.2 The settings of mass spectrometers for each PFASs.

	Selected reaction monitoring of native PFASs		Selected reaction monitoring of mass labelled PFASs		
	Q1	Q3	Label	Q1	Q3
n-PFBA	213.1	169.0	1,2,3,4-$^{13}C_4$	217.1	172.0
n-PFPeA	263.0	219.1	1,2,3,4,5-$^{13}C_5$	268.0	223.1
n-PFHxA	313.1 313.1	269.1 119.0	1,2,3,4,6-$^{13}C_5$	318.1 318.1	273.1 120.0
n-PFHpA	363.1 363.1	319.1 119.0	1,2,3,4-$^{13}C_4$	367.1 367.1	322.1 119.0
n-PFOA	413.1 413.1	369.1 169.0	1,2,3,4,5,6,7,8-$^{13}C_8$	421.1 421.1	376.1 172.0
iso-PFOA	413.1 413.1	369.1 169.0		N/A	N/A
n-PFNA	463.1 463.1	419.1 169.0	1,2,3,4,5,6,7,8,9-$^{13}C_9$	472.1 472.1	427.1 172.0
iso-PFNA	463.1 463.1	419.1 169.0		N/A	N/A
n-PFDA	513.2 513.2	469.1 169.0	1,2,3,4,5,6-$^{13}C_6$	519.2 519.2	474.1 169.0
n-PFUdA	563.2 563.2	519.1 169.0	1,2,3,4,5,6,7-$^{13}C_7$	570.2 570.2	525.1 169.0
n-PFDoA	613.1 613.1	569.1 169.0	1,2,-$^{13}C_2$	615.1 615.1	570.1 169.0
n-PFTrdA	663.2 663.2	619.2 169.0		N/A	N/A
n-PFTedA	713.2 713.2	669.2 169.0		N/A	N/A
n-PFBS	299.1 299.1	98.9 79.9		N/A	N/A
n-PFHxS	399.0 399.0	99.0 79.9	1,2,3-$^{13}C_3$	402.0 402.0	99.0 79.9
n-PFHpS	449.1 449.1	99.0 80.0		N/A	N/A
n-PFOS	499.0 499.0	99.0 79.9	1,2,3,4,5,6,7,8-$^{13}C_8$	507.0 507.0	99.0 80.0
n-PFDS	599.2 599.2	99.0 80.0		N/A	N/A
n-3:3 FTA	241.1 241.1	177.1 63.0		N/A	N/A
n-5:3 FTA	341.1 341.1	217.1 237.1		N/A	N/A
n-7:3 FTA	441.1 441.1	337.1 317.1		N/A	N/A
n-6:2 FTA	377.0 293.0	293.0 243.0	1,2-$^{13}C_2$	379.0 379.0	294.0 314.0
n-8:2 FTA	477.0 393.1	393.1 343.0	1,2-$^{13}C_2$	479.0 479.0	394.0 414.0
n-10:2 FTA	577.0 493.0	493.0 443.0	1,2-$^{13}C_2$	579.0 579.0	494.0 514.0
n-6:2 FTUA	357.0 293.0	293.0 243.0		N/A	N/A
n-8:2 FTUA	457.0 393.1	393.1 343.0		N/A	N/A
n-10:2 FTUA	557.0 493.0	493.0 443.0		N/A	N/A

Table 6.2 (continued)

	Selected ion monitoring	
	Primary	Secondary
n-4:2 FTOH	244	263
n-6:2 FTOH	344	363
n-8:2 FTOH	405	463
n-6:2 FTAcrylate	418	327
n-8:2 FTAcrylate	518	427
n-6:2 FTMethacrylate	432	327
n-8:2 FTMethacrylate	532	427
n-4:2 FTOlefin	181	227
n-6:2 FTOlefin	281	327
n-8:2 FTOlefin	381	427
n-10:2 FTOlefin	481	527
n-4:2 FTI	374	227
n-6:2 FTI	474	327
n-8:2 FTI	574	427

Method II (Telomer acid congeners)

An Acquity UPLC system and a Xevo TQ mass spectrometer were used for the quantitation of fluorotelomer acids. A FluoroSep-RP Octyl (15 cm × 2 mm i.d. 3 μm, ES Industries, West Berlin, NJ, USA) was used for quantitative analysis. Another ODS-100S was installed as well as Method I. The mobile phases A and B consisted of 5 mM ammonium formate aqueous solution adjusted at pH 4 by formic acid and methanol. The gradient, expressed as changes in mobile phase B, was as follows: 0 – 5 min, a hold at 77% B; 5 – 8 min, a linear increase from 77% to 85% B; 8 – 12 min, hold at 85% B; 12 - 13 min, a linear increase from 85% to 92% B; 13 - 20 min. hold at 92% B; 20 - 21 min, a linear increase from 92% to 100%, 21 -24 min, hold at 100%, 24 –28 min, equilibration at 77% B. The quantitation was conducted for x:2 saturated telomer acids (*n*-x:2 FTAs), x:2 unsaturated telomer acids (*n*-x:2 FTUAs), and x:3 saturated telomer acids (*n*-[x–3]:3 FTAs), where x = 6, 8, 10. ^{13}C mass labeled *n*-x:2 FTAs were used as internal standards. Four-point calibration curve (15, 50, 150, 500 ng mL^{-1}) was prepared for each analyte. The SRMs monitoring used in this analysis is summarized in Table 6.2. The settings of Xevo TQ was the same as Method I.

Method III (Volatile PFASs)

A headspace gas chromatograph/electron ionization mass spectrometer was used for the quantitation of volatile PFASs. The TurboMatrix HS-40 (PerkinElmer, Norwalk, CT, USA) and GCMS-QP2010 (Shimadzu, Kyoto, Japan) were applied to the headspace GC/MS analysis. One hundred milliliters of liquid samples were diluted in 10-mL purified water, and then 3 g of sodium chloride was added to the samples. HS-40 was set with the following conditions: oven temperature, 60 °C; thermostating time, 30 min; pressurization time, 1 min. GC was performed with a Vocol capillary column (60 m × 0.32 mm, 3 μm; Supelco, Bellefonte, PA, USA). The oven temperature was 40 °C, 2 min, 5 °C min^{-1} to 90 °C, and then 10 °C min^{-1} to 220 °C, 10 min. GCMS-QP2010 was set with the following conditions: helium gas flow, 2.25 mL min^{-1}; ion source temperature, 200 °C; ionization, EI; ionization voltage, 70 eV. Selective ion monitoring used in this analysis is summarized in Table 6.2.

Method IV (Unknown PFASs)

The Ultimate 3000 was applied to both one-dimensional (1D) and off-line 2D chromatography. Off-line 2D chromatography was applied to especially complex samples. The Exactive Orbitrap mass spectrometer, which had a resolving power of 100 000, was used to acquire the HR mass spectra. Samples were analyzed by ESI running in both positive and negative ion modes. To acquire collision induced dissociation spectra, the measurements with collision gas were conducted. In the present study, two reverse phase LC columns were used. One was a TSK-Gel ODS-100S (15 cm × 2 mm i.d., 5 µm, TOSOH). The other was an Epic-FO column (15 cm × 2 mm i.d., 3 µm, ES Industries). For the first chromatography, a gradient of mobile phase A1 (water containing 5 mM ammonium formate and adjusted to pH 4) and mobile phase B1 (methanol) was applied. The gradient, expressed as changes in mobile phase B1, was as follows: 0 – 10 min, a linear increase from 85% to 100% B1; 10 – 16 min, hold at 100% B1; 16 – 20 min, equilibration at 85% B1. The flow rate of the mobile phase was 200 µL min^{-1}. The injected volume was 10 µL. Eluates were collected into vials on the autosampler every 30 s. Ten microliters of each fraction was chromatographed on the second column. The mobile phase for the second chromatography consisted of mobile phase A2 (water) and mobile phase B2 (methanol). Both mobile phases contained 2 mM ammonium bicarbonate. The gradient, expressed as changes in mobile phase B2, was as follows: 0 – 10 min, a linear increase from 80% to 100% B2; 10 – 15 min, hold at 100% B2; 15 – 20 min, equilibration at 80% B2. A schematic diagram of the present 2D chromatography is shown in Figure 6.1. The flow rate of the mobile phase was the same as that in the first chromatography.

6.2.3 Biodegradation test

One hundred microliters of each end-user product were diluted 3000-fold in water. Biodegradability examination was conducted with reference to the Organization of Economic Co-operation and Development (OECD) guideline 301C using a Coulo Meter OM-2000 (Ohkura Electric Instruments, Tokyo, Japan). Briefly, activated sludge was added to 300 mL

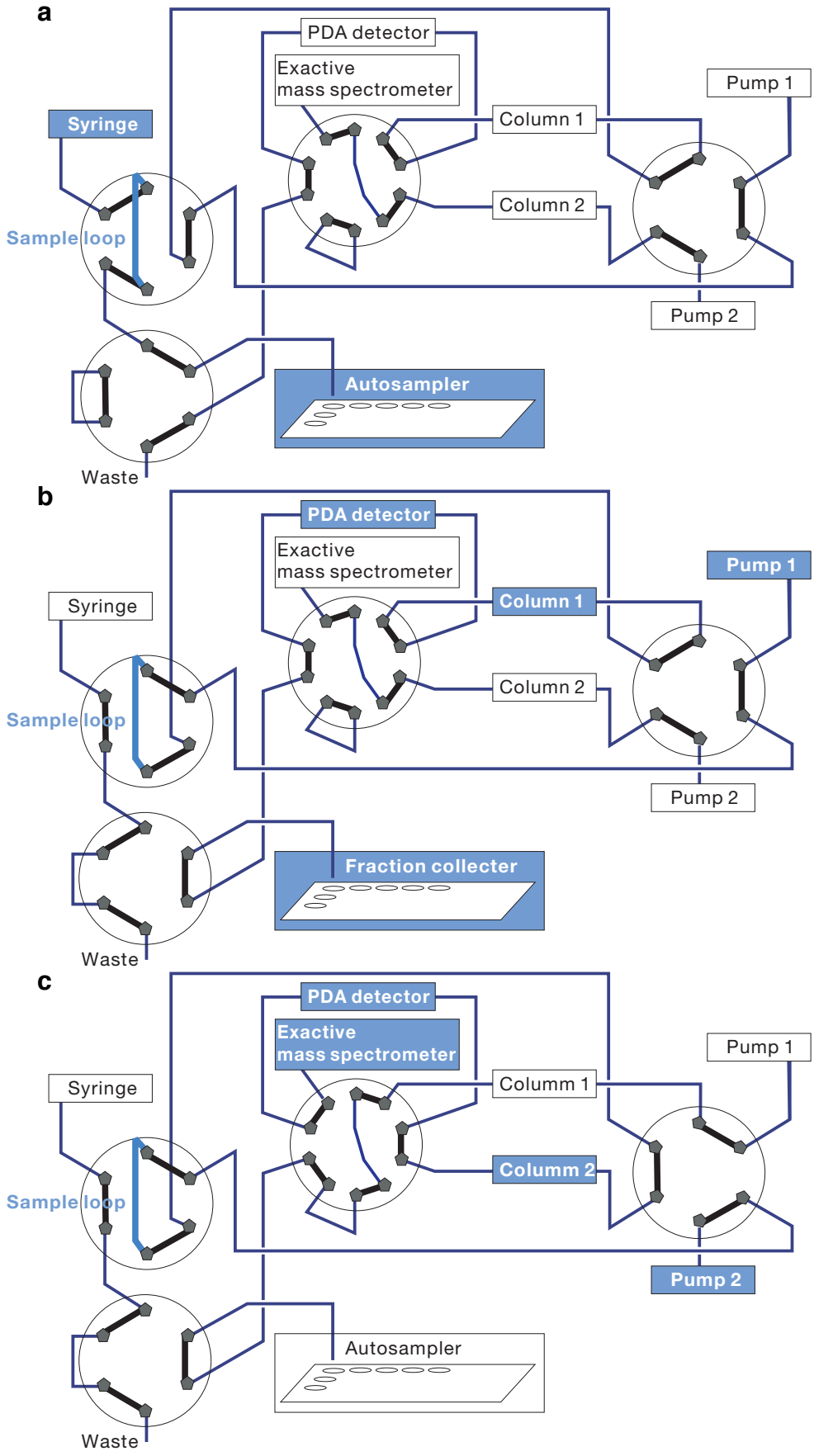

Figure 6.1 Schematic diagram of off-line 2D chromatography used in the present study: a, drawing samples; b, fractionation of eluates from Column 1; c, mass spectrometry of eluates from Column 2. Order of operation: a, b, a, and c.

of the diluted samples at a concentration of 30 ppm. Nutrient salts were also added to the samples. The samples were transferred in an enclosed biochemical oxygen demand meter, which supplied oxygen for aerobic biodegradation. A schematic representation is shown in Figure 6.2. The stirred samples were examined for a period of 28 d in a darkened, enclosed biochemical oxygen demand meter at 25 ± 1 °C. No chemical-specific analyses are prescribed in the OECD guideline. Instead, 10-mL portions of samples were withdrawn from each stirred sample once a week for chemical analyses. To extract PFASs, the portions were passed through solid-phase extraction cartridges, OASIS WAX (Waters). PFASs were eluted from the cartridges with 5 mL of 0.1% ammonia methanol. The eluates were analyzed by two LC/MS systems. After the biodegradation test, the vessel walls were washed with 5 mL of methanol. The washings were also analyzed by LC/MS.

6.3 Results and Discussions

6.3.1 Quantitation of PFASs by target analyses

Quantitative results of each end-user product by headspace GC/MS and LC/MS are summarized in Table 6.3. In this quantitation, we used selective analyses such as SIM and SRM. Few In Brand A, among targeted PFASs, the concentration of PFOS was highest, but only 11 μg mL^{-1}. In Brand A', only PFBS was detected. This finding seems to reflect the current situation in which many fluorochemical manufacturers have substituted compounds with a shorter perfluoroalkyl chain for legacy PFASs. In Brand B before the substitution, reaction intermediate products, such as telomer iodides and alcohols generated in each step of telomerization, were detected at high concentrations. The series of chemicals detected in Brand B showed an even-number-oriented polydispersity in the number of carbon atoms of their perfluoroalkyl chains with eight carbon atoms at its center. On the other hand, various PFASs were detected in Brand C. *iso*-PFOA and *iso*-PFNA were identified by authentic branched standards in Brand C and the retention time of their congeners did not match that of authentic standards of straight chain isomers. Straight chain isomers were not detected in Brand C. Authentic standards of branched isomers are commercially available only

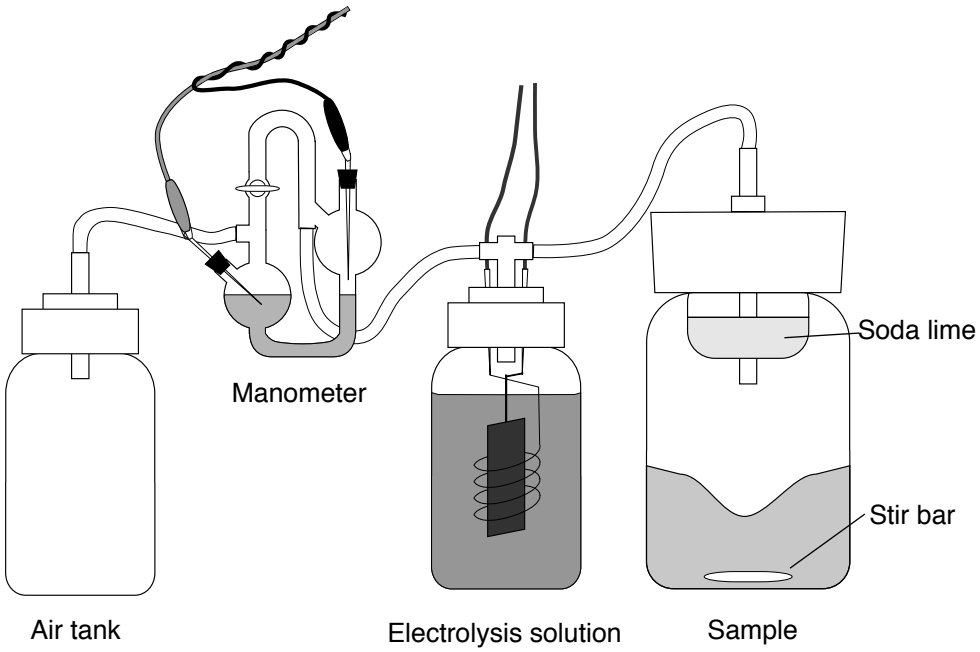

Figure 6.2 Schematic representation of the instrument used in the present biodegradation test. Carbon dioxide generated from biodegradation is adsorbed by soda lime. When the manometer detects a pressure drop, oxygen is generated by controlled-potential electrolysis.

Table 6.3 Concentration of PFCs included in each end-user product.

	Concentration / μg mL^{-1}				Analytical method
	Brand A	Brand A'	Brand B	Brand C	
n-PFBA	1.6	<0.37	1.5	0.75	Method I
n-PFPeA	1.1	<0.13	0.29	<0.13	Method I
n-PFHxA	8.4	<0.22	6.3	<0.22	Method I
n-PFHpA	1.6	<0.58	1.0	<0.58	Method I
n-PFOA	4.0	<0.55	8.7	<0.55	Method I
iso-PFOA	<0.11	<0.11	<0.11	330	Method I
n-PFNA	<0.53	<0.53	0.58	<0.53	Method I
iso-PFNA	<0.10	<0.10	<0.10	3200	Method I
n-PFDA	<0.27	<0.27	4.6	<0.27	Method I
n-PFUdA	<0.2	<0.2	<0.2	<0.2	Method I
n-PFDoA	<0.15	<0.15	1.7	<0.15	Method I
n-PFTrdA	<0.15	<0.15	<0.15	<0.15	Method I
n-PFTedA	<0.27	<0.27	1.1	<0.27	Method I
n-PFBS	<0.18	0.36	<0.18	<0.18	Method I
n-PFHxS	<0.4	<0.4	<0.4	<0.4	Method I
n-PFHpS	<0.4	<0.4	<0.4	<0.4	Method I
n-PFOS	11	<0.87	<0.87	<0.87	Method I
n-PFDS	<0.35	<0.35	<0.35	<0.35	Method I
n-4:2 FTOH	<0.3	<0.3	<0.3	<0.3	Method III
n-6:2 FTOH	<0.3	<0.3	4.5	<0.3	Method III
n-8:2 FTOH	<3	<3	130	<3	Method III
n-6:2 FTAcrylate	<0.04	<0.04	<0.04	<0.04	Method III
n-8:2 FTAcrylate	<1.5	<1.5	45	<1.5	Method III
n-6:2 FTMethacrylate	<0.02	<0.02	<0.02	<0.02	Method III
n-8:2 FTMethacrylate	<20	<20	<20	<20	Method III
n-4:2 FTOlefin	<0.02	<0.02	<0.02	<0.02	Method III
n-6:2 FTOlefin	<0.3	<0.3	<0.3	<0.3	Method III
n-8:2 FTOlefin	<0.1	<0.1	300	<0.1	Method III
n-10:2 FTOlefin	<4	<4	110	<4	Method III
n-4:2 FTI	<0.002	<0.002	<0.002	<0.002	Method III
n-6:2 FTI	<0.003	<0.003	0.2	<0.003	Method III
n-8:2 FTI	<0.03	<0.03	22	<0.03	Method III

for perfluorooctyl and perfluorononyl compounds (i.e. *iso*-PFOA and *iso*-PFNA). Quantitation of octyl and nonyl congeners was successfully performed using these authentic branched isomers. Although only comparison of peak area was demonstrated, the series of chemicals detected in Brand C seemed to show an odd-number-oriented polydispersity in the number of carbon atoms of their perfluoroalkyl chains with nine carbon atoms at its center.

6.3.2 Accurate mass analysis of Brand A

The analytical results of Brand A using HR-MS in negative-ion ESI are shown in Figure 6.3. Several series of ions with a constant *m/z* interval of 49.9970 were present. These intervals correspond to CF_2, and the *m/z* values of the ions with the highest intensity among each series were 718.0684, 804.1052, and 1315.0584. Even with an HR of 100 000, the number of candidate chemical formulas was over 100 when the chemical formulas were estimated only from these accurate masses. Although the isotope patterns were helpful for reducing the number of candidates, a possible chemical formula could not be unambiguously identified. The product ion spectra obtained by the Xevo TQ showed that these ions fragmented into ions with *m/z* values of 419 and 526. The HR mass spectrum also included these ions, 418.9737 and 525.9778. Based on an accurate mass of 418.9734, the chemical formula, C_8F_{17} could be determined with a mass error of 0.0003. If the ion of 526 includes a perfluorooctyl group, the remaining group has a mass of 107.004. This group was determined to be $C_2H_5O_2NS$. Therefore, this ion was considered to be an *N*-ethyl prefluorooctane sulfonamide anion. The extracted ion chromatograms of 525.9778 are shown in Figure 6.4 and indicate the presence of compounds that have similar structures. Moieties that remain following the removal of the *N*-ethyl prefluorooctane sulfonamide anions from 718.0684 and 804.1052 had *m/z* values of 192.0906 and 278.1274, respectively. The formulas of these moieties were determined to be $C_{10}H_{12}O_2N_2$ and $C_{14}H_{18}O_4N_2$. These structures were considered to comprise a heteroatom bond, such as an ester, amido, or urethane bond, because these formulas included many oxygen and nitrogen atoms. Urethane

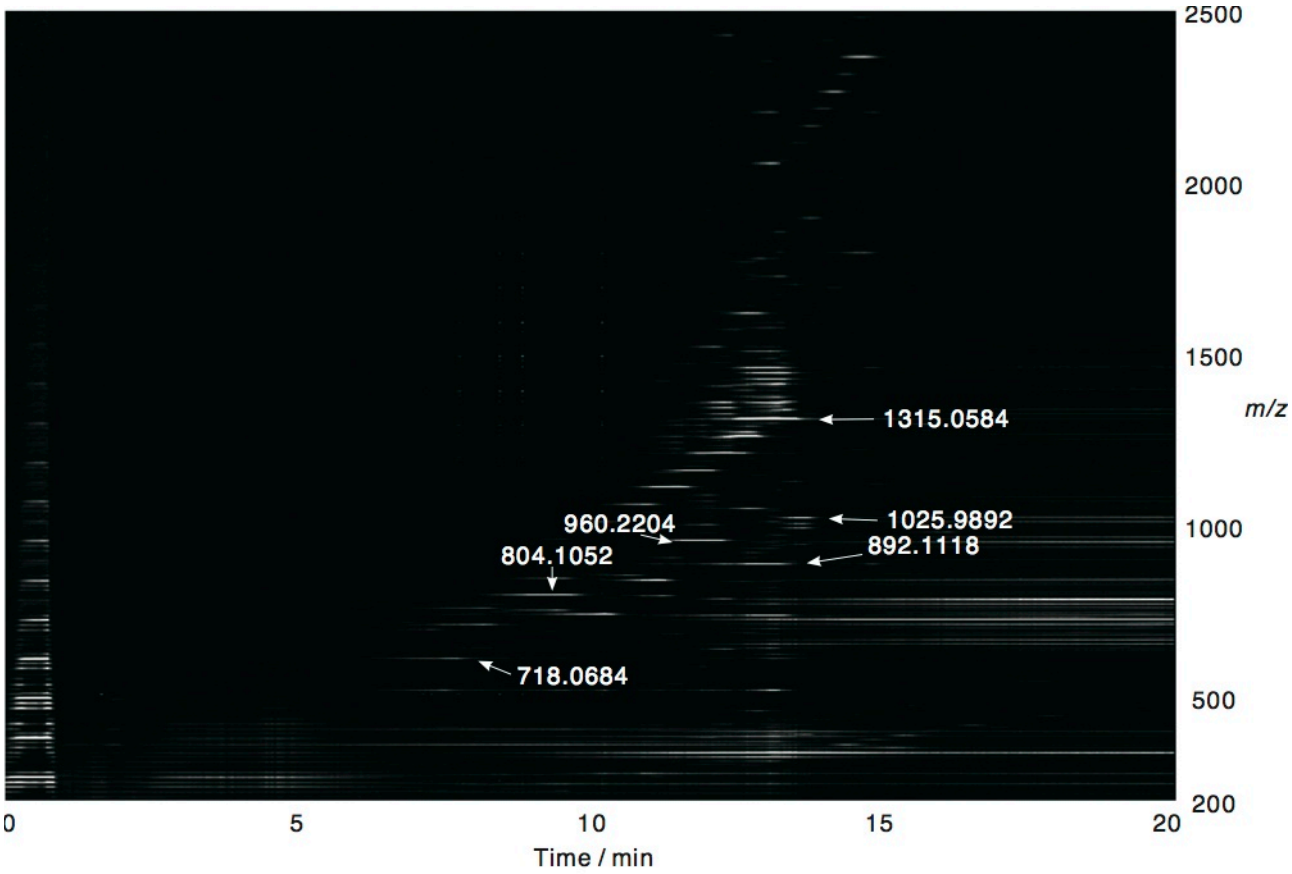

Figure 6.3 Mass spectrum observation of Brand A using LC/MS running in negative-ion ESI. Horizontal axis denotes retention time and vertical axis denotes *m/z*. Bright dots indicate the presence of ions. The *m/z* values of ions that accompany a series of ions with a constant m/z interval of 49.997 are shown in the figure.

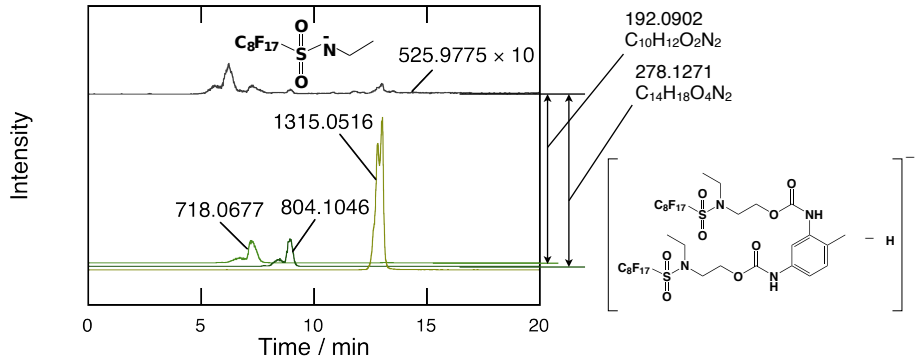

Figure 6.4 Extracted ion chromatograms of the analysis of Brand A. Extracted accurate masses are shown in the figure. The chromatogram of 525.9774 is magnified 10 times. Chemical formulas estimated from the difference of accurate masses are shown in the margin. The structure of the most abundant ion is also shown in the margin.

bonds are usually generated by the reaction of isocyanate and alcohol. In the manufacture of polyurethane, methylene diphenyl diisocyanate and toluylene diisocyanate are the most common isocyanate (*19*). When toluylene diisocyanate reacts with *N*-ethyl perfluorooctane sulfonamide ethanol (*N*-EtFOSE), the product will likely have the structure shown in Figure 6.4. If this compound generates monovalent deprotonated molecules in negative-ion ESI, the exact mass of the ion would be 1315.0576. The ion detected in the Exactive Orbitrap mass spectrometer had an *m/z* of 1315.0584. Given that the perfluorooctyl chains were generated by electrochemical fluorination, the occurrence of ions with a constant interval *m/z* of 49.997 is consistent. In addition, positive-ion ESI observation also showed the presence of the protonated molecule. Moreover, a urethane with two perfluorooctyl groups is common in lubricants (*5*). Therefore, the structure included in Brand A was a fluorinated urethane compound with two perfluoroalkyl chains. The ions with masses of 718.0677 and 804.1045 were considered to be impurities with a single perfluorooctyl chain. The procedure that subsequently determines the whole structure from partial structures is helpful for identifying unknown compounds.

6.3.3 Accurate mass analysis of Brand A'

The analytical result of 1D-LC/HRMS in negative-ion ESI using an ODS column is shown in Figure 6.5. None of the ions of Brand A' had an *m/z* interval of 49.997, unlike in Brand A. The most abundant ion had an *m/z* of 1574.2809. It was difficult to identify the structures of prominent ions because these ions accompanied numerous other ions with the separation of 1D-LC. In addition, because these ions seemed to comprise various ion species, such as deprotonated molecules, adduct ions, and fragment ions, it was hard to distinguish them from each other by 1D-LC. Therefore 2D-LC separation was conducted, and the number of accompanying ions in the same retention time as the most abundant ion decreased. It was believed that this ion was $[M - H]^-$ because the corresponding $[M + H]^+$ was detected in positive-ion ESI at 1576.2854. The negative-ion mass spectra of the fraction, including the most abundant ion with and without collision gas, are shown in

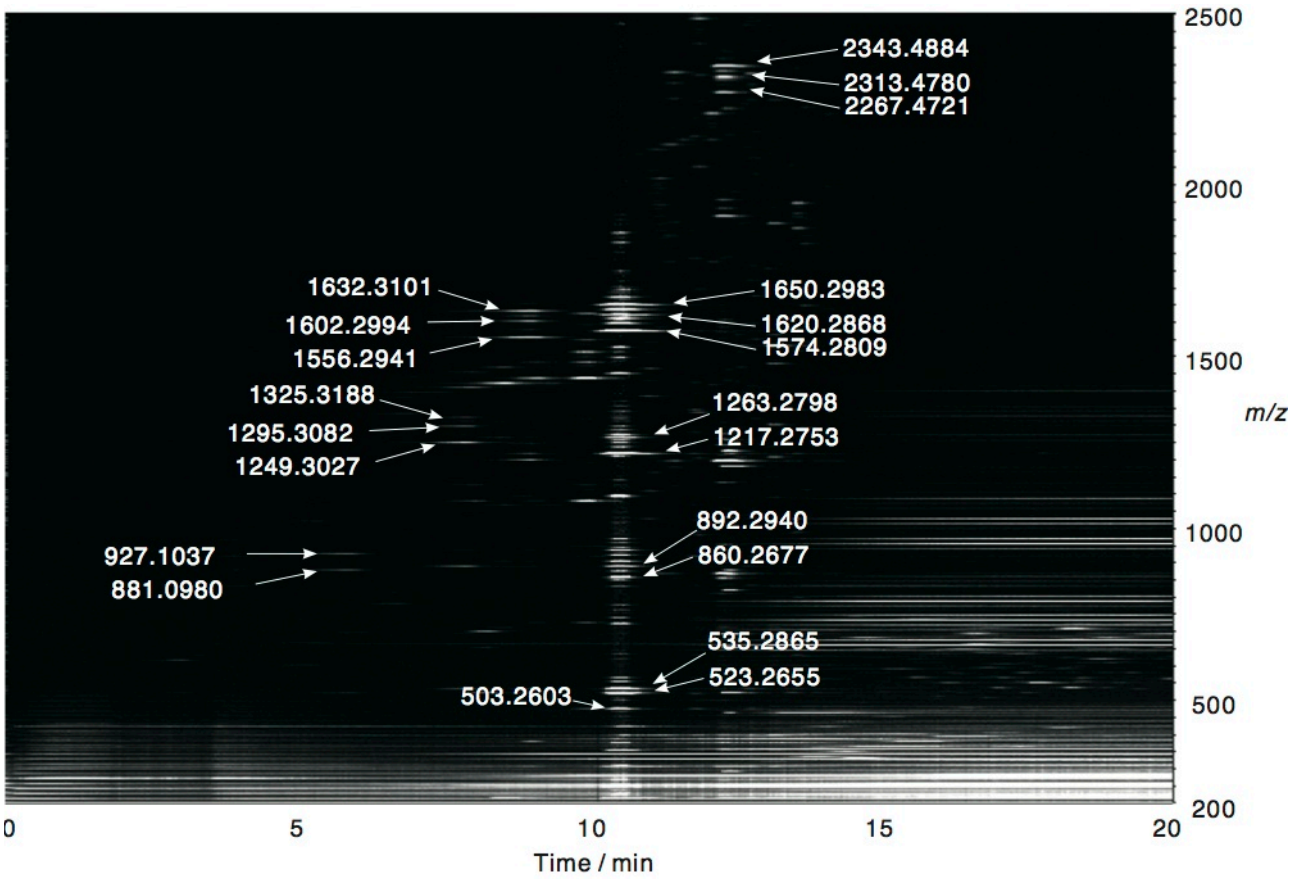

Figure 6.5 Mass spectrum observation of Brand A' using LC/MS running in negative-ion ESI. There are no ions with a constant interval of 49.997. The *m/z* values of characteristic ions are shown in the figure.

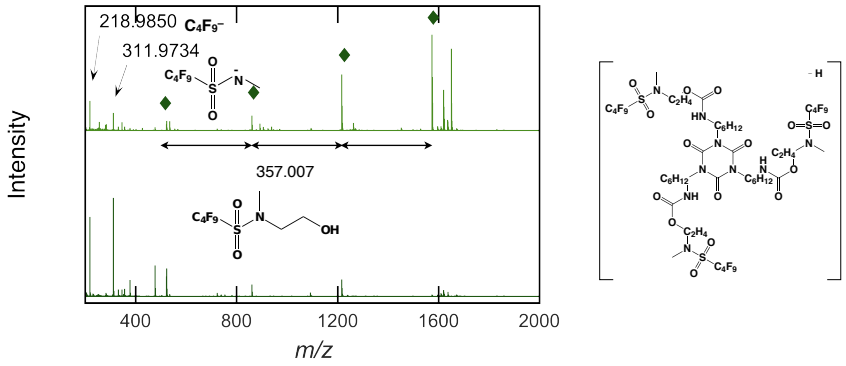

Figure 6.6 Mass spectra of the fraction including the most abundant ion. Upper spectrum was acquired without collision gas. Lower spectrum was acquired with collision gas. Ion marked by the filled diamond appeared at constant *m/z* intervals of 357.007. Structures are also shown in the figure.

Figure 6.6. In the mass spectrum with collision gas, two ions, 218.9850 and 311.9734, were abundantly observed. If a similar urethane structure to Brand A was used in Brand A', 218.9850 and 311.9734 were considered to be the nonafluorobutyl group C_4F_9, and the *N*-methyl-nonafluorobutane sulfonamide group, i.e. $C_4F_9SO_2NCH_3$, respectively. In addition, three ions with a constant *m/z* interval of 357.007 were observed. If this interval included the *N*-methyl-nonafluorobutane sulfonamide group, this interval would indicate that *N*-methyl-nonafluorobutane sulfonamide ethanol was present because the residual moiety was estimated from the residual mass of 45.0336 to be C_2H_5O. It appeared that the original ion had three such moieties. In addition, hexamethylene diisocyanate trimer is commonly applied in urethane coatings. Given that the original molecule was generated by *N*-methyl-nonafluorobutane sulfonamide ethanol and a trimer of hexamethylenediisocyanate, the structure will be the compound shown in Figure 6.6. The exact *m/z* value of the deprotonated molecule of this structure is 1574.2867 and coincided with the accurate *m/z* value. The identified structure was consistent with the manufacturer's statements that longer perfluorinated alkyl chains are not used in the current product line.

6.3.4 Accurate mass analysis of Brand B

Negative-ion ESI HR-MS with 1D-LC of Brand B showed the presence of four series of ions with a constant interval of *m/z* 99.994 (Figure 6.7). This value corresponds to C_2F_4. One of the series was identified as telomer alcohols by authentic standards. Under the present measurement conditions, we observed telomer alcohol congeners with even-numbered carbon atoms, corresponding to perfluoroalkyl chains, up to 16. That is, we observed $C_{2n}F_{4n+1}C_2H_4O^-$, where n = 3–8. Each congener accompanied ions with intervals corresponding to hydrogen fluoride of *m/z* 20.006 and CH_2O of 30.010. In addition, CO_2 adduct ions were found in both the Exactive Orbitrap and XevoTQ mass spectrometers. At a high pH and in the presence of dissolved CO_2, the formation of CO_2 adducts by various compounds having amino groups is common. Terrier and Douglas showed adduct formation with CO_2 of amino acids in ESI (*20*). Furthermore, Kumar et al. reported the

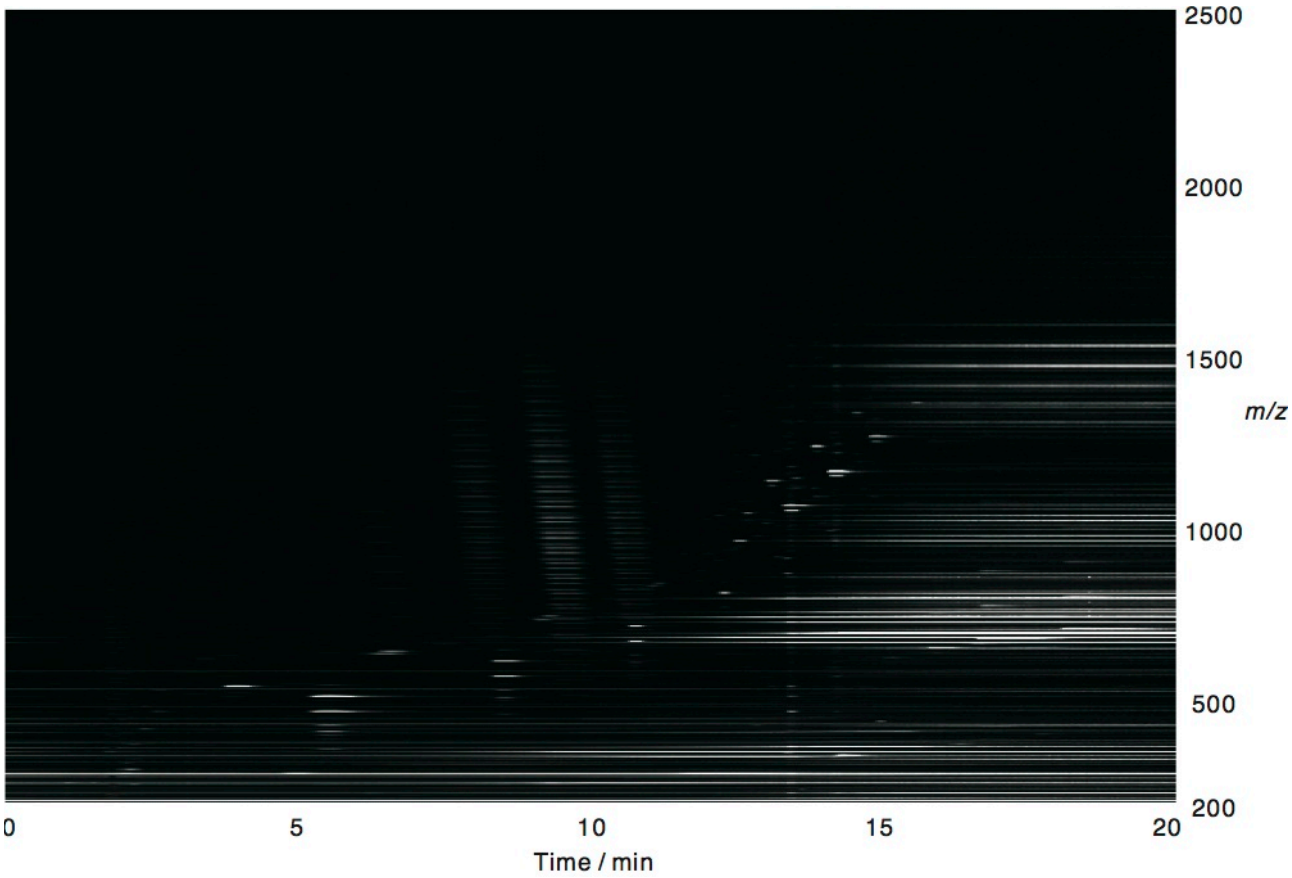

Figure 6.7 Mass spectrum observation of Brand B using LC/MS running in negative-ion ESI. Four series of ions with an *m/z* intervals of 99.994 were detected, suggesting the presence of long-chain FTOHs up to 16:2 FTOH in Brand B.

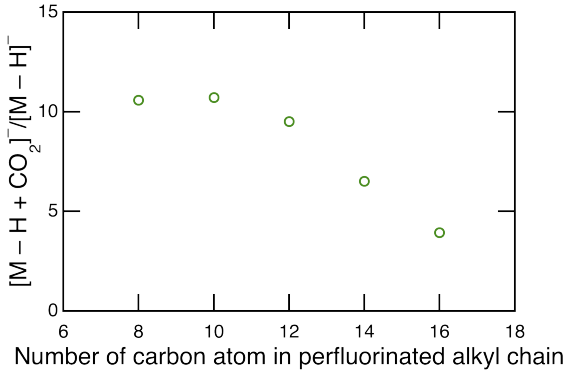

Figure 6.8 Abundance ratio of $[M - H + CO_2]^-$ and $[M - H]^-$ with respect to the number of carbon atoms of perfluorinated alkyl chain.

generation of carbonate from the gas phase reaction between aliphatic alkoxide and CO_2 (*21*). They concluded that the generation of carbonate depended on the stability of the alkoxide. The ratio $[M - H + CO_2]^-/[M - H]^-$ among the fluorotelomer congeners found in Brand B decreased with an increase in the length of the perfluorinated alkyl chain (Figure 6.8). The group with a longer perfluorinated alkyl chain becomes the stronger electron-withdrawing group. The decreased ratio was consistent with the stability of alkoxide.

Fragmentation of PFAS in MS was thoroughly reviewed by Frömel and Knepper and hydrogen atoms in the polyfluorinated alkyl chain are eliminated in the form of hydrogen fluoride (*4*). Four hydrogen fluoride eliminations were consistent with the number of hydrogen atoms in the polyfluorinated alkyl chain. Berger previously reported the same results in telomer alcohols (*22*). The others of the four series coincided with neither telomer acrylate nor telomer olefin with respect to the accurate masses, although both telomers were abundantly detected in the headspace GC/MS observation. Therefore, identification of chemical formulas was demonstrated from partial structures as well as Brands A and A'. The accurate mass of one series revealed the formula to be $C_{2n}F_{4n+1}C_5H_8O_3^-$. From the product ion spectrum, these compounds seemed to have a moiety of telomer alcohol. The remaining part after removal of a moiety of telomer alcohol was $\cdot C_3H_4O_2^-$. Because the reaction of telomer alcohol with acrylonitrile and hydrolysis of the nitrile formed yield a fluorinated carboxylic acid (*5*), this compound was identified as 1*H*,1*H*,2*H*,2*H*-perfluoroalkyl propionic acid. In the analysis of different mobile phases including ammonium formate, we detected the corresponding formate adduct anions ($C_{2n}F_{4n+1}C_6H_{10}O_5^-$). The remaining two series of the four series appeared to have two perfluoroalkyl chains. The formula $[C_{2n}F_{4n+1}C_2H_4O]_2C_5H_7O_4^-$ was estimated for one of remaining two series from its accurate mass.

6.3.5 Accurate mass analysis of Brand C

The analytical result of 1D-LC/HR-MS using an ODS column is shown

in Figure 6.9. Similar to Brand A', the mass spectrum was too complex to identify the structures of the observed ions with 1D-LC. A 2D chromatogram of Brand C, which was acquired by the Exactive Orbitrap mass spectrometer running in positive-ion ESI, is shown in Figure 6.10. Each peak in the 2D chromatogram had a series of ions in the mass spectrum with an *m/z* interval of 44.026. This interval corresponded to an ethoxy unit, C_2H_4O. Therefore, it can be considered that Brand C contains polymers with many ethoxy units. In addition, these ethoxy series were accompanied by other ethoxy series with an *m/z* interval of 99.994. To reveal their chemical structure, collision-induced dissociation spectra were also acquired (Figure 6.11). In the spectrum of Brand C in negative ion mode with collision gas, precursor ions having a perfluoroalkyl chain length generated only one prominent product ion, $C_{2n}F_{4n-3}^-$. In the case shown in Figure 6.11, it was $C_{10}F_{17}^-$ with an *m/z* of 442.9705. The precursor ions that had different numbers of ethoxy units generated an identical fragment ion. Because the ring and double bond equivalent of $C_{2n}F_{4n-3}^-$ was 2.5, the precursor ions appeared to trigger the elimination of two hydrogen fluoride molecules and an ethoxy chain. Therefore, the structural formula of the precursor ions was estimated to be $C_{2n-1}F_{4n-1}CH_2(OCH_2CH_2)_xO^-$. In the mass spectra, related ions such as $[M + Cl]^-$ and $[M - H - HF]^-$ were also found as well as $[M - H]^-$. The structure can set up two hydrogen fluoride eliminations. On the other hand, in the spectrum in positive ion mode with collision gas, ions with a shortened ethoxy chain were observed. Schröder reported a cleavage between the carbon-oxygen bond in ethoxy units in the product ion spectrum of the ammonium adduct of fluorotelomer ethoxylate in positive-ion APCI (*23*). In the present observation of the fragment ions, the *m/z* value of a fragment ion with the shortest ethoxy chain was 527.0109. Considering the cleavage position reported by Schröder, the same fragmentation appeared to occur because the exact mass of $C_9F_{19}CH_2OCH_2CH_2^+$ was 527.0110. The fragmentation path that occurred on this ion is depicted in Figure 6.11. It is highly likely that the terminal of the perfluoroalkyl chain is branched because this product includes a high concentration of *iso*-PFOA and *iso*-PFNA. Other than the fluorotelomer ethoxylate described in this formula,

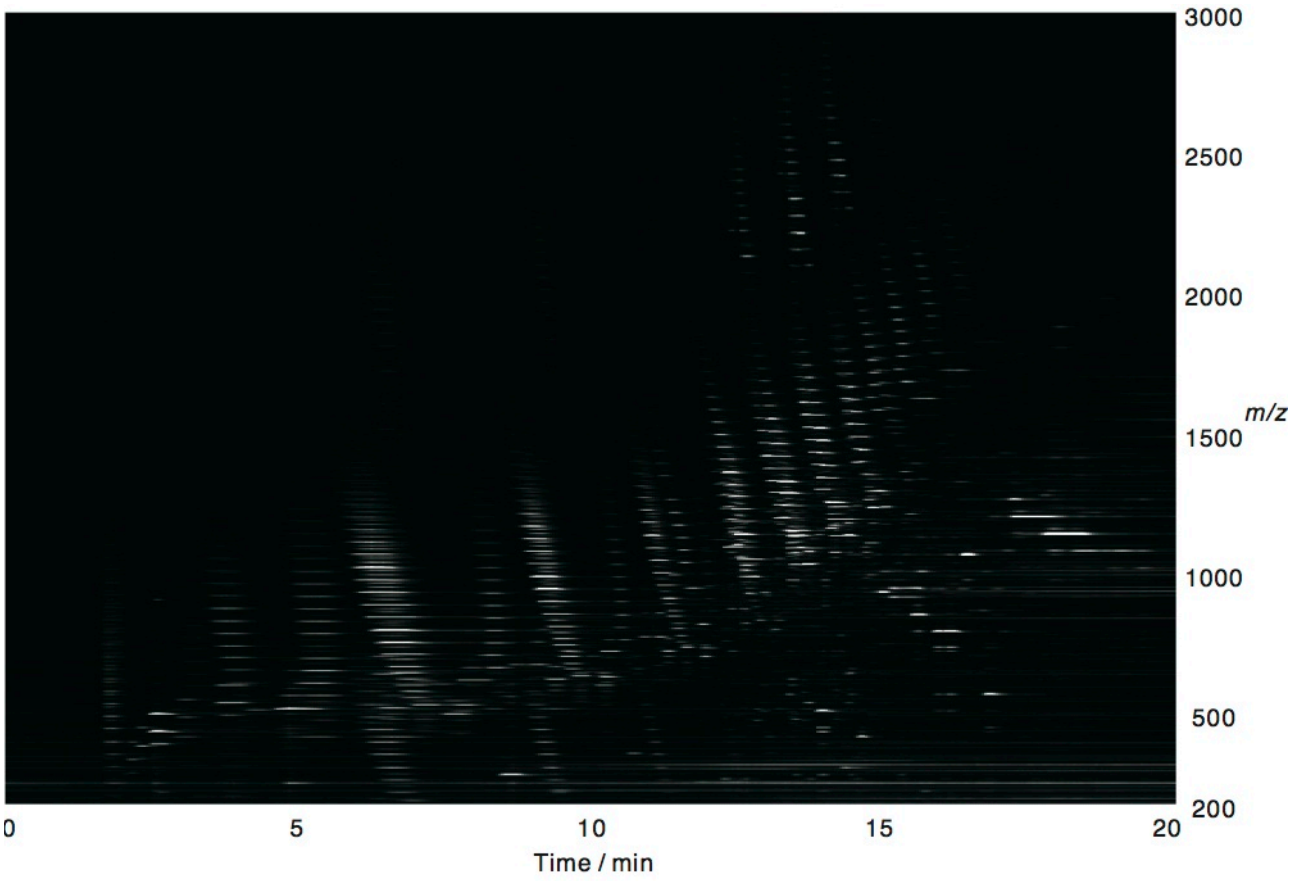

Figure 6.9 Mass spectrum observation of Brand C using LC/MS running in negative-ion ESI. Ions with *m/z* intervals of 44.026 and 99.994 suggest the polydispersity of the ethoxy chain and perfluoroalkyl chain, respectively.

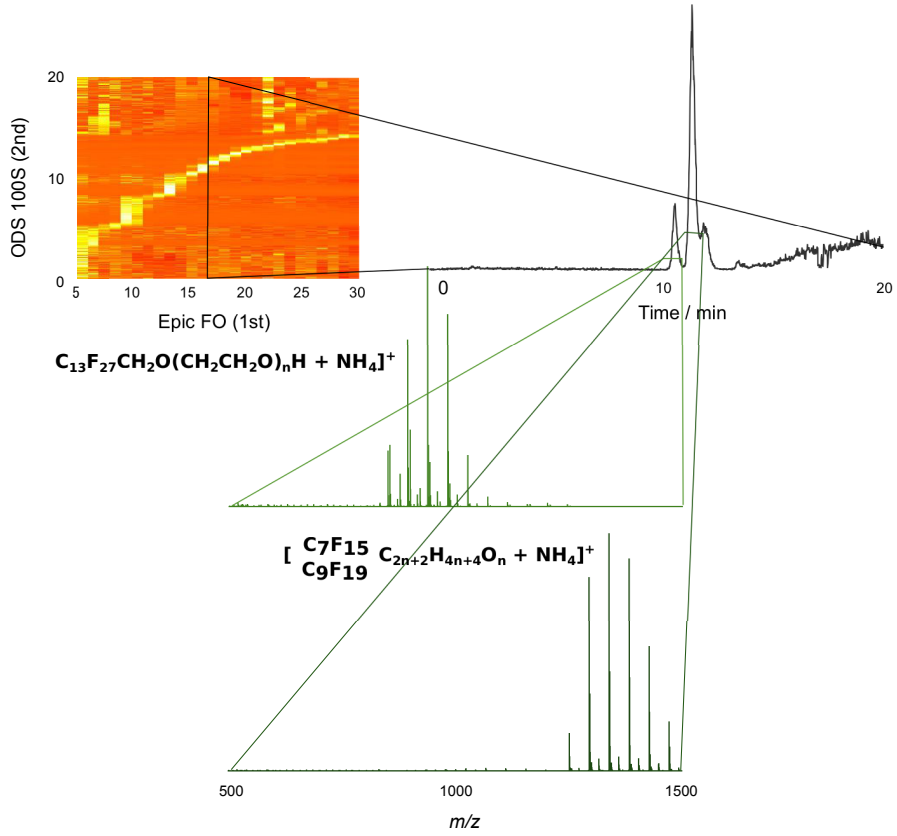

Figure 6.10 Two-dimensional total ion chromatograms of Brand C. A 2nd-chromatogram of one of fractions extracted from 2D is shown in the upper right. Mass spectra and estimated structures of the marked two peaks are shown in the bottom.

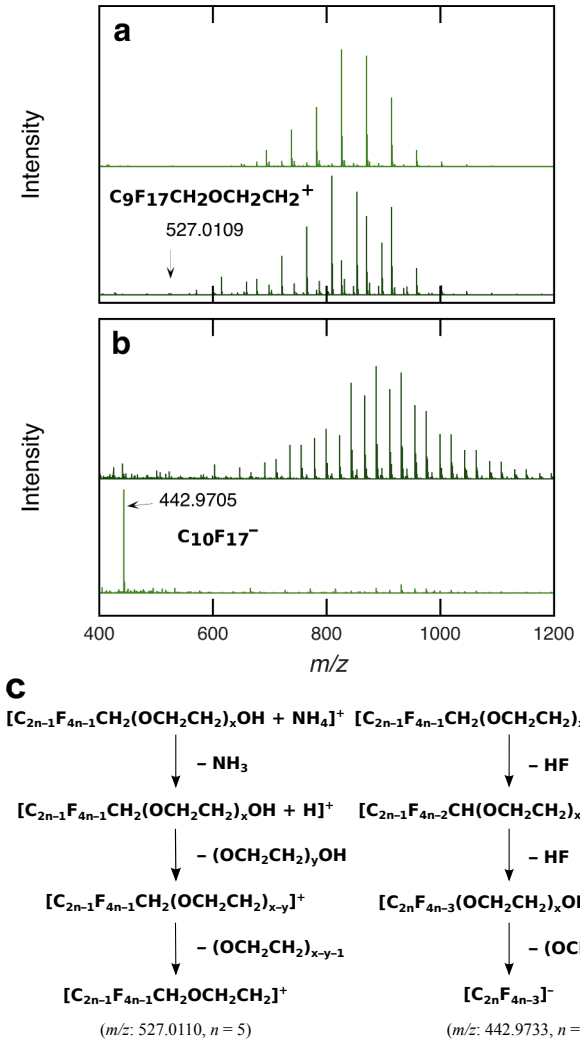

c

$[C_{2n-1}F_{4n-1}CH_2(OCH_2CH_2)_xOH + NH_4]^+$ → (– NH_3) → $[C_{2n-1}F_{4n-1}CH_2(OCH_2CH_2)_xOH + H]^+$ → (– $(OCH_2CH_2)_yOH$) → $[C_{2n-1}F_{4n-1}CH_2(OCH_2CH_2)_{x-y}]^+$ → (– $(OCH_2CH_2)_{x-y-1}$) → $[C_{2n-1}F_{4n-1}CH_2OCH_2CH_2]^+$ (*m/z*: 527.0110, *n* = 5)

$[C_{2n-1}F_{4n-1}CH_2(OCH_2CH_2)_xOH - H]^-$ → (– HF) → $[C_{2n-1}F_{4n-2}CH(OCH_2CH_2)_xOH - H]^-$ → (– HF) → $[C_{2n}F_{4n-3}(OCH_2CH_2)_xOH - H]^-$ → (– $(OCH_2CH_2)_xO$) → $[C_{2n}F_{4n-3}]^-$ (*m/z*: 442.9733, *n* = 5)

Figure 6.11 Mass spectra of a prominent peak included in Brand C: a, positive-ion mode; b, negative-ion mode. Upper spectra in each figure were acquired without collision gas. Lower spectra were acquired with collision gas. c, proposed fragmentation paths.

there were three major series of fluorotelomer ethoxylates. Considering their similar structure, one series could be explained by the formula, $C_{2n-1}F_{4n-1}CH_2CH_2O(CH_2CH_2O)_xH$. The remaining two fluorotelomer ethoxylates were more hydrophobic than $C_{2n-1}F_{4n-1}CH_2O(CH_2CH_2O)_xH$ and $C_{2n-1}F_{4n-1}CH_2CH_2O(CH_2CH_2O)_xH$ and appeared to have two perfluoroalkyl chains, but the structure could not be determined.

6.3.6 Overview of identification using accurate mass spectra of perfluorinated compounds

To identify the compounds, ions generated from objective compounds must be distinguished from the numerous ions observed. By using one mass spectrum, it is difficult to distinguish which of the ions were adduct ions or fragment ions. Various ion-molecule reactions might occur in the ion source. Further elucidation of the ion-molecule reactions that occur in the ionization process with atmospheric pressure and commonly-used LC mobile phases is anticipated. Even with high-resolving power, the larger *m/z* value increases the number of candidate chemical formulas. Therefore, sufficient separation prior to mass spectrometry is advisable. After chromatographic separation, the partial structure should be examined for each fragment because a small accurate mass has less chemical formula candidates than does a large mass. Then, the whole structure can be determined using the differences between the whole mass and the mass of the partially determined structure. The intensity ratio of a monoisotopic ion and isotopolog ions and mass defects of ions are helpful for identifying the chemical formula. In addition, ions with constant intervals observed in mass spectrum and product ion spectrum are also helpful because PFASs generate specific fragment ions in collision-induced dissociation. Furthermore, the type of mobile phase often changes the ion species generated and their ratio. Sometimes, only adduct or fragment ions are observed. In such a case, analyses in both positive and negative polarities could be definite in consideration of the original structure (*24*). In addition, the estimated structure should be consistent with the general reaction of fluorochemistry.

6.3.7 Identification of the biodegradation product

For each brand, the difference in the accurate mass spectra before and after biodegradation was examined. Numerous ions exhibited differences. An ion with *m/z* of 583.9729 was observed only in samples of Brand A after the biodegradation test. Because the ion showed a negative mass defect, the ion seemed to have many atoms with a negative mass defect, such as fluorine, sulfur, and phosphorus. This ion was identified as *N*-ethyl perfluorooctanesulfonamidoacetic acid (*N*-EtFOSAA) using an authentic standard. The concentration of *N*-EtFOSAA increased during the biodegradation test. On the other hand, perfluorooctanesulfonamide (FOSA) and *N*-ethyl perfluorooctanesulfonamide (*N*-EtFOSA) were not detected in the present biodegradation test. Among the PFASs quantitated by Method I, the concentration of *n*-PFOS slightly increased. Although *N*-EtFOSAA is a known biodegradation product of *N*-ethyl perfluorooctanesulfonamidoethanol (*N*-EtFOSE) (*25*), *N*-EtFOSE was hardly detected in Brand A before biodegradation. The activated sludge used in the present study could easily degrade the high-molar-mass compounds to *N*-EtFOSAA. On the other hand, degradation into further products such as *N*-EtFOSA and FOSA was not smooth.

With the respect to Brand A', the replacement of Brand A, an ion with an *m/z* of 369.9721 was observed only in samples after the biodegradation test. If degradation occurred around the urethane bond similar to in Brand A, this ion corresponded to *N*-methyl perfluorobutanesulfonamidoacetic acid (*N*-MeFBSAA). The exact mass of the deprotonated molecule is 369.9801. Unfortunately, an authentic standard of *N*-MeFBSAA is not commercially available. Therefore, confirmation with an authentic standard could not be conducted. The peak area of *N*-MeFBSAA increased during the period of biodegradation test. As for PFASs quantitated by Method I, the concentrations of *n*-PFBA and *n*-PFBS slightly increased. On the other hand, perfluorobutanesulfonamide and *N*-methyl perfluorobutanesulfonamide were not observed throughout the biodegradation test.

The biodegradation of telomer alcohol has been thoroughly investigated (*26–28*). We thus considered that similar biodegradation products to telomer

alcohols might be generated in the biodegradation of Brand B. x:2 saturated telomer acids (*n*-x:2 FTAs), x:2 unsaturated telomer acids (*n*-x:2 FTUAs), and x:3 saturated telomer acids (*n*-x:3 FTAs) are commercially available and quantitation using an authentic standard is possible by Method II. The changes in the concentrations of each compound by Methods I and II during the biodegradation test are shown in Figure 6.12. The most dominant degradation congener was the congener with a perfluoroalkyl chain with eight carbon atoms. Among its homologs, the most dominant homolog was unsaturated telomer acid. Telomer acids are considered to be biodegradation products because no telomer acids were observed in the samples before biodegradation. Compounds with an alkyl chain having more than eight carbon atoms are strongly hydrophobic and were hardly detected. On the other hand, degradation products with shorter alkyl chains showed no monotonic increase. Although confirmation using an authentic standard could not be conducted, the generation of *n*-7:3 FTUA, 3OH-*n*-7:3 FTA, and 3OH-*n*-5:3 FTA was inferred. Another biodegradation product reported by Wang (*28*), namely 2*H*-PFOA, was not found in the present biodegradation test.

With regard to Brand C, comparison of the spectra before and after biodegradation was quite challenging due to its complexity. Frömel reported the rapid biodegradation of fluorotelomer ethoxylate and the generation of its carboxylate (*29*). Such rapid biodegradation, however, was not observed during the present biodegradation test. The peak area change with respect to the number of ethoxy units in fluorotelomer ethoxylate described in the formula $C_9F_{19}(CH_2CH_2O)_xH$ is shown in Figure 6.13. The ethoxy unit profile hardly changed during the biodegradation test. The increase in the amounts of *iso*-PFOA and *iso*-PFNA was also obscure because the amounts preliminarily included in the product were enormous. On the other hand, every peak with a constant interval of *m/z* 44.026 had an adjacent peak. Only a high resolving power of more than 30 000 could separate these peaks. These peaks had a very small *m/z* difference of 0.036. This value is possible when different structures have an *m/z* difference of 43.989 or 44.061. Two structures, CO_2 and C_3H_8, can be estimated from these values. It would

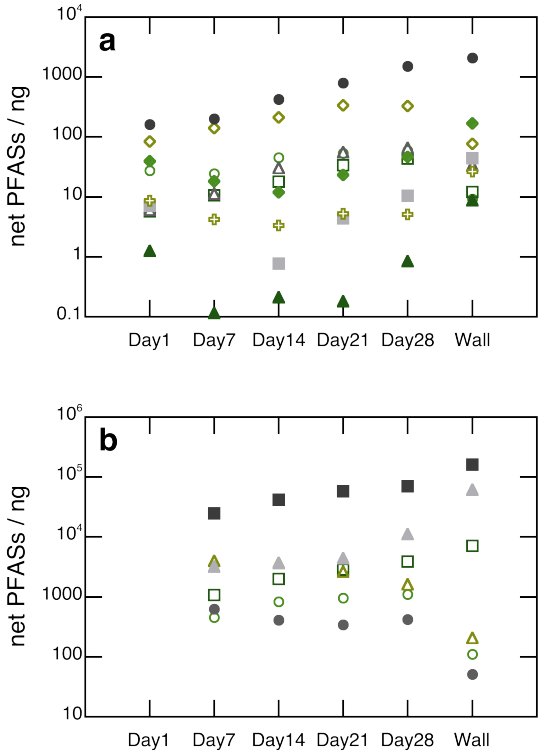

Figure 6.12 Net amount of degradation products during the biodegradation test with Brand B. Results of PFOA congeners were shown in a), where open circle, n-PFBA; open square, n-PFPeA; open diamond, n-PFHxA; open triangle, n-PFHpA; filled circle, n-PFOA; filled square, n-PFNA; filled diamond, n-PFDA; filled triangle, n-PFUdA; cross, n-PFDA. Results of telomer acids were shown in b), where open circle, n-5:3 FTA; open square, n-7:3 FTA; open triangle, n-6:2 FTUA; filled circle, n-6:2 FTA; filled square, n-8:2 FTUA; filled triangle, n-8:2 FTUA.

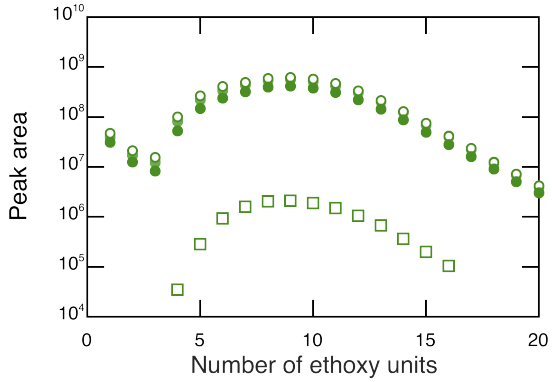

Figure 6.13 Ethoxy unit profile found in Brand C (circle) and in effluent sample (open square). The color of circle get darker as the degradation period increases: open circle, before biodegradation; filled circle, after 4 weeks biodegradation.

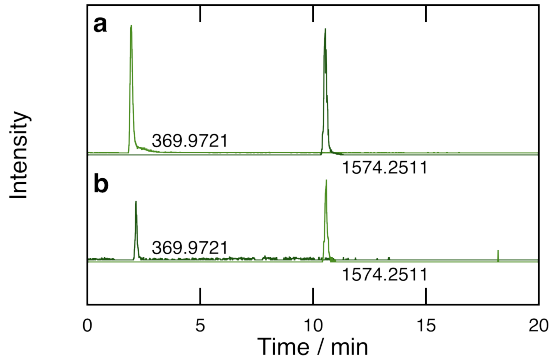

Figure 6.14 Extracted ion chromatograms of the same compound included in Brand A' and its degradation product. Extracted ion chromatograms a) of Brand A and b) of leachate sample from a disposal facility. The m/z values of extracted ions are also denoted in the figure.

appear that $C_{2n-1}F_{4n-1}(CH_2CH_2O)_xCOOH$ was also the degradation product as well as $C_{2n-1}F_{4n-1}(CH_2CH_2O)_xCH_2COOH$ reported by Frömel and Knepper (*29*).

6.3.8 Detection of ions determined in accurate mass observation from the environment

Leachate samples were collected from a disposal facility located in the Kansai area in 2010. The leachate samples had been treated by coagulating sedimentation and filtration. The analytes were extracted using a Presep PFC-II cartridge (Wako Pure Chemicals, Kyoto, Japan) and analyzed using an Exactive Orbitrap mass spectrometer. The same ion having an *m/z* value of 1574 as found in Brand A' and its degradation product were detected, as shown in Figure 6.14. Although quantitation with an authentic standard could not be conducted, it is highly probable that the same compounds exist in the environment. The fluorotelomer ethoxylates observed in Brand C were also detected in the leachate sample. With respect to the number of ethoxy units, the peak area of each fluorotelomer ethoxylate with a C_9F_{19} group is also shown in Figure 6.13. This profile is remarkably similar to that of Brand C. If these fluorotelomer ethoxylates were readily degradable, their ethoxy profiles would differ.

6.4 Conclusions

In the present study, various PFASs included in commercial products and their biodegradation products were structurally identified using HR-MS. Spectra appearing in ESI included isotopolog ions, protonated ions, and deprotonated ions, as well as fragment ions and adduct ions. Therefore, when each eluent from LC includes complex components, the interpretation of mass spectra became remarkably difficult even with HR-MS. Despite being very time-consuming, off-line 2D chromatography provided satisfactory separation. Structural identifications of PFASs could be demonstrated from interpretation of ions that appeared with some regularity, such as a constant interval of an *m/z* value, and some knowledge of fluorochemistry. In addition, some structures were determined and

quantitated by authentic standards. Readily biodegradable PFASs could exist even when they had molar masses ranging from 1000 to 2000. On the other hand, the present observations differed from previous studies with regard to the fluorotelomer ethoxylate. To date, the contribution of fluorinated polymers to PFOS and PFOA has been mostly ignored. Some PFASs, however, were detected from the environment in an unchanged form, indicating the importance of estimating their contribution to the environment using authentic standards.

References

(1) Secretariat of the Stockholm Convention on Persistent Organic Pollutants, *The Nine New POPs*, United Nations Environment Programme, Geneva Switzerland, 2009.

(2) Paul, A. G.; Jones, K. C.; Sweetman, A. J. *Environ. Sci. Technol.*, **2009**, *43*, (2), 386–392.

(3) de Voogt, P. *Perfluorinated alkylated substances.* Rev Environ Contam Toxicol Vol 208. Springer, Berlin, 2010.

(4) Frömel, T.; Knepper, T. P. In: Knepper TP and Lange FT (ed) *Polyfluorinated chemicals and transformation products.* Hdbk Env Chem Vol 17. Springer, Berlin, 2012.

(5) Kissa, E. *Fluorinated surfactants and repellents 2nd ed.* CRC Press, New York, 2001.

(6) 3M Company *Fluorochemical Use, Distribution and Release Overview.* U.S. EPA Administrative Record AR226-0550, 1999.

(7) Ministry of Economy, Trade and Industry, Japan *Fact-finding investigation about production and import of chemical substances*. 2007. (in Japanese) http://www.meti.go.jp/statistics/sei/kagaku/index.html

(8) DuPont *DuPont Global PFOA Strategy*. U.S. EPA Administrative Record AR226-1914, 2005.

(9) Martin, J. W.; Asher, B. J.; Beesoon, S.; Benskin, J. P.; Ross, M. S. *J. Environ. Monit.*, 2010, 12, (11), 1979–2004.

(10) D'eon, J. C.; Mabury, S. A. *Environ. Sci. Technol.*, **2011**, *45*, (19), 7974–

7984.
(11) Russell, M. H.; Berti, W. R.; Szostek, B.; Buck, R. C. *Environ. Sci. Technol.*, **2008**, *42*, (3), 800–807.
(12) Washington, J. W.; Ellington, J.; Jenkins, T. M.; Evans, J. J.; Yoo, H.; Hafner, S. C. *Environ. Sci. Technol.*, 2009, 43, (17), 6617–6623.
(13) Opiteck, G. J.; Lewis, K. C.; Jorgenson, J. W.; Anderegg, R. J. *Anal. Chem.*, **1997**, *69*, (8), 1518–1524.
(14) Julka, S.; Cortes, H.; Harfmann, R.; Bell, B.; Schweizer-Theobaldt, A.; Pursch, M.; Mondello, L.; Maynard, S.; West, D. *Anal. Chem.*, **2009**, *81*, (11), 4271–4279.
(15) Hogenbooma, A. C.; van Leerdama, J. A.; de Voogt, P. *J. Chromatogr. A*, **2009**, *1216*, (3), 510–519.
(16) Hernández, F.; Sancho, J. V.; Ibáñez, M.; Abad, E.; Portolés, T.; Mattioli, L. *Anal. Bioanal. Chem.*, **2012**, *403*, (5), 1251–1264.
(17) Arsenault, G.; McAlees, A.; McCrindle, R.; Riddell, N. *Rapid Commun. Mass Spectrom.*, **2007**, *21*, (23), 3803–3814.
(18) Flaherty, J.M.; Connolly, P.D.; Decker, E.R.; Kennedy, S.M.; Ellefson, M. E.; Reagen, W. K.; Szostek, B. *J. Chromatogr. B*, **2005**, *819*, (2), 329-338.
(19) Allport, D. C.; Gilbert, D. S.; Outterside, S. M. *MDI & TDI: Safety Health and the Environment.* John Wiley and Sons, New York, 2003.
(20) Terrier, P.; Douglas, D. J. *J. Am. Soc. Mass Spectrom.*, 2010, 21, (9), 1500–1505.
(21) Kumar, M. R.; Prabhakar, S.; Reddy, T. J.; Vairamani, M. *Eur. J. Mass Spectrom.*, **2006**, *12*, (1), 19–24.
(22) Berger, U.; Langlois, I.; Oehmeb, M.; Kallenborna, R. *Eur. J. Mass Spectrom.*, **2004**, *10*, (5), 579–588.
(23) Schröder, H. F. *J. Chromatogr. A*, **2003**, *1020*, (1), 131–151.
(24) Holčapek, M.; Jirásko, R.; Lísa, M. B. *J. Chromatogr. A*, **2010**, *1217*, (25), 3908–3921.
(25) Rhoads, K. R.; Janssen, E. M. L.; Luthy, R. G.; Criddle, C. S. *Environ. Sci. Technol.*, **2008**, *42*, (8), 2873–2878.
(26) Martin, J. W.; Mabury, S. A.; O'Brien, P. J. *Chem-biol. Interact.*, **2005**, *155*, (3), 165–180.

(27) Fasano, W. J.; Sweeney, L. M.; Mawn, M. P.; Nabb, D. L.; Szostek, B.; Buck, R. C.; Gargas, M. L. *Chem-biol Interact.*, **2009**, *180*, (2), 281–295.
(28) Wang, N.; Szostek, B.; Buck, R. C.; Folsom, P. W.; Sulecki, L. M.; Gannon, J. T. *Chemosphere*, **2009**, *75*, (8), 1089–1096.
(29) Frömel, T.; Knepper, T. P. *Chemosphere*, **2010**, *80*, (11), 1387–1392.

General Overview

In this thesis, the advantages of application of APPI and accurate mass measurements to solve various problems of the public health and the environmental research fields were demonstrated. Compounds with nitro group or organochlorine compounds are generally considered unsuitable for LC/ESI-MS. APPI was a dominant tool for the analyses of organochlorines and lipids with low polarity, and neonicotinoids with high polarity. The APPI process sometimes included various side reactions such as ion-molecule reaction during the ionization and generated inconceivable ions considering the analyte structures. Accurate mass measurement by high-resolution mass spectrometry could correctly determine the ion species generated in the ionization process. This is great advantage in the elucidation of the reactions that take place in APPI. As well as in the ionization process, in the fragmentation process, the mechanisms of fragmentation would be elucidated by accurate mass measurements. In the present study, the structural identification of unknown PFASs was demonstrated by accurate mass measurements and the information of fluorochemistry. In the future, data of accurate masses will be accumulated and data library will noticeably improve. Therefore unknown compounds can be identified only by the knowledge obtained from accurate mass measurements at an early date. The strategy proposed here has great positive impact on the public health and the environmental research fields.

Epitaph

I dedicate this thesis to my mother Yukiko Yamamoto who passed away shortly before completion of the manuscript. Yukiko was very diligent in her work and an affectionate mother. It's a privilege to be your son.

Acknowledgements

I wish to express my gratitude to Professor Ryuichi Arakawa and Professor Hideya Kawasaki for giving me great direction regarding the accomplishment of my studies. I appreciate the useful advise of Dr. Rie Kakehashi and Dr. Hiroshi Maeda, and the technical assistance of Dr.

Mikiya Kitagawa and Mr. Toru Yasuhara on liquid chromatography, and Mr. Hirotaka Hisatomi and Mr. Tomoshige Ando on the experiments of Exactive Orbitrap, and Ms. Fumie Adachi on the experiments of resistant bacteria, and Professor Nagatoshi Fujiwara and Assistant Professor Takayuki Wada on the donation of mycloic acid samples, and Ms. Cyndi Morley on the support of manuscript editing. I would like to sincerely thank my father Hitoshi Yamamoto and everybody in my laboratory for supporting me and having many helpful discussions. This thesis would not be finished without you all. Thank you very much!

List of Publications

(1) Yamamoto, A.; Kakutani, N.; Yamamoto, K.;' Kamiura, T.; Miyakoda, H. *Environ. Sci. Technol.* **2006,** *40,* (13), 4132–4137.
(2) Yamamoto, A.; Miyamoto, I.; Kitagawa, M.; Moriwaki, H.;' Miyakoda, H.; Kawasaki, H.; Arakawa, R. *Anal. Sci.* **2009**, *25*, (5), 693–697.
(3) Yamamoto, A.; Terao, T.; Hisatomi, H.; Kawasaki, H.; Arakawa, R. *J. Environ. Monit.* **2012**, *14*, (8), 2189–2194.
(4) Adachi, F.; Yamamoto, A.; Takakura, K.; Kawahara, R. *Sci. Total Environ.* **2013**, *444*, 508–514.
(5) Yamamoto, A.; Hisatomi, H.; Ando, T.; Takemine, S.; Terao, T.; Tojo, T.; Yagi, M.; Ono, D.; Kawasaki, H.; Arakawa, R. *Anal. Bioanal. Chem.* **2014**, *406*, 4745–4755.